PREPARATION AND STUDY OF THE ELECTRICAL PROPERTIES OF PLASMA POLYMERIZED THIN FILMS OF N,N,3,5 TETRAMETHYLANILINE
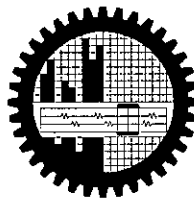
A thesis submitted to the department of Physics of Bangladesh
University of Engineering and Technology in partial
fulfillment of the requirement for the degree of
MASTER OF PHILOSOPHY IN PHYSICS

By
Hasina Akther

#99100#

Department of Physics
Bangladesh University of Engineering and Technology(BUET)
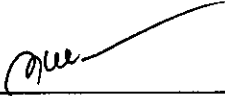January, 2004

BANGLADESH UNIVERSITY OF ENGINEERING AND TECHNOLOGY DHAKA
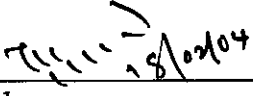## DEPARTMENT OF PHYSICS
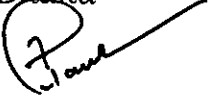
Certification of Thesis work

The thesis titled **"PREPARATION AND STUDY OF THE ELECTRICAL PROPERTIES OF PLASMA POLYMERIZED THIN FILMS OF N,N,3,5 TETRAMETHYLANILINE"** submitted by **HASINA AKTHER,** Roll No. 100114010F Session: October 2001 has been accepted as satisfactory in partial fulfillment of the requirement for the degree of **Master of Philosophy in Physics** 18 February, 2004.
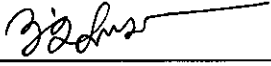
Board of Examiners

1. _____
    Dr. Md. Abu Hashan Bhuiyan (Supervisor)
    Professor,
    Department of Physics,
    BUET, Dhaka   Chairman

2. _____
    Head,
    Department of Physics,
    BUET, Dhaka   Member

3. _____
    Dr. Mominul Huq
    Professor,
    Department of Physics,
    BUET, Dhaka   Member

4. _____
    Dr. Md. Feroz Alam Khan
    Associate Professor,
    Department of Physics,
    BUET, Dhaka   Member

5. _____
    Dr. A. B. M. Obaidul Islam
    Associate Professor,
    Department of Physics,
    University of Dhaka, Dhaka   Member (External)

Declaration

It is hereby declared that this thesis or any part of it has not been submitted elsewhere for the award of any degree or diploma.

Signature of the candidate

H. Akther
_____

(Hasina Akther)

1001140101F

i

Dedication

To My Father and
My Elder Sister

Contents

CHAPTER 3   EXPERIMENTAL DETAILS

CHAPTER 4   CHEMICAL, THERMAL AND OPTICAL PROPERTIES OF PPTMA

CHAPTER 5   DC ELECTRICAL PROPERTIES OF PPTMA

CHAPTER 6   CONCLUSIONS

List of Figures

List of Tables

Abbreviations and symbols used in this thesis

ABS	Absorbance
AC/ac	Alternating Current
Al	Aluminium
B	Tauc Parameter
Cr-Al	Chromel-Alumel
CC/cc	Capacitively Coupled
d	Thickness
DC/dc	Direct Current
DTA	Differential Thermal Analysis
EA	Elemental Analysis
FL	Fermi Level
FTIR	Fourier Transform Infrared
I	Current
I	Intensity of Radiation
IR	Infrared
J	Current Density
k	Boltzmann Constant
K	Extinction Co-efficient
LB	Langmuir-Blodgett
MHz	Mega Hertz
PECVD	Plasma Enhanced Chemical Vapour Deposition
PF	Poole Frenkel
PPDP	Plasma-polymerized Diphenyl
PPm-X	Plasma-Polymerized m-Xylene
PPPA	Plasma-Polymerized Polyaniline
PPTMA	Plasma-Polymerized N,N,3,5 Tetramethylaniline
PVD	Physical Vapour Deposition
RF/rf	Radio Frequency
SCLC	Space Charge Limited Current
SEM	Scanning Electron Microscopy

T_g	Glass Transition Temperature
T_m	Melting Point
TMA	N,N,3,5 Tetramethylaniline
TGA	Thermogravimetric Analysis
TSDC	Thermally Stimulated Depolarization Current
UV-Vis	Utraviolet-Visible
V	Voltage
XPS	X-ray Photoelectron Spectroscopy
α	Absorption Coefficient
λ	Wavelength
ΔE	Activation Energy
σ	Electrical Conductivity
ε	Dielectric Constant
ε_o	Permittivity of free space
μ	Mobility of the Charge Carrier
θ	Trapping Factor

Acknowledgements

Abstract

Plasma polymerized N, N, 3, 5 tetramethylaniline (PPTMA) thin films were deposited on to glass substrates at room temperature by a capacitively coupled parallel plate reactor. The as-grown PPTMA thin films were characterized by elemental analysis (EA), infrared (IR) spectroscopy, differential thermal analysis (DTA)/ thermogravimetric analysis (TGA), ultraviolet-visible(Uv-vis) spectroscopy and dc electrical measurements.

The EA and IR spectroscopic analyses indicate that the PPTMA is chemically and structurally different from that of the N, N, 3, 5 tetramethylaniline (TMA) monomer. The empirical formula of the PPTMA film is $C_{7.70}H_{10.30}N_{1.50}O_{0.80}$. The structural investigation reveals that PPTMA thin films may be formed with certain amount of conjugation. The DTA/TGA analyses shows that the degradation in the structure and evaluation of gases may occur temperatures between 373 to 873K most probably due to dehydrogenation and oxidative reactions in the thin films. It is observed that the PPTMA films are thermally stable up to about 505 K. From the Uv-vis absorption spectra, allowed direct transition (E_{qd}), allowed indirect transition (E_{qi}) energy gaps, Tauc parameter, B and extinction coefficient were determined. The E_{qd} and E_{qi} are 2.80 and 1.44 eV respectively. The value of B is 188 $cm^{-1/2} (eV)^{-1/2}$.

The current density-voltage(J-V) measurements were performed on the PPTMA thin films of different thicknesses in a aluminium/PPTMA/aluminium configuration over 0 to 13 V and temperature range from 300 to 450 K. The J-V characteristics of PPTMA showed a power law dependence, $J \infty V^n$, with a linear behavior ($n \approx 1$) at the lower voltage region followed by a non ohmic dependence with an exponent about 2 at higher voltage region. These results emphasize that the conduction mechanism is space charge limited (SCL) conduction. Measurements of current density as a function of temperature at constant applied voltages yielded different activation energies. The values obtained are 0.81 ± 0.02 and 0.85 ± 0.05 eV for 2(ohmic) and 10 V(non ohmic) in the high temperature region respectively and 0.19 ± 0.01 and 0.19 ± 0.02 eV in the low temperature region respectively. The conduction in PPTMA may be dominated by hopping of carriers between the localized states at low temperatures and thermally excited carriers from energy levels within the band gap in the vicinity of high temperature.

CHAPTER 1

INTRODUCTION
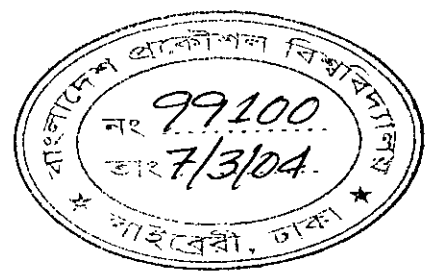
1.1 Introduction

Polymers are widely used in a great number of applications because of their many advantageous general properties, such as, low density and ease of processability and low cost. For applications requiring electrical conductivity, the choice of a suitable polymer is limited to polymers with a conjugated chemical structure e.g. polyaniline, polypyrrole, polythiophene, etc.[1-3]. In a number of applications, both conductivity and transparency are required, for which metals, inorganic conductors and ion-conducting polymer can be used. In the strive for reduction in size, costs and weight of electronic equipment, the combination of polymeric properties and conductivity would be highly advantageous. This has long been recognized by the scientific and industrial community and has resulted in extensive research in this field.

Organic materials have been the subject of intense scientific investigation for the past 50 years. Due to often weak bonding between organic molecules in the solid state, they share many of the properties of both semiconductors and insulators, and hence their study has led to a deepening of fundamental understanding of the electronic and optical properties of polymers. Thin films of these organic materials have received a great deal of interest due to their extensive applications in the fields of mechanics, electronics and optics [4,5].

Generally, thin polymer films can be formed in two ways: one is wet processing, such as the Langmuir-Blodgett film method, spin-coating, dip-coating and chemical vapor deposition (CVD). Although excellent results have been achieved this way, there are a number of problems that can arise such as pinholes, inclusion of solvents in different polymer layers, and contaminants. An alternative approach, which can avoid such difficulties, is plasma polymerization. This type of vapor deposition under vacuum provides a clean environment. It is solvent free and is well suited to sequential depositions.

Now a days, material preparation, processing and surface modification have become a prominent area of research in the development of science and technology. Among

different kinds of polymerization techniques, plasma polymerization emerges as a most important technique for the preparation of organic thin films. Plasma polymerization has been dealt as an extension of polymerization from the academic view point and as a new technology to prepare thin films from a practical view point. The concept of plasma polymerization has been based on the application of the concept of polymerization and/or of polymers developed in preceding decades to the formation of organic material under plasma conditions. Plasma polymerization is an attractive technique, using which it is possible to modify the surface properties of a substrate, while retaining the transparency and bulk properties of the substrate materials. Furthermore, it is a solvent-free, fast and versatile process [6-9]. In the thin film technology, plasma polymerization is accepted and is preferred owing to the desirable features of the thin films it yields, because the films produced in plasma have strong adhesion to the substrate surface and pinhole-free character [10-14].

In this thesis, preparation of plasma polymerized N,N,3,5 tetramethylaniline(PPTMA) thin films and study of different properties are described. The chemical structure of PPTMA observed to be little different than that of monomer keeping its aromatic ring structure. This film was found to be deficit in carbon and hydrogen and contained oxygen, which was not a part. The observed value of indirect band gap is 1.44 eV and that of direct band gap is 2.80 eV. The electrical conduction mechanism in this thin film was found to be space charge limited conduction. The activation energies determined from the current-temperature measurements are 0.19 ± 0.01 and 0.81 ± 0.02 eV respectively in the lower and higher temperature regions for 2 V. The activation energies are 0.19 ± 0.02 and 0.85 ± 0.05 eV respectively in the lower and higher temperature regions for 10 V. The thermally activated conduction in PPTMA is attributed to be a transition from a hopping regime to a regime determined by distinct energy levels from lower to higher temperature regions.

1.2 Review of Earlier Research Work

Glow discharge or plasma polymerization is widely used to prepare polymer thin films. The plasma polymerization as a plasma assisted deposition process is a well-known and efficient method to produce organic thin films and offers good control over the film properties. The term plasma polymerization should not be limited to the formation of organic materials but should cover a wider area that includes metallic or inorganic elements. Thus plasma polymerization is gaining recognition as an important process for the formation of entirely new kinds of materials. The recent development of science and technology of thin films of organic compounds produced through plasma polymerization has drawn much attention of the scientists to investigate their various properties.

At the beginning Bradley and Hammes [15,16], Stuart [17], Ozawa [18], Gregor [19] and Hirai and Nakada [20] developed plasma polymerized thin films and studied some of their chemical and electrical properties. In these developments, the concept of plasma polymerization has been based on the application of polymers developed to the formation of organic material under plasma conditions. Then the process has attracted the attention of scientists and engineers in different disciplines as an exotic method of polymerization. Today plasma polymerization is based on the molecular processes by which the size of molecules increases. The arrangement of the atoms that constitute the molecules of a monomer is accomplished during the organic synthesis of the monomer.

The structural behavior of plasma polymerized thin films is different than that of the conventionally prepared polymer thin films. Infrared (IR) spectroscopic analysis, X-ray photoelectron spectroscopy (XPS), Scanning electron microscopy(SEM), Elemental analysis(EA), etc. provide information about the chemical structure of the plasma polymers. Nakamura et al. [21] prepared thin films from cobalt tetraphenylporphyin (CoTPP) by plasma polymerization at different radio frequency(rf) power ranging from 10 to 100W. They observed that the plasma polymerized CoTPP thin films has cross-linked structure in which the original structure porphyin in CoTPP was retained to some extent depending on the rf power. Then the chemical structure of the vacuum deposited

and plasma polymerized thin film have been analyzed by Uv-visible(Uv-vis), XPS, Atomic force microscopy (AFM) and their hardness, adhesive force to a glass substrate and current–voltage characteristics were measured. Investigation of a sandwich type device of Au/ CoTPP/ ITO (Indium Tin Oxide) glass revealed that the plasma polymerized CoTPP thin film has p–type semi-conducting characteristics. The structural, electrical and optical properties of plasma-polymerized pyrrole and iodine-doped pyrrole have been studied by John and Kumar [22]. A comparative study of the IR spectra of the monomer and plasma-polymerized pyrrole showed that the ring structure was retained during plasma polymerization. With the help of SEM micrographs it has been observed that the iodine filled up the voids in the polymer, thus smoothing the surface of the polymer, which increased the connectivity, and continuity of the polymer units, thereby increasing in the electrical conductivity. Because of the strong dependence of film properties on various energy input levels and various monometer parameter, an electrical conductivity of about $1.3 \times 10^{-6} \ \Omega^{-1} \ cm^{-1}$ at low plasma polymerization power density and a high monomer flow rate. The optical emission spectroscopy(OES) was used to characterize the plasma during plasma deposition of thiophene(C_4H_4S) and iodothiophene(C_4H_4SI) by Kiesow and Heilman[23]. They showed that the conductivity of the thiophene and iodothiophene plasma polymer film has still far below that of doped-conducting bulk polymers.

Uv-vis spectroscopic analyses of organic or inorganic materials can provide the information about electronic structure and can ascertain the existence of optical transition mechanisms: allowed direct and indirect transitions and forbidden transitions. The plasma polymerized thiophene thin films were studied by Kim et al. [24] using Uv-vis spectroscopy. Uv-vis spectra showed an energy band gap shift from 3.78 to 4.02 eV with increasing r f power and quite high optical transmittance up to 95%. XRD and AFM results showed that the as-grown films have some oriented structures. As the plasma power was increased, the refractive index of thin films increased. The maximum growth rate of this study is obtained to be 115nm/min. Optical properties have been evaluated from Uv-vis spectroscopic measurements of as-deposited heat treated and aged(as deposited and heat treated) plasma polymerized diphenyl(PPDP) thin films by

Chowdhury and Bhuiyan[25]. They investigated the effect of heat treatment on the band gap, allowed direct and indirect transition energy the gap.

The effects of post deposition H_2+He plasma treatment on the electrical and thermal properties of plasma polymerized paraxylene(PPp-X) thin films were investigated by Quan et al.[26]. They observed that dielectric constant was decreased and thermal stability was increased due to plasma treatment. Plasma polymerized hexamethyldisiloxane thin films have been produced using a capacitively coupled electrode apparatus by Lee and Lee [27]. Fourier transform infrared spectroscopy(FTIR) has indicated that the spectra of the thin film was composed not only of the corresponding monomer bands but also of several new bands. They observed that the increase of relative dielectric constant and decrease of dielectric loss tangent with the discharge power was originated from high cross-linking of the films. Chowdhury et al. [28] prepared plasma polymerized diphenyl (PPDP) thin films using glow discharge technique. They characterized PPDP thin films by SEM, EA, IR, and XPS. They observed that the surface morphology of the PPDP thinfilms were uniform and pinhole free. Zhang et al. [29] has prepared Hydrophobic plasma polymer films from perflurohexane and octafluorotoluene and hydrophilic plasma polymer film from acrylic acid. Using in situ laser interferometer, FTIR and contact angle measurement, the deposition rate was correlated with the precursor structure, the deposition parameters and the plasma film structure. The results indicated that the deposition relied not only on the deposition power but also on the structure of the precursors to a large extent. Singh et al.[30] studied on a pH-dependent polyaniline with monovalent and multivalent ions. They observed that the conductivity decreased in case of multivalent ion doping. Sharp changes in conductivity took place in a particular pH range for both monovalent and multivalent ions, and accompanied by structural changes.

Many researchers have been devoted in studying the direct current (dc) electrical conduction mechanisms in various plasma–polymerized organic compounds. Shah Jalal et al. [31] studied dc electric conduction mechanism in plasma polymerized m-xylene thin films. They found Poole–Frenkel mechanism to be operative in PPm-X thin films. Measurements of the temperature dependence of ohmic and space-charge-limited(SCL) currents on thin films of polycrystalline particles of B-magnesium

phthalocyanine(MgPc) dispersed in a polymer binder in Schottky junction cells have been carried out by Riad et al.[32]. When MgPc material was sandwiched between an ohmic contact (Au) and a blocking contact (Al), the resulting cell showed rectification. The square power dependence in SCLC indicated that current conduction was limited by a discrete trapping level above the valence band edge. They also determined that the conduction process was Schottky emission in the lower voltage range and the Poole-Frenkel effect for higher voltage levels. Silva and Amaratunga[33] characterized diamond-like carbon thin films using the space-charge limited current (SCLC) under electron and hole injection. They showed that the midgap states were similar to those in a-Si:H with a large dangling-bond density.

Mathai et al. [34] prepared polyaniline thin films of different thickness by ac plasma polymerization technique. The study of asymmetric electrode configuration showed that barrier heights play a significant role in the conduction process. An activated process with activation energy decreased from 0.73 to 0.65 eV as the bias voltage increased. From their observations, they inferred that electrode limited Schottky-type conduction was dominant in plasma polymerized polyaniline thin films. Gong et al. [35] synthesized polyaniline thin films of various chemical compositions by radio-frequency plasma-polymerization technique and they showed a correlation between the C/N ratio and their different properties. The plasma-polyaniline films have been characterized by Uv-vis spectroscopy, FTIR spectroscopy, electron spin resonance, XPS, SEM and contact angle measurements, which indicated that the contents of quinoid sequences and aliphatic cross linking moieties increase with increasing plasma power input and discharge duration. The dielectric properties from a set of molybdenum(Mo)-containing diamond-like carbon films were investigated by Huang et al. [36]. They found that the permittivity greatly increased by the introduction of Mo. The relaxation time decreases with increasing the Mo content in the films at room temperature. The effect of voltage on the permittivity of the films is insignificant at frequencies above 10 kHz.

Pandey et al. [37] fabricated Schottky device by thermal evaporation of indium on chemically synthesized polyaniline, poly(o-anisidine), and poly(aniline-co-

orthoanisidine) co-polymer. They performed electrical characterization of each of these devices using current(I)-voltage(V) and capacitance(C)- voltage(V) measurements. Good rectification(0.6V) was found in the case of In/Poly(aniline-co-o-anisidine) junction.   Ram et al. [38] studied aluminium-polyaniline-aluminium(Al-PANI-Al) capacitor configurations and found that the moment of charge carriers under the influence of an electric field gives rise to the space charge phenomenon, leading to the interfacial polarization. The relaxation phenomenon seen in this configuration has been attributed to the damping of dipole oscillators originating due to the application of external electric field. The increase in the value of mobility both with increasing temperature and thickness observed in the case of Al-PANI-Al configuration support the formation of space charge in doped polyaniline.

Yamada et. al. [39] investigated poly(vinylsulfonic acid) chains having cation-exchangeable groups introduced onto a surface of polyaniline film by means of plasma-graft polymerization. The redox reaction mechanism of the plasma grafted polyaniline film has been examined with a combination of electrochemical and microgravimetric techniques. The development of the graft layer of which the thickness was ununiformed was realized by increased polymerization time. Plasma-grafting has effective on cation migration which take place in order to maintain electrioneutrality of the polyanline film during redox process in the electrolyte. Kumar et al.[40] worked on plasma polymerization of pyrrole(PPPy) in the presence and absence of iodine, and characterized it's optical and electrical properties. The studied of IR and SEM revealed that iodine was not bonded in any manner to the polymer chain of PPPy but that it made the surface morphology of the PPPy film smoother. An analysis of the electronic spectra gave band gap energies of 1.3 and 0.8 eV for the undoped and doped PPPy films respectively. The current-voltage characteristics of the two types of polymer films revealed that the conductivity of the doped PPPy film was approximately two times greater than that of the undoped one. R. Valaski et al.[41] reported their investigation of charge transport properties of thin electrodeposited polypyrrole (PPy) films. The positive charge carrier mobility was estimated and demonstrated that its value was higher for thinner films.

Polyaniline was prepared using redox polymerization by Sayed and Salem[42] They measured its dc electrical conductivity. The electrical conductivity of polyaniline salt and polyaniline base was compared with composites prepared by the hot press of polyaniline base with Potassium Bromide (KBr), Cobalt acetate [Co(CH_3COO)_2] and picric acid. Takeda [43] formed polyaniline thin film by using plasma polymerization of gasified liquid aniline. He observed that the film conductivity of the sensor with an active area of 34.3 mm^2 increased approximately six times in magnitude, which is proportional to the area and to the level of the flowing CO_2 gas. An electrical study of aging of conductivity of polyaniline-polystyrene(PANI-PSt) blend has been demonstrated by Jousseaume et al. [44]. Their study showed that the electrical conductivity decreased with time following a first order or a non first order kinetic depending principally on the nature of the dopant.

Han et al. [45] analyzed the dielectric spectra of PANI salt films by changing the dopants and film-formation methods. In the film-doping method the increase in dopant size resulted in subsequent displacement of the dielectric relaxation peak toward lower frequency which was found to be the result of an increased inter-chain distance on the PANI surface leading to lower carrier hopping. Polyaniline, an amine aromatic, has interesting combination of properties that make them very attractive in the area of electrical and electronic application. And the electronic property may be modified by adding electron donor groups like –N(CH_3)_2 in the aniline structure. Ab initio quantum mechanical investigations have been carried out by Mhin and Park [46] to examine the effects of constituents on structural deformations and electronic properties. Using a superposition approximation, they obtained good structural parameter to describe the electrical properties of push-pull para-disubstituted benzene derivatives. The amount of charge transfer and the length of the path were important parameters explaining the behavior of the electronic properties and these two structural parameters have no relationship.

1.3 Objectives of the Present Study

Thin films of organic materials have received a great deal of interest due to their extensive applications in the fields of mechanics, electronics and optics. Among many methods of depositing thin films of organic compounds or of polymers, plasma polymerization by glow discharge can be considered as an attractive technique for the formation of new kinds of materials. This work is aimed at preparing thin films of N,N,3,5 Tetramethylaniline (TMA) by plasma polymerization and characterizing them using different physical techniques. Plasma polymerized N,N,3,5 Tetramethylaniline (PPTMA) thin films would be deposited at different deposition conditions such as different power, different flow rate, etc. to find the optimum condition for good sample deposition. The structural and physical properties of the deposited PPTMA would be investigated by the following ways.

The chemical structure of PPTMA thin films would be characterized by EA. The functional groups of TMA and PPTMA would be identified by IR spectroscopy. DTA and TGA would be employed for thermal analysis.

Uv-visible spectroscopy would be used to determine the absorption co-efficient, direct and indirect transitions, Tauc parameter, etc. of PPTMA. The dc current-voltage characteristics of PPTMA thin films of different thicknesses would be investigated to elucidate dc electrical conduction mechanism. The variation of current with temperature at different applied voltages of samples of different thicknesses would be measured to ascertain the type of conduction in PPTMA.

1.4 Thesis Layout

Organization of this thesis is divided into six chapters.

Chapter 1 gives general introduction followed by a review of earlier research work, the objectives of the study and the thesis layout.

Chapter 2 illustrates briefly polymers and their general properties, different polymerization processes, overview of gas discharge plasma, plasma polymerization

mechanism, advantages and disadvantages of plasma polymers. Application of plasma polymerized organic thin films is focused at the end of the chapter.

The experimental techniques are briefly explained in chapter 3 along with description of the plasma polymerization set up, generation of glow discharge, deposition parameters, film thickness measurements, sample formation, electrode deposition etc. The Monomer, substrate materials and its cleaning process are also described here.

Chapter 4 begins with introduction to EA, experimental procedure, and results of elemental analysis followed to IR spectroscopy in the next section. The details of Uv-vis absorption measurement and calculated values of direct and indirect transition energy gaps are discussed at the end of the chapter.

Chapter 5 begins with a brief account of the existing theories on dc conduction mechanism followed by the experimental procedures of current voltage measurements and temperature dependence of current. Chapter 5 ends with the analyses of J-V characteristics and temperature dependence of current data. And finally the thesis is folded up with conclusions and suggestions for future work in chapter 6.

References

1. R.G. Lindford, "In applications of electroactive polymers", Scrosati, B, Ed.; Chapman and Hall: London (1993).

2. J.R. Reynods, C. K. Baker, C.A. Jolly, P.A. Poropatic, J. P. Ruiz, "In conductive polymers and plastics", J.M. Margolis, Ed.; Chapmann and Hall: New York (1989).

3. R.S. Sethi, M.T.Goosey, "In special polymers for electronics and optoelectronics", J.A. Chilton and M.T., Ed: Chapman and Hall, London (1995).

4. S.R. Forrest, IEEE journal on selected topics in Quantum Electronics, **6(6)** (2000) 1072-1083.

5. Frank F. Shi, "Developments in plasma-polymerized organic thin films with novel mechanical, electrical, and optical properties", J.M.S.-Rev. Macromol. Chem. Phys., **36(4)** (1996) 795-826.

6. H. Yasuda, "Plasma polymerization", Academic Press; Orlando, (1985).

7. A T. Bell and M. Shen (Eds.), "Plasma Polymerization", Am. Chem. Soc., Washington, D.C. (1979).

8. R. d' Agostino, Ed.;"Plasma deposition, treatment, and etching of polymers", Academic Press, Boston (1990).

9. H. Suhr and A.T. Bell, "In Techniques and applications of plasma chemistry; Hollahan", Ed.; John Wiley & Sons, New York (1974).

10. J. Fang, H. Chen, X. Yu, "Studies on plasma polymerization of Hexamethyldisiloxane in the presence of different carrier gases", J. Appl. Polym. Sci, **88** (2001) 1434-1438.

11. S.E. Evsyukov, F. Gautheron, H. W. Hoffken, K. Born, "Synthesis, X-ray structure, and polymerization of 1-Vinyl-3-cyanomethylimidazolium Chloride", J. Appl. Polym. Sci, **82** (2001) 499-509.

12. E.M. Moser, Ch. Faller, S. Pietrzko, F. Eggimann, "Modeling the functional performance of plasma polymerized thin films", Thin Solid Films, **355-356** (1999) 49-54.

13. S. Dahl, D. Rats, J. von Stebut, L. Martinu, J.E. Klemberg-Sapieha, "Micromechanical characterisation of plasma treated polymer surface", Thin Solid Films, **355-356** (1999) 290-294.

14. N. Inagaki, S. Tasaka, H. Hiramatsu, "Preparation of oxygen gas barrier poly(ethylene terephthalate) films by deposition of silicon oxide films plasma-polymerized from a mixture of etramethoxysilane and oxygen", J. Appl. Polym. Sci, 71(1999) 2091-2100.

15. A Bradely and J.P. Hammes, J. Electrochem. Soc., 110(1) (1963) 15-22.

16. A Bradely and J.P. Hammes, J. Electrochem. Soc., 110(1) (1963) 543-548.

17. M. Stuart, Nature (London), 199 (1963) 59-60.

18. P.J. Ozawa, IEEE Trans. Parts, Packag. PMP-5(2) (1919) 112-116.

19. L. V. Gregor, Thin Solid Films, 2 (1968) 235-246.

20. T. Hirai and O. Nakada, Jpn. J. Appl. Phys., 7(2) (1968) 112-121.

21. K. Nakamura, M. Watanabe, M. Zhou, M. Fujishima, M. Tsuchiya, T. Handa, S. Ishii, H. Noguchi, K. Kashiwagi and Y. Yoshida, "Plasma polymerization of cobalt tetraphenylporphyrin and the functionalities of the thin films produced", Thin Solid Films, 345 (1999) 99-103.

22. R.K. John, D.S. Kumar, "Structural, Electrical, and Optical Studies of Plasma polymerized and Iodine-Doped Poly Pyrrole" J. Appl. Polym Sci, 83 (2002) 1858-1859.

23. A Kiesow, A. Heilmann, "Deposition and properties of plasma polymer films made from thiophenes", Thin Solid Films, 343-344 (1999) 338-341.

24. M.C. Kim, S.H. Cho, J.G. Han, B.Y. Hong, Y.J. Kim, S.H. Yang and J.H. Boo, "High-rate deposition of plasma polymerized thin films using PECVD method and characterization of their optical properties", Surface and Coatings Technology, 169-170 (2003) 595-599.

25. F.-U.-Z. Chowdhury and A.H. Bhuiyan,"An investigation of the optical properties of plasma-polymerized diphenyl thin films", Thin Solid Films, 306(1-2) (2000) 69-74.

26. Yong Chun Quan, Sanghak Yeo, Cheonman Shim, Jaeyoung Yang, and Donggeun Jung," Significant improvement of electrical and thermal properties of low dielectric constant plasma polymerized paraxylene thin films by postdeposition H_2+He plasma treatment", J. Appl. Phys, 89(2) (2001) 1402-1404.

27. S.H. Lee and D. C. Lee, "Preparation and characterization of thin films by plasma polymerization of hexamethyldisiloxane", Thin Solid Films, 325 (1998) 83-86.

28. F.-U.-Z. Chowdhury, A.B.M.O. Islam, A.H. Bhuiyan, "Chemical analysis of the plasma-polymerized diphenyl thin films", Vacuum **57** (2000) 43-50.

29. J. Zhang, W.V. Ooij, P. France, S. Datta, A. Radomyselkiy, H. Xie, "Investigation of deposition rate and structure of pulse DC plasma polymers", Thin Solid Films, **390** (2001) 123-129.

30. R. Singh, V. Arora, R.P. Tandon, S. Chandra, N. Kumar, A. Mansingh, "Transport and structural properties of polyaniline doped with monovalent and multivalent ions", Polymer, **38(19)** (1997) 4897-4902.

31. A.B.M.S. Jalal, S. Ahmed, A.H. Bhuiyan and M. Ibrahim, "On the conduction mechanism in plasma polymerized m-xylene thin films", Thin Solid Films, **295** (1997) 125-130.

32. A.S. Riad, M. El-Shabasy and R.M. Abdel-Latif, "D.C. electrical measurements and temperature dependence of the Schottky-barrier capacitance on thin films of β–MgPc dispersed in polycarbonate." Thin Solid Films, **235** (1993) 222-227.

33. S.R.P. Silva, G.A.J. Amaratunga, "Use of space-charge-limited current to evaluate the electronic density of states in diamond-like carbon thin films", Thin Solid Films, **253** (1994) 146-150.

34. C.J. Mathai, S. Saravanan, S. Jayalekshmi, S. Venkitachalam, M.R. Anantharaman, " Conduction mechanism in plasma polymerized aniline thin films", Materials Letters, **57** (2003) 2253-2257.

35. Xiaoyi Gong, Liming Dai, Albert W.H. Mau, and Hans J. Griesser, " Plasma-polymerized polyaniline films: Synthesis and Characterization", J. Polym. Sci.: PartA: Polym. Chem., **36** (1998) 633-643.

36. Q.F. Huang, S.F. Yoon, Rusli, Q. Zhang, J.Ahn, "Dielectric properties of molybdenum-containing diamond-like carbon films deposited using electron cyclotron resonance chemical vapor deposition", Thin Solid Films, **409** (2002) 211-219.

37. S.S. Pandey, S. Annapoorni, B.D. Malhotra, "Synthesis and Characterization of Poly(aniline-co-o-anisidine): A processable Conducting Copolymer", Macromolecules, **26** (1993) 3190-3193.

38. M.K. Ram, S. Annapoorni, S.S. Pandey , B.D. Malthotra, "Dielectric relaxation in thin conducting polyaniline films", Polym., **39(15)** (1998) 3399-3404.

39. K. Yamada, T. Haraguchi and T. Kajiyama, Polym."Surface modification of polyaniline film by plasma-graft polymerization and its effect on the redox reaction", J. Polymer, **30(2)** (1998) 133-137.

40. D.S. Kumar, K. Nakamura, S Nishiyama, S. Ishil, H. Noguchi, K. Kashiwagi, Y Yoshida, "Optical and electrical characterization of plasma polymerized pyrrole films", J. Appl. Phys., **93(5)** (2003) 2705-2711.

41. R. Valaski, S. Ayoub, L. Micaroni, I.A. Hummelgen, " Influence of thin thickness on charge transport of electrodeposited polypyrrole thin films", Thin Solid Films, **415** (2002) 206-210.

42. W.M. Sayed, T.A. Salem,"Preparation of polyaniline and studying its electrical conductivity", J. Appl. Polym. Science, 77 (2000) 1658-1665.

43. S. Takeda, "A new type of CO_2 sensor built up with plasma polymerized polyaniline thin film", Thin Solid Films, **343-344** (1999) 313-316.

44. V. Jousseaume, M. Morsli, and A. Bonnet, "Aging of electrical conductivity in conducting polymer films based on polyaniline", J. Appl. Phys., **88(2)** (2000) 960-966.

45. M.G. Han and S.S. Im, "Dielectric spectroscopy of conductive polyaniline salt films", J. Appl. Plyom. Sci., **82** (2001) 2760-2769.

46. B.J. Mhin and B.H. Park, "Relationship between charge transfer and the structural deformation in para-substituted aniline derivatives", Chem. Phys. Letters, **325** (2000) 61-68.

CHAPTER 2

FUNDAMENTAL ASPECTS OF POLYMER AND PLASMA POLYMERIZATION

2.1 Introduction

A literature survey on polymers and their general properties, different polymerization processes is presented in this chapter. The details of plasma, overview of gas discharge plasma, plasma polymerization, different types of glow discharge reactors, plasma polymerization mechanism, advantages and disadvantages of plasma polymerized thin films are illustrated in this chapter. Application of plasma polymerized organic thin films is focused at end of the chapter.

2.2 Polymers [1]

The word 'Polymer' literally means many (poly) units (mer). A simple chemical unit repeats itself a very large number of times in the structure of a polymer molecule: this unit may consist of a single atom or more commonly, a small group of atoms linked chemically. In some cases the repetition is linear, such as a chain is built up from its links and in other cases the chains are branched or interconnected to form a three dimensional network. The repeat unit of the polymer is usually equivalent or nearly equivalent to the monomer, or starting material from which the polymer is formed. The length of the polymer chain is specified by the number of repeat units in the chain, which is known as the degree of polymerization (DP). Polymers are thought to be colloidal substance i.e. glue-like materials. From chemical point, the colloidal substances are in fact large molecules and that their behavior could be explained interns of the size of the individual molecules. Polymer materials, some of which are naturally occurring are in use from historical time, some are new and of recent products. When more than one kind of repeat units are present in a polymer, it is known as a copolymer. Polymers having molecular weight roughly in the range of 1000-20,000 are called low polymers and those having molecular weights higher than 20,000 as high polymers.

2.2.1 Classification of polymer

Depending on the different functional groups and structures in the field of macromolecules, polymers are classified in various ways listed in Table 2.1.

Table 2.1 Classification of polymer:

Basic Classification	Polymer types
Origin	Natural, Semisynthetic, Synthetic
Thermal response	Thermoplastic, Thermosetting
Mode structure	Addition, Condensation
Line structure	Linear, Branched, Cross–linked
Tacticity	Isotactic, Syndiotactic, Atactic
Crystallinity	Non-crystalline(amorphous),Semi-crystalline, Crystalline.

2.2.2 States of polymer

Usual description of three States (Solid, Liquid and Gaseous) of matter is not sufficient to characterize polymers. The concept of phase state is also not enough for these specifications either. The polymer structure is liquid in physical state, but it is in fact in the solid state of aggregation and there is no three-dimensional long-range order. Polymers can exist in three different states: a) the viscofluid state b) the rubbery state and c) the glassy state.

a) The viscofluid state

The viscofluid state of polymer is characterized by the intensive thermal motion of individual units, large fragments of the polymeric chain and the movement of the macromolecule as a whole. This state is typical of most liquids. The most important specific feature of polymers existing in this state is the ability to flow under the influence of the applied stress (fluidity).

b) The rubbery state

The rubbery(high elastic) state is the characteristic of polymer only. In the rubbery state individual units, atomic groups and segments undergo intensive thermal motion. Polymers in these states possess remarkable mechanical properties. The folded flexible long chains straighten out under the influence of the applied stress and return to their original shape after the stress is removed as a result of thermal motion.

c) The glassy state

When the temperature is lowered a liquid can crystalline or pass to the glassy state, which sets in when highly viscous liquids are overcooled. The transition to the glassy state is possible for both low-molecular mass substances and polymers. In this state polymers are no longer capable of undergoing segmental motion. The glassy state is characterized by the vibrational motion, small units in the main chain and also atomic groups.

There are two ways in which a polymer can pass from the solid to the liquid phase, depending on the chains in the sample. The different types of thermal response, illustrated by the following change in specific volume, are shown in Fig. 2.1.
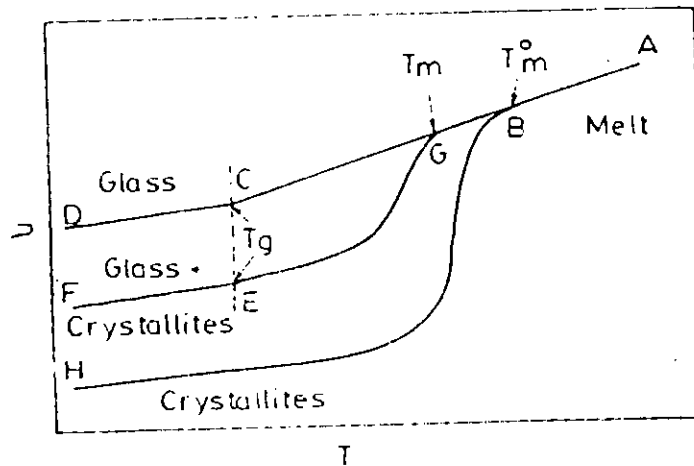
Fig. 2.1 Schematic representation of the change of specific volume of a polymer with temperature T for i) a complete amorphous sample (A-C-D), ii) a semi-crystalline sample(A-G-F) and iii) a perfectly crystalline material(A-B-H).

A polymer may be completely amorphous(Curve A-D) in the solid state, which means that the chains in the specimen are arranged in a totally random fashion. In the region C-D the polymer is a glass, but as the sample is heated it passes through a temperature T_g, called the glass transition temperature beyond which it softens and becomes rubberlike. A continuing increase in temperature along C-B-A leads to a change of the rubbery polymer to a viscous liquid. The crystalline polymer on heating would follow curve H-B-A, at T_m° melting would be observed and the polymer would become a

viscous liquid. Semi-crystalline polymers usually exhibit both T_g and T_m, corresponding to the ordered and disordered portions and follow curves similar to F-E-G-A.

2.3 Different Polymerization Process

Polymerization may generally be defined as intermolecular reaction between bifunctional or polyfuntional compounds avoiding formation of ring or cyclic structures and in a manner that make the process functionally capable of proceeding to infinity. Functional groups or atoms are: reactive hydrogen(-H), hydroxy(-OH), carboxyl group(-COOH), amino group(-NH$_2$), halogen atoms(-Cl,-Br) and C=C double bond etc. The process of polymerization may be divided into two ways (i) Chemical process and (ii) Physical process

2.3.1   Chemical process or conventional polymerization process

A variety of methods are employed for producing polymer films and the three most important groups are step growth, addition, and free radical polymerization [2,3].

i) Step growth polymerization

In step-growth polymerization, a linear chain of monomer residues is obtained by the stepwise intermolecular condensation or addition of the reactive groups in bifunctional monomers. These reactions are analogous to simple reactions involving monofunctional units as typified by a polyesterification reaction,

$$HO\text{-}R\text{-}OH + HOOC\text{-}R\text{-}COOH \Leftrightarrow HO\text{-}R\text{-}OCO\text{-}R\text{-}COOH + H_2O$$
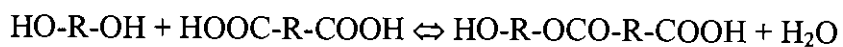
Two major groups, both distinguished by the type of monomer involved, can be identified in step-growth polymerization. In the first group two polyfunctional monomers take part in the reaction, and each possesses only one distinct type of functional group

$$A\text{-}A + B\text{-}B \rightarrow (\text{-}A\text{-}AB\text{-}B\text{-})$$
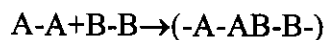
The second group is encountered when the monomer contains more than one type of functional group such as a hydroxyacid(HO-R-COOH), represented generally as A-B where the reaction is

$$nA\text{-}B \rightarrow (\text{-}AB\text{-})n$$
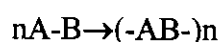
or $n(HO-R-COOH) \rightarrow H(-ORCO-)n$ OH

ii) Addition polymerization or chain-growth polymerization

Addition or chain-growth polymerization is a process by which unsaturated monomers are converted to polymers of high molecular weight, exhibiting the characteristics of a typical chain reaction.

A large number of unsaturated monomers with C-C structure undergo addition polymerization. The initiation of the chain polymerization may be activated and induced by heat, light, high-energy radiation or a host of chemical additives, commonly known as initiator (I) or catalysts for polymerization. The initiation is usually a direct consequence of generation or introduction of highly reaction species R*, through dissociation or degradation of some monomer molecules (M), under the influence of physical agencies such as heat, light, radiation, etc., or as a consequence of dissociation or decomposition of the initiator represented as

$$I \rightarrow R*$$

Addition or chain-growth polymerization is usually done in gas phase in liquid bulk monomer or under melt condition, or by solution suspension or emulsion techniques.

iii) Free radical polymerization

A free radical is an atomic or molecular species whose normal bonding system has been modified such that an unpaired electron remains associated with the new structure. The radical is capable of reacting with an olefinic monomer to generate a chain carrier which can retain its activity long enough to propagate a macromolecular chain under the appropriate conditions. The most important aspects of free radical polymerization are:

a) The rate of polymerization is proportional to the square root of the initiator concentration or the square root of the rate of the initiation.

b) The degree of polymerization is inversely proportional to the square root of the initiator concentration or the square root of the rate of the initiation.

Accordingly, faster polymer formation leads to a shorter chain length of the resulting polymers.

Except these methods, thin polymer films can be prepared in the two ways: one includes wet process like Langmuir-Blodgett (LB), spreading, dipping or solvent casting methods and the other is dry processing, such as physical vapor deposition(PVD) and chemical vapor deposition(CVD).

2.3.2   Physical process

The important processes of film formation are that a) Evaporation and b) Plasma polymerization.

i) Evaporation

The thermal evaporation method is simple and can produce good quantity film and hence this method becomes a good technique for thin film fabrication. Here vacuum evaporation is described, one of the physical methods, which is usually used to prepare thin film.

Vacuum evaporation[4,5]: The Vacuum evaporation is a kind of technique for the preparation of thin films, which includes sublimation and a condensation process. The condensation process where the film formation occurs is related with a balance among the adsorption of sublimated molecules at the substrate surface, the surface-diffusion of the adsorbed molecules, and the secession of the adsorbed molecules from the substrate surface. The important characteristic features of this technique are that the transport of vapors from the source to the substrate takes place by physical means. In this process, a vacuum chamber evacuated to about 10^{-5} torr or below, contains a vapor source for example a resistive foil source and a substrate. The material to be evaporated is in thermal contact with foil source. When the vapor source is heated by passing an electric current, the vapor pressure of the evaporate becomes substantial and liberated atoms are sent out into the vacuum chamber and stick to the substrate where a thin film consequently formed.

As the name implies vacuum evaporation technique consists of vaporization of the solid material by heating it to sufficiently high temperature and condensing it onto a cooler substrate to form a film. The deposition of thin films by vacuum evaporation consists of several distinguishable steps.

i. Transition of a condensed phase, which may be solid or liquid into the gaseous state.

ii. Vapor traversing the space between the evaporation source and the substrate at reduced gas pressure.

iii. Condensation of the vapor upon arrival on the substrates.

The liquid vapor transformation is called evaporation and solid to vapor transformation is called sublimation. Thus by evaporation method films of high quantity are produced with a minimum of interfering conditions. In practice they are applicable to all substances and to a great range of thicknesses.

ii) Plasma polymerization

As this technique is used in the preparation of the organic thin films to be investigated in the present study, a little details about plasma and plasma polymerization is documented in the following sections.

2.4 Plasma and Plasma Polymerization

2.4.1　Plasma

Plasmas are ionized gases. An ionized gas consists mainly of positively charged molecules or atoms and negatively charged electrons. A gaseous complex that may be composed of electrons, ions of both polarity, gas atoms and molecules in the ground or any higher state of any form of excitation as well as of light quanta is referred to as plasma. The ionization degree can vary from 100%(fully ionized gases) to very low values (partially ionized gases). When the temperatures greater than 10,000K all molecules and atoms tend to become ionized. Plasma is considered as being a state of materials, and the state is more highly activated than in the solid liquid, or Gas State. Besides the astroplasmas there are two main groups of laboratory plasmas, i.e. the high-temperature or fusion plasma and the so-called low temperature plasma or gas discharge[6,7]. Generally subdivision can be made between plasmas, which are in thermal equilibrium, and those, which are not in thermal equilibrium. Thermal equilibrium implies that the temperature of all species (electrons, ions, neutral species) is the same. Often the term 'Local thermal equilibrium (LTE) is used, which implies

that the temperatures of all plasma species are the same in localized areas in the plasma. On the other hand, interstellar plasma matter is typically not in thermal equilibrium also called 'non-LTE'.

The gas discharge plasmas can also be classified into LTE and non-LTE plasmas. This subdivision is typically related to the pressure in the plasma. Indeed a high gas pressure implies many collisions in the plasma, leading to a efficient energy exchange between the plasma species and hence equal temperatures. A low gas pressure, on the other hand, results in only a few collisions in the plasma species due to inefficient energy transfer.

In recent years, the field of gas discharge plasma applications has rapidly expanded [8-11]. The wide variety of chemical non-equilibrium conditions is possible since parameters can easily be modified such as,

- the chemical input,
- the pressure,
- the electromagnetic field structure,
- the discharge configuration,
- the temporal behavior.

Because of this multi- dimensional parameter space of the plasma conditions, there exists a large variety of gas discharge plasmas employed in a large range of applications. Four types of plasma i.e., the glow discharge (GD), capacitively coupled (CC), inductively coupled plasma (ICP), and the microwave-inductively plasma (MIP), are commonly used in plasma spectrochemistry and are therefore familiar to most spectrochemists. However these plasmas, as well as related gas discharges, are more widely used in technological fields.

2.4.2   An overview of gas discharge plasma

Plasma polymerization take place in a low pressure (or low temperature) plasma that is provided by a glow discharge operated in an organic gas or vapor(monomer) at low pressure between two electrodes. When a sufficient high potential difference is applied

between two electrodes placed in a gas, the letter will break down into positive ions and electrons, giving rise to a gas discharge. The mechanism of the gas breakdown can be explained as follows; a few electrons are emitted from the electrodes due to the omnipresent cosmic radiation.

However, when a potential difference is applied the electrons are accelerated by the electric field in front of the cathode and collide with the gas atoms. The most important collisions are the inelastic collisions leading to excitation and ionization. The excitation collisions create new electrons and ions. The ions are accelerated by the electric field toward the cathode, where they release new electrons by ion-induced secondary electron emission. The electrons give rise to new ionization collisions, creating new ions and electrons. These processes of electron emission at the cathode and ionization in the plasma make the glow discharge self-sustaining plasma.
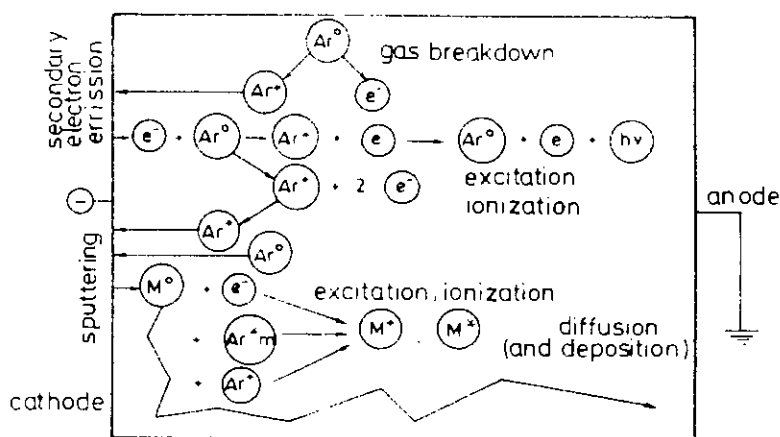
Fig. 2.2 Schematic overview of the basic processes in a glow discharge.

Another important process in the glow discharge is the phenomenon of sputtering, which occurs at sufficiently high voltage. When the ions and fast atoms from the plasma bombard the cathode, they not only release secondary electrons, but also atoms of the cathode materials, which is called sputtering. This is the basis of the use of glow discharges for analytical spectrochemistry. The ions can be detected with a mass spectrometer and the excited atoms or ions emit characteristic photons, which can be measured with optical emission spectrometry. Alternatively, the sputtered atoms can

also diffuse through the plasma and they can be deposited on a substrate, this technique is used in materials technology e.g. for the deposition of thin films
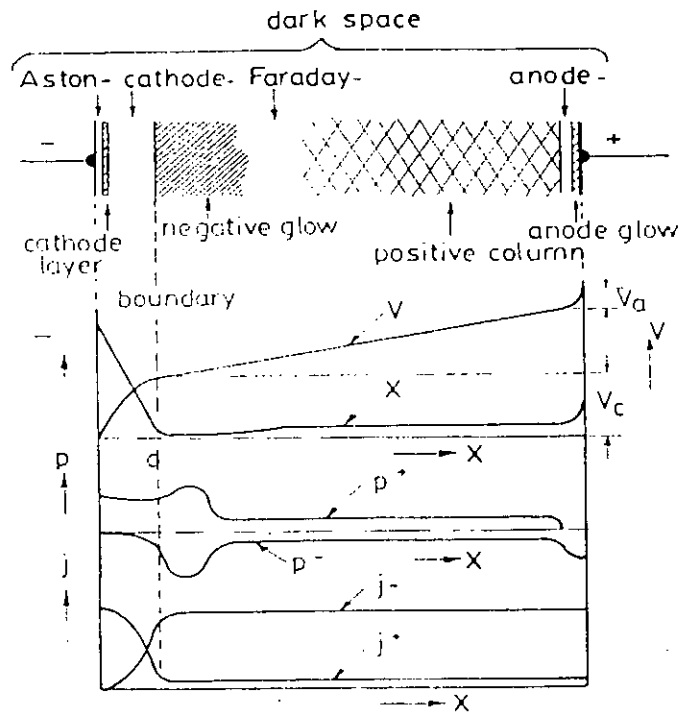
Fig.2.3 Normal glow discharge; (a) the shaded areas are luminous, (b) distribution of potential among luminous zones.

Glow discharge is characterized by the appearance of several luminous zones and by a constant potential difference between the electrodes independent of current. The relative size of these zones varies with pressure and the distance between the electrodes. A typical distribution is shown in Fig.2.3(a), the distribution of potential among different zones is shown in Fig.2.3(b). As the pressure decreases the negative glow and the Faraday dark space expand at the expense of the positive glow, which may disappear altogether. If the discharge between the electrodes decreases, the positive glow diminishes while the size of the other zones remains intact.

Basically the operation of the glow discharge depends critically on the role of the cathode dark space. In order to have a steady state each electron emitted by the cathode must produce sufficient ionization and excitation to effect the release of a sufficient number of secondary electrons from the cathode upon impact of the ions.

The role of the anode is to transform current from the glow discharge to the external circuit. When there is no positive column, the anode is usually in the Faraday dark space. In this case, the anode fall of potential can be very small, or even negative, because ions and electrons diffuse together to the anode from the negative glow in such a way that charges neutrality is maintained.

2.4.3   Direct current (dc) glow discharge

Plasma polymerization process takes place usually in a low temperature generated by glow discharge. The space between the electrodes becomes visible when a glow discharge is established, the actual distribution of light in the glow discharge is significant and is dependent on the current-voltage characteristics of the discharge[12-15].

When a constant potential difference is applied between the cathode and anode, a continuous current will flow through the discharge; giving rise to a direct current (dc) glow discharge. In a dc glow discharge the electrodes play an essential role for sustaining the plasma by secondary electron emission. The potential difference applied between the two electrodes is generally not equally distributed between cathode and anode, but it drops almost completely in the first millimeters in front of the cathode. However, for most of the other applications of dc glow discharges (sputtering, deposition, chemical etching, analytical chemistry etc.), the distance between cathode and anode is generally short. So normally a short anode zone is present beside cathode dark space and negative glow, where the slightly positive plasma potential returns back to zero at the anode.

A dc glow V can operate over a wide range of discharge conditions. The pressure can vary from below 1 pa to atmospheric pressure. The product of pressure and distance between the electrode(PD) is a better parameter to characterize the discharge. For instance, at lower pressure, the distance between cathode and anode should be longer to create a discharge with properties comparable to these of high pressure with small distance. The discharge can operate in a rare gas (most often argon or helium) or in a reactive gas (N_2, O_2, H_2, CH_4, SiH_4, SiF_4, etc.), as well as in a mixture of these gases.

2.4.4   Alternating current (ac) glow discharge

The mechanism of glow discharge generation will basically depend on the frequency of the alternation. At low frequencies(60 Hz), the effect is simply to form dc glow discharges of alternating polarity. However the frequency is higher than 60Hz the motion of ions can no longer follow the periodic changes in field polarity. But above 500 KHz the electrode never maintains its polarity long enough to sweep all electrons or ions, originating at the opposite electrode, out of the inter-electrode volume. In this case the regeneration of electrons and ions that are lost to the walls and the electrodes takes place within the body of the plasma. The mechanism by which electrons pick up sufficient energy to cause bond dissociation or ionization involves random collisions of electrons with gas molecules, the electron picking up an increment of energy with each collision. A free electron in a vacuum under the action of an alternating electric field oscillates with its velocity 90 out of phase with the field, which obtains no energy, on the average, from the applied field. The electron can gain energy from the field only as a consequence of elastic collisions with the gas atoms, as the electric field converts the electron's resulting random motion back to ordered oscillatory motion. Because of its interaction with the oscillating electric field, the electron gains energy on each collision until it acquires enough energy to be able to make an inelastic collision with a gas atom. In that case the process of these inelastic collisions is termed volume ionization.

Thus the transfer of energy from the electric field to electrons at high frequencies is generally accepted as that operative in microwave discharges. It has also been put forward as that applicable to the widely used rf of 13.56 MHz.

2.4.5   Plasma polymerization

Plasma polymerization is a process in which organic materials are reacted in an ionizing gas environment to form cross-linked polymer films. An ultra thin film can be formed by this process where thin films deposit directly on surfaces as comprising the vacuum deposition of covalently bonded materials. In this process, the growth of low-molecular-weight molecules (Polymer) occurs with the assistance of the plasma energy, which involves activated electrons, ions and radicals. The mechanisms of plasma

polymerization and that of free radical polymerization have some similarity but the fundamental processes are vastly different. The materials obtained by plasma polymerization are significantly different from conventional polymers and also different from most inorganic materials. Hence plasma polymerization should be considered as a method of forming new types of materials rather than a method of preparing conventional polymers. This polymerization process covers a wide interdisciplinary area of physics, chemistry, science of interfaces and materials science and so on[16-22]. Thus plasma polymerization is a versatile technique for the deposition of films with functional properties suitable for a wide range of modern applications.

Historically, it was known that electric discharge in a glass tube forms oily or polymer-like products at the surface of the electrodes and at the wall of the glass tube. This undesirable deposit however had extremely important characteristics that are sought after in the modern technology of coating that is, i) excellent adhesion to substrate materials and ii) strong resistance to most chemicals. To explain the reaction mechanism, many investigators discussed the effects of discharge conditions such as polymerization time monomer pressure, discharge current, and discharge power and substrate temperature on the polymerization rate.

In many cases, polymers formed by plasma polymerization show distinguished chemical composition and chemical and physical properties from those formed by conventional polymerization, if the same monomer is used for the two polymerization. To appreciate the uniqueness of plasma polymerization, it is useful to compare the steps necessary to obtain a good coating by a conventional coating process and by plasma polymerization. Coating a certain substrate with a conventional polymer, at least several steps are required (1) synthesis of a monomer, (2) polymerization of the monomer to form a polymer, (3) preparation of coating solution, (4) cleaning, (5) application of the coating, (6) drying of the coating and (7) curing of the coating. Polymers formed by plasma polymerization aimed at such a coating are in most cases branched and cross-linked [23-26]. Such polymers are also depend on (1) synthesis of a monomer, (2) Creation of plasma medium, (3) polymerization of the monomer to form a polymer, (4) cleaning, (5) application of the polymer film, and (7) curing of the film.

The important forms of plasma polymers are ultra thin films require special attention. Many bulk properties of a polymer film, such as permeability, electric volume resistively, and dielectric constant may be considered material constants, a thickness factor is included, and therefore these parameters do not change as the thickness of the film varies. This is true for a film as long as its thickness is above a certain critical value, which is 0.05-0.1μm depending on parameters under consideration. As the thickness of the film decreases below the critical value, the constancy of such parameters is no longer observed, probably due to increased contribution of flaws to the total film, which progressively increases as the thickness of the film decreases. Polymers are formed, from solid or liquid monomers, by plasma-induced polymerization through essential chemical reaction that is believed to be conventional molecular polymerization that occurs with the influence of plasma. Thus, the capability of plasma polymerization to form an ultra thin film containing a minimal amount of flaws, if not completely flawless is unique and is a valuable asset.
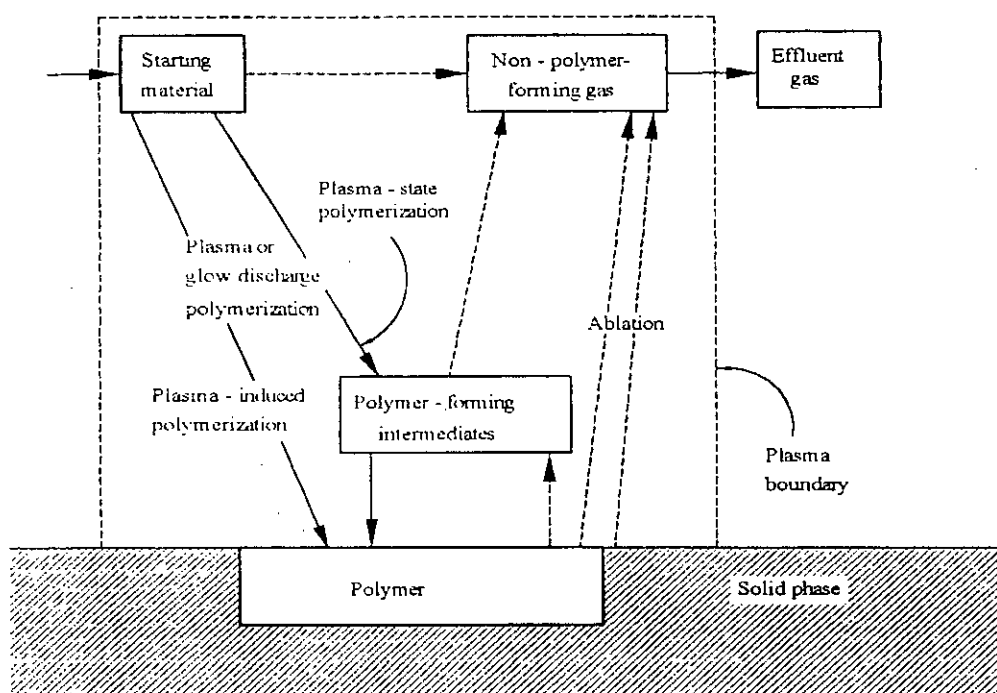
Fig.2.4 Competitive ablation and polymerization, scheme of glow discharge
        polymerization.

Among the many types of electric discharge, glow discharge is by far the most frequently used in plasma polymerization. Some other models were proposed based on ion or electron bombardment. The role of ion bombardment and pointed to a competition between etching and deposition processes in plasma polymerization was given by Yasuda in Fig.2.4.

2.5 Different Types of Glow Discharge Reactors [4, 6,27]

Glow discharge reactor is the important part of plasma polymerization system. Because reactor geometry influences the extent of charge particle bombardment on the growing films which affects the potential distribution in the system. Different kinds of reactors including capacitively coupled and inductively coupled RF reactors, microwave, dual-mode (MV/RF), etc. can be used for plasma polymerization processes. The presence of insulating layers on the electrodes deflects plasma current into any surrounding conducting areas and thus leads to gross plasma non-uniformity or plasma extinction. Therefore, when insulating materials are involved, AC power is usually employed so that power may pass through the insulator by capacitive coupling.

The most widely used reactor configurations for plasma polymerization can be broadly divided in to three classes.

```
                    ┌─────────────┐
                    │  Reactors   │
                    └──────┬──────┘
          ┌────────────────┼────────────────┐
  ┌───────┴────────┐  ┌────┴──────────┐  ┌──┴────────────┐
  │Internal electrode│ │External electrode│ │Electrode less │
  │    reactors     │  │    reactors    │  │   reactors    │
  └─────────────────┘  └────────────────┘  └───────────────┘
```
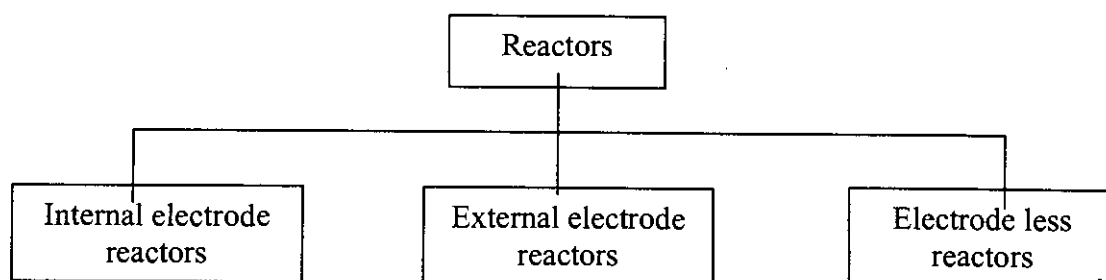
Reactors with internal electrodes have different names, e.g. flat bed, parallel plates, planar, diode etc. Their main features are power supply, coupling system, vacuum chamber, RF driver electrode, grounded electrode, and eventually one or most substrate holders. Among the internal electrode arrangements a bell-jar-type reactor with parallel

plate metal electrodes is most frequently used by using ac(1-50 kHz) and rf fields for plasma excitation.

(a)

(b)

(c)
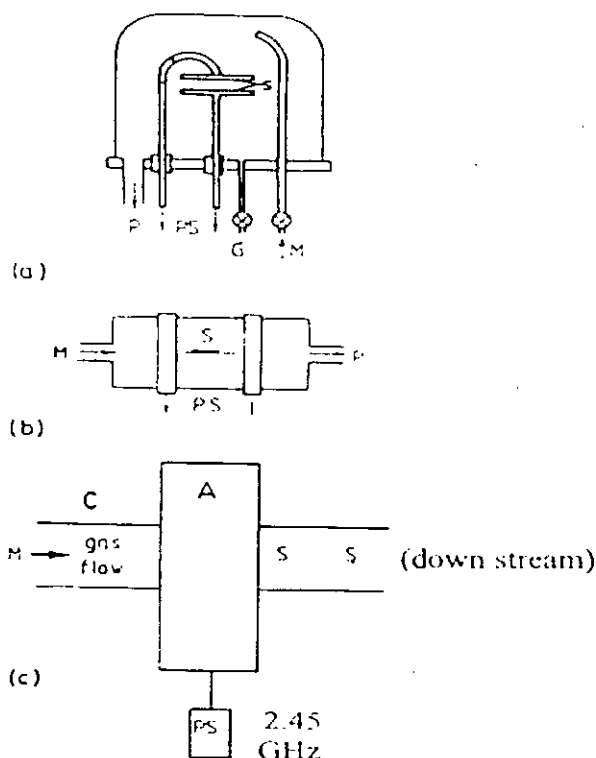
Fig.2.5 Different types of reactor configuration used for plasma polymerization.

The vacuum chambers can be made either of glass or of conductive materials, such as metal. In the case of bell-jar reactors, no particular care is taken for the grounded electrode apart from its area. On the contrary, the design and arrangement of the cathode require special attention: a metallic shield surrounding the electrode highly improves the glow confinement inside interelectrodic space; electrode material and area greatly affect the extend of sputtering on the target.

In the current research, capacitively coupled reactor (glow discharge plasma) system was used for the formation of thin films.

2.5.1   Capacitively coupled (cc) radio-frequency(rf) discharge

If an ac voltage(Up to kHz) is used, the discharge is still basically of a dc type and each electrode really acts as a cathode and anode alternatively. The frequencies generally used for the alternating voltages are typically in the radiofrequency (rf) range.

Capacitively coupled(cc) discharge can also be generated by alternating voltages in another frequency range. Therefore, the term 'alternating current(ac)' discharges as opposed to dc discharges might be more appropriate. The term 'capacitively coupled' refers to the way of coupling the input power into the discharges i.e. by means of two electrodes and their sheaths forming a kind of capacitor. The cc rf discharges which also results from the differences in mass between electrons and ions, is the phenomenon of self bias. The self-bias or dc-bias is formed i) when both electrodes differ in size and ii) when a coupling capacitor is present between the rf power supply and the electrode or when the electrode is non conductive (because it then acts as a capacitor). When a certain voltage is applied over the capacitor formed by the electrodes, the voltage over the plasma will initially have the same value as the applied voltage.

When the applied voltage is initially positive the electrons will be accelerated toward the electrode. Hence the capacitor will be rapidly charged up by the electron current and the voltage over the plasma will drop. When the applied potential changes polarity after one half-cycle, the voltage over the plasma changes with the same amount. The capacitor will now be charged up by the ion current and the voltage over the plasma will, therefore drop as well, but this second drop is less pronounced, because of the much lower mobility of the ions and hence the lower ion flux. At the next half-cycle, the applied potential, and hence also the voltage over the plasma, again changes polarity. The voltage over the plasma drops again more rapidly, because the capacitor is again charged up by the electron flux. This process repeats itself, until the capacitor is finally sufficiently negatively charged so that the ion and electron fluxes integrated over one rf-cycle, are equal to each other. This results in a time-averaged negative dc bias at the rf-powered electrode.

Because of the negative dc bias, the ions continue to be accelerated toward the rf-powered electrode, and they can, therefore cause sputtering of the rf-electrode material. In fact, the cc rf discharge often resembles a dc glow discharge with a similar subdivision in different regions, similar operating conditions, and with similar processes occurring in the plasma.
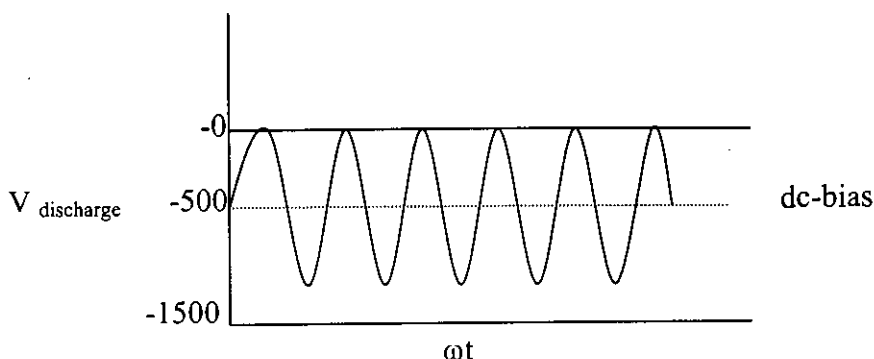
Fig.2.6 Typical sinusoidal voltage in a cc-rf discharge in the case of a large
negative dc bias.

2.5.2   Inductively coupled (ic) glow discharges

In the inductively coupled source, the plasma chamber is mostly surrounded by a coil.
Simply speaking, the rf currents in the coil (inductive element) generate an rf magnetic
flux, which penetrates the plasma region.

Following Faraday's law:

$$\nabla \times E = -\partial B / \partial t$$

the time-varing magnetic flux density induces a solenoidal rf electric field, which
accelerates the free electrons and sustains the discharge[27,28].

Basically, two different coil configurations can be distinguished in inductive discharges
for processing applications, i.e. cylindrical and planar. In the first configuration, a coil is
wound around the discharge chamber, as a helix. In the second configuration, which is
more commonly used for materials processing, a flat helix or spiral is wound from near
the axis to near the outer radius of the discharge chamber, separated from the discharge
region by a dielectric. Advantages of the latter are reduced plasma loss and better ion
generation efficiency; disadvantage is the higher sputter-contamination, UV-damage
and heating of neutrals at the substrate. Multipole permanent magnets can be used
around the process chamber circumference to increase radial plasma uniformity. The
planar coil can also be moved close to the wafer surface, resulting in near-planar source
geometry, having good uniformity properties, even in the absence of multipole
confinement.

It should be mentioned that the coupling in IC plasma is generally not purely inductive,
but has a capacitive component as well, through the wall of the reactor. Indeed, when an

inductive coupling is used, deposition on the wall is often observed to follow a pattern matching the shape of the coil. This is an indication of localized stronger electric fields on the walls, showing that the coupling is at least partly capacitive through the walls of the reactor.

It is mentioned that inductively coupled plasma are not only used as materials processing discharges, but they are also applied in other fields, albeit in totally different operating regimes. So IC plasmas are the most popular plasma sources in plasma spectrochemistry.

2.6 Plasma Polymerization Mechanism

The mechanism of reaction by which plasma polymerization occurs is quite complex and cannot be specifically described for the general case. Operational parameters such as monomer flow rate, pressure frequency, and power affect the deposition rate and structure of the plasma film. The electrons or atoms generated by partial ionization of the molecules are the principle sources for transferring energy from the electric field to the gas in all glow discharges[29, 30].

In plasma polymerization, free electrons gain energy from an imposed electrical field and then transfer the energy to neutral gas molecules, which lead to the formation of many chemically reactive species. By applying greater power to the rf source, the energy per unit mass of the monomer is increased and may bring about changes in the fragmentation process. As a result, free radicals may become entrapped in the plasma-polymerized film and increase in concentration with increasing rf power.

The deposition of polymer films in low-pressure plasma is a complex phenomenon involving reactions, which occur both in the plasma phase and at the surfaces bounding the plasma. Plasma polymerization can be represented by the following schematics where I and k are numbers of repeating units and M^* is a reactive species, which can be positive and negative ions, a free radical, or excited molecule. Since the radical concentration is very high, the combination of radical fragments predominates:

Initiation: $M_i \rightarrow M^*_i$

$M_k \rightarrow M^*_k$

Propagation: $M^*_i + M^*_k \rightarrow M_{i+k}$

Termination: $M^*_i + M_k \rightarrow M_{i+k}$
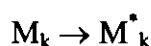
Due to high concentration of radicals produced in the plasma polymerization process, termination reactions tend to dominate over propagation reactions. In the plasma polymerization, the product of a reaction is subjected to a repeated initiation process in the presence of plasma. The phenomenon of radical combination does not stop polymer propagation reactions because the combined molecules can also be attacked through a continual cycle of initiation, combination, and reinitiation.

In plasma polymerization, deposition rates and polymer film densities have been shown to vary with substrate temperature and discharge power. Some authors have observed that deposition rate decreases with increasing substrate temperature. Polymeric films produced by plasma polymerization have branched and cross-linked structures and are difficult to dissolve in organic solvents. Their structure is irregular and amorphous and there may be no distinction between the main chain and branches.

2.7 Advantages and Disadvantages of Plasma Polymers

Besides the surface activation of polymers thin polymer films can also be deposited by so-called plasma polymerization. It refers to the deposition of polymer films through plasma dissociation and to the excitation of an organic monomer gas and subsequently deposition and polymerization of the excited species on the surface of a substrate. Plasma polymerization is used to deposit films with thickness from several tens to several thousands of angstroms. The deposited films are called plasma polymers and are generally chemically and physically different from conventional polymers. Plasma polymerization takes place through several reaction steps. In the initiation stage, free radicals and atoms are produced by collisions of electrons and ions with monomer molecules, or by dissociation of monomers adsorbed on the surface of the sample. The next step ie. propagation of the reaction, is the actual formation of polymeric chain. Finally termination can also take place in the gas phase or at the polymer surface, by similar process as in the propagation step, but ending either with the final product or with a closed polymer chain.

Plasma-polymerized films are generally chemically inert, insoluble, mechanically tough, and thermally stable have been used in a wide variety of applications such as

protective coating, electrical, optical and biomedical films. The plasma polymerization process offers several advantages over conventional polymer synthesis.

i. The starting feed gases used may not contain the type of functional groups normally associated with conventional polymerization.

ii. Such films are often highly coherent and adherent to a variety of substrates including conventional polymers, glasses and metals.

iii. Polymerization may be achieved without the use of solvents.

iv. Plasma polymer films can be easily produced with thickness of 500°A to 1 μm.

v. Ultra thin 'Pinhole' free films may be prepared.

The main advantage of plasma polymerization is that it can occur at moderate temperatures compared to conventional chemical reactions because the cracking of monomers and the formation of radicals occur by electron impact reactions in the plasma.

The specific advantages of plasma-deposited films are summarized in here:

i) Conformal: Because of the penetrating nature of low-pressure gaseous environment in which mass transport is governed in part by both molecular (line of sight) diffusion and convective diffusion, complex geometry shapes can be treated.

ii) Pinhole-free: Under common reaction conditions, the plasma film appears to coalesce during formation into a uniform over layer free of voids. Transport studies and electrical property studies suggest this continuous barrier structure.

iii) Barrier film: The pinhole-free and dense, cross-linked nature of these films suggests they have potential as barrier and protective films.

iv) Unique substrates: Plasma-deposited polymeric films can be placed upon almost any solid substrate including metals, ceramics, and semiconductors. Other surface grafting or surface modification technologies are highly dependent upon the chemical nature of the substrate.

v) Good adhesion to the substrate: The energetic nature of the gas phase species in the plasma reaction environment can induce some mixing and implantation between the overlayer film and the substrate.

vi) Unique film chemistry: The chemical structure of the polymeric overlayer films produced by rf plasma deposition cannot be synthesized by conventional organic chemical methods. Complex gas phase molecular rearrangements account for these unique surface chemical compositions.

vii) Easy preparation: Once the apparatus is set up and optimized for a specific deposition, treatment of additional substrates is rapid and simple.

Through careful control of the polymerization parameters, it is possible to tailor the films with respect to specific chemical functionality, thickness, and other chemical and physical properties[31-34].

Disadvantages

The disadvantages of plasma deposition and treatment for surface modification are:

i.   the chemistry produced on a surface is often not well defined, sometime a complex branched hydrocarbon polymer will be produced,

ii. the apparatus used to produce plasma depositions can be expensive,

iii. contamination can be a problem and care must be exercised to prevent extraneous gases, grease films, and pump oils from entering the reaction zone.

In spite of the drawbacks, plasma polymerization is far well developed process for many types of modification that simply cannot be done by any other technique.

2.8 Applications of Plasma-polymerized Organic Thin Films

Research and development of plasma and plasma-polymerized organic thin films have been undertaken very actively in the last few years and some of the products have been applied in a variety of technologies. Surface modification is probably the most important application field, plasma processes appear to have some distinct advantages compared to conventional processes. Plasma polymers are used as dielectric and optical coating to inhibit corrosion. A number of different plasma technologies are essential to different steps in the fabrication of ICs. The use of plasmas as lamps, more specifically fluorescent lamps is probably the oldest application. Nowadays, new types of so-called electrode less lamps are being developed, and the use of low temperature plasmas for

displays as large and flat television screens. Applications of plasma-polymerized films are associated with biomedical uses, the textile industry, electronics, optical applications, chemical processing and surface modification [35-37]. The main advantage of plasma polymerization is that it can occur at moderate temperatures compared to conventional chemical reactions because of cracking of monomers and the formation of radicals occurs by electron impact reactions in the plasma. Segui described two applications and the problems that prevent their industrial application, ie the reactor geometry and neutralization of free radicals in the case of microcapacitors and contact openings and mobile charge quantity reduction in the case of component passivation. Typical uses of plasma-polymerized films are listed in Table 2.2

Table 2.2 Potential applications of plasma-polymerized films.

Electronics	Integrated ckt, amorphous semiconductor, amorphous fine ceramic etching.
Electrics	Insulator, thin film dielectrics, separation membrane for batteries.
Chemical processing	Adhesive improvement, protective coating, abrasion-resistant coating, anti-crazing and scratching.
Surface modification	Adhesive improvement, protective coating, abrasion-resistant coating, anti-crazing and scratching..
Optical	Anti-reflection coating, anti-dimming coating, improvement of transparency, optical fiber, optical wave-guide laser and optical window, contact lens.
Textile	Anti-flammability, anti-electrostatic treatment, dying affinity, hydrophilic improvement, water repellence, shrink-proofing.
Biomedical	Immobilized enzymes, organelles and cells, sustained release of drugs and pesticides, sterilization and pasteurization, artificial kidney, blood vessel, blood bag, anti-coating.

References

1. J.M.G. Cowie, "Polymers: chemistry & physics of modern materials", Glasgow (1991).

2. R. Hollahan and A.T. Bell(Eds;), "Plasma polymerization", Am. Chem. Soc., Washington, D.C. (1979).

3. N. Morosoff, "An Introduction to plasma polymerization", in "Applications of plasma polymers", in plasma deposition, treatment, and etching of polymers (R. d'Agostino, Ed;.), Academic press, San Diego, CA (1990).

4. Andrew Guthrie, "Vacuum technology", John Wiley and Sons, Inc, New York (1963).

5. J. Ohkubo, N. Inagaki, "Influences of the system pressure and the substrate temperature of plasma polymer ", J. Appl. Polym. Sci., **41**(1990) 349-359.

6. A. Bogaerts, E Neyts "Gas discharge plasma and their applications", Spectrochimica Acta Part B, **57**(2002) 609-658.

7. H. Biederman, Y. Osada, "Plasma chemistry of polymers", Springer-Verlag, Berlin (1990).

8. M.A. Lieberman, A.J. Lichtenberg, "Principles of plasma discharges and materials processing", Wiley, New York (1994).

9. A. Grill, "Cold plasma in materials fabrication: from fundamentals to applications", IEEE press, New York (1994).

10. A. Bogaerts, L. Wilken, V. Hoffmann, R. Gijbels, K. Wetzig, " Comparison of modeling calculations with experimental results for rf glow discharge optical emission spectroscopy", Spectrochimica. Acta Part B, **57**(2002) 109-119.

11. S.M. Levitskii, An investigation of the sparking potential of a HF discharge in a gas in the transition range of frequencies and pressure, Sov. Phys.-Tech. Phys., **2** (1957) 887-893.

12. H. Yasuda, "Plasma polymerization" Academic Press, Inc, Tokyo (1985).

13. R.H. Stark, K.H. Schoenbach, "Direct current high pressure glow discharges", J. Appl. Phys., **85** (1999) 2075-2080.

14. R.H. Stark, K.H. Schoenbach, "Direct current glow discharges in atmospheric air", Appl. Phys. Lett., **74** (1999) 3770-3772.

15. J.C.T. Eijkel, H. Stori, and A. Manz. "A dc microplasma on a chip employed as an optical emission detector for gas chromatograph", Anal. Chem. **72** (2000) 2547-2552.

16. H. Biederman and D. Slavinska, "Plasma polymer films and their future prospects", Surface and Coatings Technology, **125(1-3)** (2000) 371-376.

17. K. Nakamura, M. Watanabe, M. Zhou, M. Fujishima, M. Tsuchiya, T. Handa, S. Ishii, H. Noguchi, K. Kashiwagi and Y. Yoshida, "Plasma polymerization of cobalt tetraphenylporphyrin and the functionalities of the thin films produced", Thin Solid Films, **345** (1999) 99-103.

18. F.-U.-Z. Chowdhury, A.H. Bhuiyan, " An investigation of the optical properties of plasma- polymerized diphenyl thin films", Thin Solid Films, **360** (2000) 69-74.

19. Xiaoyi Gong, Liming Dai, Albert W.H. Mau, and Hans J. Griesser, " Plasma-polymerized polyaniline films: synthesis and characterization", J. Polym. Sci.: PartA: Polym. Chem., **36** (1998) 633-643.

20. A. Kiesow and A. Heilmann, "Deposition and properties of plasma polymer films made from thiophenes", Thin Solid Films, **343-344** (1999) 338-341.

21. M.G. Han and S.S. Im, "Dielectric spectroscopy of conductive polyaniline salt films", J. Appl. Polym. Sci., **82** (2001) 2760-2769.

22. A.B.M. Shah Jalal, S. Ahmed, A.H. Bhuiyan and M. Ibrahim, "On the conduction mechanism in plasma polymerized m-xylene thin films", Thin Solid Films, **295** (1997) 125-130.

23. N. Inagaki, "Plasma surface modification and plasma polymerization", Wiley New York (1996).

24. D. Ratner, and A. Chilkoti, "Plasma deposition and treatment for biomaterial applications", Academic Press, New York (1990).

25. F. F. Shi, "Developments in plasma-polymerized organic thin films with novel mechanical, electrical and optical properties", J.M.S-Rev, Macromol Chem. Phys., **C36(4)** (1996) 795-826.

26. S.D. Anghel, T. Frentiu, E.A. Cordos, A. Simon, A. Popescu,"Atmospheric pressure capacitively coupled plasma source for the direct analysis of non-conducting solid samples", J.Anal. At. Spectrom, **14** (1999) 541-545.

27. J. Hopwood, "Review of inductively coupled plasmas for plasma processing", Plasma Source Sci. Technol., **1** (1992) 109-116.

28. A. Montaser, "Inductively Coupled Plasma Mass Spectrometry", Wiley, New York (1998).

29. H. Yasuda, J.L. Vossen, and W. Kern, "Thin Film Processes", Academic Press, New York (1978).

30. H. Yasuda and T. Hirotsu, J Polym. Sci: Polymer Chemistry Edition, **16** (1978) 313-17.

31. F.B. Vurzel, Acad.Sci., Moscow, USSR, "Plasma chemistry, technology, application", Inst. Plasma Chem. and Technol., Carlsbad, CA (1983).

32. T. Hammer, "Applications of plasma technology in environmental techniques, contrib.", Plasma phys. **3** (1999) 441-462.

33. R.G. Lindford, "In Applications of electroactive polymers"; Scrosati,B.Ed; Chapman and Hall, London (1993).

34. A.T. Bell and R.Hollahan, "Techniques and applications of plasma chemistry", John Wiley & Sons, New York (1974).

35. C.J. Mathai, S. Saravanan, S. Jayalekshmi, S. Venkitachalam, M.R. Anantharaman, "Conduction mechanism in plasma polymerized aniline thin films", Materials Letters, **57** (2003) 2253-2257.

36. B. J. Mhin and B.H. Park, "Relationship between charge transfer and the structural deformation in para-substituted aniline derivatives", Chem. Phys. Letters, **325** (2000) 61-68.

37. Y. Segui and Bui Ai, "Microelectronic applications of plasma-polymerized films", Thin Solid Films, **50** (1978) 321-324.

CHAPTER 3

EXPERIMENTAL DETAILS

3.1 Introduction

This chapter describes the details of the monomer, substrates materials, capacitively coupled plasma polymerization set up for thin film deposition, modification of the system, generation of glow discharge plasma, thickness measurement, formation and electrode deposition.

3.2 The Monomer

N,N,3,5 Tetramethylaniline was collected from BDH chemical limited, England. Its chemical formula is $(CH_3)_2C_6H_3N(CH_3)_2$. It is a colorful(orange) liquid with boiling point $499 \pm 2°$ K. Its density is 0.91 gm/cm^3 and refractive index is 1.54. It was used without further purification. N,N,3,5 Tetramethylaniline(TMA) contains four methyl groups where two groups are attached to the nitrogen atom. The chemical structure of the monomer is shown in Fig.3.1. The ionic form of N,N,3,5 tetramethylaniline was dissolved in the organic phase after formation of a salt soluble. The reasons for choosing TMA as monomer has been described chapter 1.
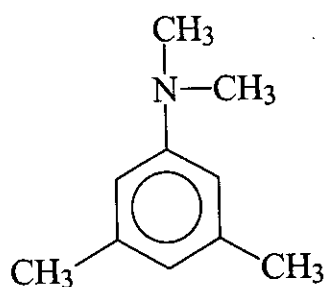
Fig. 3.1 The structure of N,N,3,5 tetramethylaniline

3.3 Substrate Materials

The substrates used were pre-cleaned glass slides (25.4mm X 76.2mm X 1.2mm) from Sail Brand, China, purchased from local market. Electrodes and plasma polymerized TMA thin films were deposited onto them.

Before depositing the films, each substrate was chemically cleaned. For chemical cleaning, the substrates were kept in concentrated nitric acid for an hour and then

cleaned with distilled water. After rinsing with distilled water the substrates were put in concentrated sodium hydroxide solution for more than half an hour and then washed with distilled water. The substrates were then kept in potassium dichromate solution for more than half an hour and then rinsed with distilled water. Finally, the cleaned substrates were rinsed with carbon tetrachloride and distilled water. Then the substrates were dried in the vacuum oven for 10 min at 453 K and were preserved in desiccator for use.

3.4 Capacitively Coupled Plasma Polymerization Set-up

Plasma polymerization takes place in a glow discharge excited in a monomer gas or vapor, or their mixture with argon, providing thus the dielectric (polymeric) component of the composite[1-4].
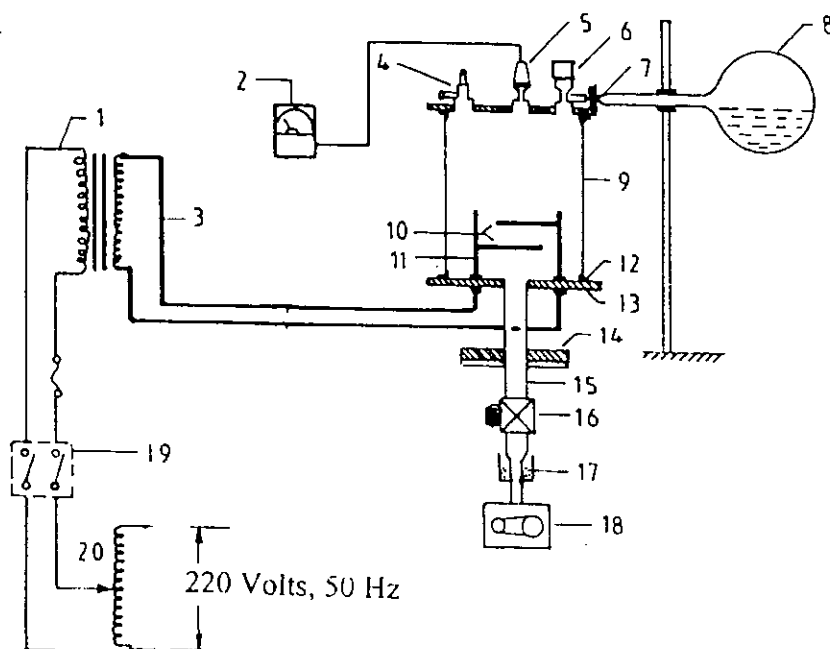
Fig.3.2 Schematic diagram of the plasma polymerization system (1 high voltage power supply, 2 pirani gage, 3 high tension leads, 4 gas inlet valve, 5 guage head, 6 monomer injection valve, 7 flowmeter, 8 monomer container, 9 Pyrex glass dome, 10 metal electrodes, 11 electrode stands, 12 gasket, 13, lower flange, 14 bottom flange, 15 brass tube, 16 valve, 17 liquid nitrogen trap, 18 rotary pump, 19 switch and 20 variac).

The glow discharge plasma deposition set-up consists of the following components is shown in Fig.3.2.

i) Plasma reaction chamber.

The plasma chamber consists of a cylindrical Pyrex® glass bell-jar having 0.15m in inner diameter and 0.18 m in length. The top and bottom edges of the glass bell-jar are covered with two rubber L-shaped (height and base 0.015m, thickness, 0.001 m) gaskets. The cylindrical glass bell jar is placed on the lower flange. The lower flange is well fitted with the diffusion pump by a I joint. The upper flange is placed on the top edge of the bell-jar. The flange is made up of brass having 0.01 m in thickness and 0.25 m in diameter. On the upper flange a laybold pressure gauge head, Edwards high vacuum gas inlet valve and a monomer injection valve are fitted. In the lower flange two highly insulated high voltage feed-through are attached housing screwed copper connectors of 0.01m high and 0.004 m in diameter via Teflon™ insulation.

ii) Electrode system

In the present set-up capacitively coupled electrode system was used. Two circular stainless steel plates of diameter 0.09 m and thickness of 0.001 m, are connected to the high voltage copper connectors. The inter-electrode separation can be changed by moving the electrodes through the electrode stands. After adjusting the distance between the electrodes they are fixed with the stands by means of screws. The substrates are usually kept on either of the electrodes for plasma deposition.

iii) Pumping unit

For creating laboratory plasma, first step is pumping out the air/gas from the plasma chamber. In this system a rotary pump of vacuubrand (Vacumbrand GMBH & Co: Germany) is used.

iv) Vacuum pressure gauge

A vacuum pressure gauge head (Laybold AG) and a meter (ThermotronTM 120) of Laybold, Germany, are used to measure inside pressure of the plasma deposition chamber.

v) Input power for plasma generation

The input power supply for plasma excitation comprises of a step-up high-tension transformer and a variac. The voltage ratio at the output of the high-tension transformer

is about 16 times that of the output of the variac. The maximum output of the variac is 220V and that of the transformer is about 3.5 KV with a maximum current of 100 mA. The deposition rate increases with power at first and then becomes independent of power at high power values at constant pressure and flow rate.
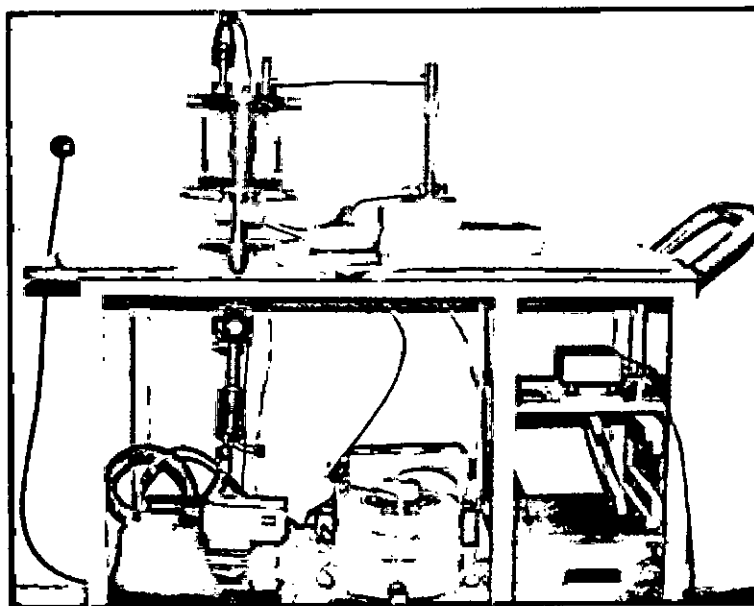
Fig.3.3 Plasma polymerization system in laboratory.

vi) Monomer injecting system

The monomer injecting system consists of a conical flask of 25 ml capacity and a pyrex glass tube with capillarity at the end portion. The capillary portion is well fitted with metallic tube of the nozzle of the high vacuum needle valve. The conical flask with its components is fixed by stand-clamp arrangement.

vii) Supporting frame

A metal frame of dimension 1.15mX0.76mX0.09m is fabricated with iron angle rods, which can hold the components described above. The upper and lower bases of the frame are made with polished wooden sheets. The wooden parts of the frame are varnished and the metallic parts are painted to keep it rust free. The pumping unit is placed on the lowed base of the frame. On the upper base a suitable hole is made in the wooden sheet so that the bottom flange can be fitted with nut and bolts.

3.5 Modifications of the Plasma Polymerization System

A flowmeter and a liquid nitrogen trap are incorporated to plasma polymerization system; details are given below.

3.5.1 Flowmeter

The system pressure of a gas flow is determined by the feed in rate of a gas and the pumping out rate of a vacuum system. The monomer flow rate is determined by a flowmeter. So flowmeters are used in plasma polymerization system to control the monomer deposition rate[1, 4]. In the plasma polymerization set up a flowmeter (Glass Precision Engineering LTD, Meterate, England) is attached between the needle valve and the monomer bottle.

3.5.2 Liquid nitrogen trap

Cold trap, particularly a liquid N_2 trap, acts as a trap pump for different type gas. The liquid N_2 trap system is placed in the fore line of the reactor chamber before the pumping unit in the plasma deposition system. It consists of a cylindrical shape chamber having 6.4 cm diameter and 11.5 cm in length using brass material. The cross-sectional view of the liquid N_2 chamber is shown in Fig3.4.
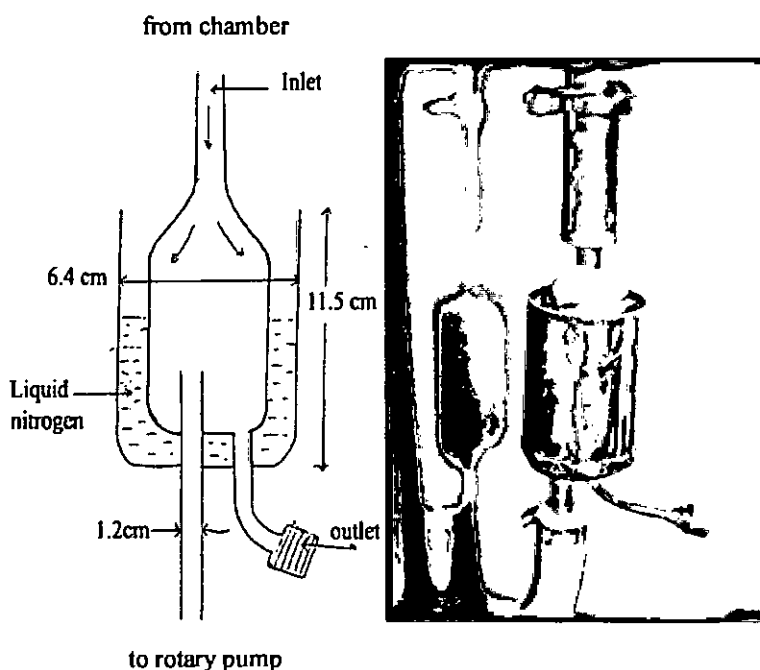
Fig. 3.4 The cross-sectional view and photograph of liquid nitrogen trap.

3.6 Generation of Glow Discharge Plasma in the Laboratory

Glow discharges are produced by an applied static or oscillating electric field where energy is transferred to free electrons in vacuum. Inelastic collisions of the energetic free electrons with the gas molecules generate free radicals, ions, and species in electronically excited states. This process also generates more free electrons, which is necessary for a self-sustaining glow [5-8]. The excited species produced are very active and can react with the surfaces of the reactors as well as themselves in the gas phase.
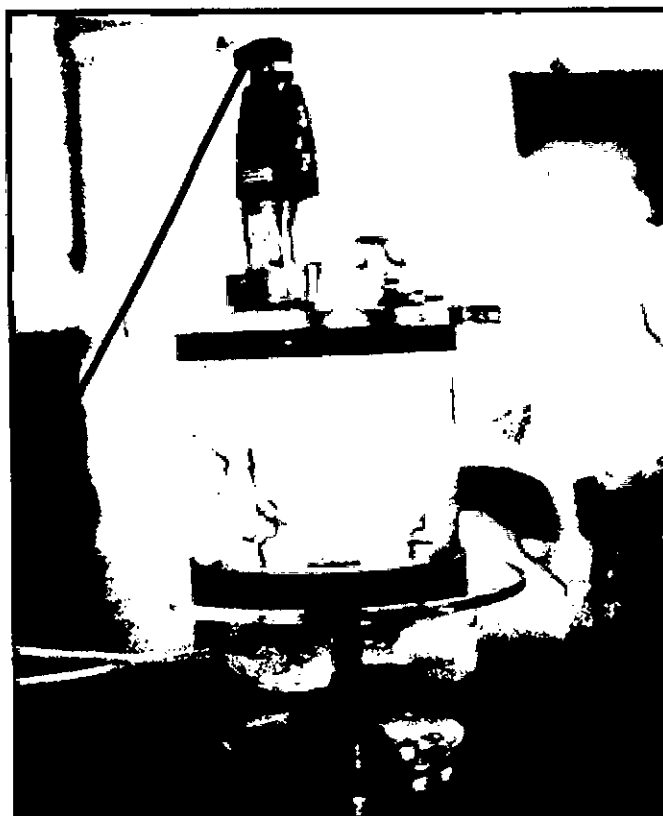
Fig.3.5 Glow discharge plasma during deposition.

The important feature of glow discharge plasma is the non-equilibrium state of the overall system. In the plasmas considered for the purpose of plasma polymerization, most of the negative charges are electrons and most of the positive charges are ions. Due to large mass difference between electrons and ions, the electrons are very mobile as compared to the nearly stationary positive ions and carry most of the current. Energetic electrons as well as ions, free radicals, and vacuum ultraviolet light can

possess energies well in excess of the energy sufficient to break the bonds of typical organic monomer molecules which range from approximately 3 to 10 eV. Some typical energy of plasma species available in glow discharge as well as bond energies encountered at pressure of approximately 0 .01 mbar.

The chamber of the plasma polymerization unit and monomer container is evacuated to about 0.01 mbar. The monomer vapor is then injected to the chamber slowly for some time. A high-tension transformer along with a variac is connected to the feed-through attached to the lower flange. While increasing the applied voltage, light bluish colors monomer plasma is produced across the electrodes at around 0.15-mbar-chamber pressure. Fig.3.3 shows the photograph of plasma deposition set-up and Fig.3.5 is the photograph of glow discharge plasma across the electrodes in the capacitively coupled parallel plate discharge chamber.

3.7 Measurement of Thickness of the Thin Films

Thickness is the single most significant film parameter. Any physical quantity related to film thickness can in principle be used to measure the film thickness. It may be measured either by several methods with varying degrees of accuracy. The methods chosen on the basis of their convenience, simplicity and reliability. Several of the common methods are i) During Evaporation, ii) Multiple-Beam Interferometry, iii) Using a Hysteresisgraph and other methods used in film-thickness determination with particular reference to their relative merits and accuracies. Multiple-Beam Interferometry technique was employed for the measurement of thickness of the thin films. This technique described below.

Multiple-Beam Inferferometry [9]

This method utilize the resulting interference effects when two silvered surfaces are brought close together and are subjected to optical radiation. This interference technique, which is of great value in studying surface topology in general, may be applied simply and directly to film-thickness determination. When a wedge of small angle is formed between unsilvered glass plates, which are illuminated by

monochromatic light, broad fringes are seen arising from inteference between the light beams reflected from the glass on the two sides of the air wedge.
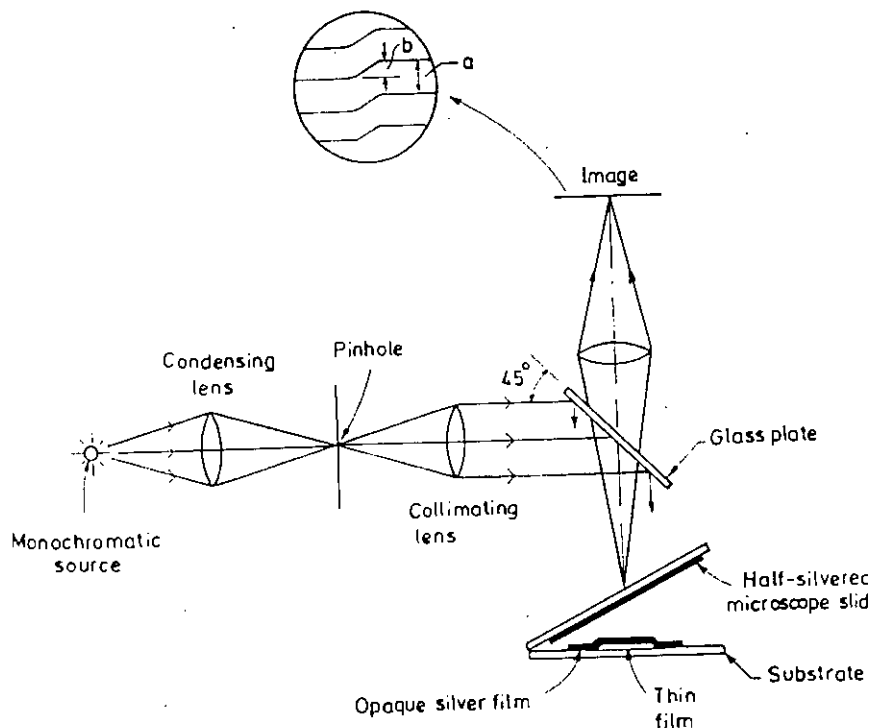
Fig3.6 The schematic diagram of multiple-beam interferometer.

Where the path difference is an integral and odd number of wavelengths, bright and dark fringes occur. If the glass surfaces of the plates are coated with highly reflecting layers, one of which is partially transparent, then the reflected fringe system consists of very fine dark lines against a bright background. A schematic diagram of the multiple-beam interferometer along with a typical pattern of Fizeau fringes from a film step is shown in Fig3.6.

As shown in this figure, the film whose thickness is to be measured is over coated with a silver layer to give a good reflecting surface and a half-silvered microscope slide is laid on top of the film whose thickness is to be determined. The thickness of the film d can then be determined by the relation

$$d = \frac{\lambda}{2}\frac{b}{a}$$

where λ is the wavelength and *b/a* is the fractional discontinuity identified in the figure. In general, the sodium light is used, for which λ = 5893 A°. In practice, several half-silvered slides of varying thickness and therefore of varying transmission are prepared, and one of these is selected for maximum resolution. Accurate determinations of fringe spacings are difficult and time consuming; but a method of image comparison, which considerably improves the ease, and rapidity of measurement has recently been developed. Alternatively, a simple film- thickness gauge utilizing Newton's rings may be developed, which involves no critical adjustment of wedges, etc., and which reduces error in film-thickness determination.

In conclusion, it might be mentioned that the Tolansky method of film-thickness measurement is the most widely used and in many respects also the most accurate and satisfactory one.

3.8 Plasma Polymer Thin Film Formation

The electric field, when applied to the gaseous monomers at low pressures (0.01 to 1 mbar), produces active species that may react to form cross-linked polymer films. In this experiments, air was used as the primary plasma, and the monomer(N,N,3,5 tetramethylaniline) vapor was injected downstream of the primary air glow discharge. In laboratory plasma polymerized N,N,3,5 tetramethylaniline(PPTMA) thin films were prepared using a bell-jar type capacitively coupled glow discharge system described earlier. The boiling point of N,N,3,5 tetramethylaniline is about 499K. So in order to deposit good PPTMA films the natural flow of monomer gas during deposition is not suitable. To increase the flow rate the container filled with N,N,3,5 tetramethylaniline liquid is heated using a heating mantle. The conditions to prepare PPTMA thin films were 40W RF power, 0.15mbar system pressure, and the monomer flow rate was kept 20cm^3/min. The deposition times for these films were varied from 20 minute to 60 minute in order to get films of different thicknesses.

3.9 Contact Electrodes for Electrical Measurements

3.9.1 Electrode materials

Aluminium(Al) (purity of 4N British Chemical Standard) was used for electrode deposition. Al has been reported to have good adhesion with glass slides [9]. Al film has advantage of easy self-healing burn out of flaws in sandwich structure [10].

3.9.2 Electrode deposition

Electrodes were deposited using an Edward coating unit E-306A(Edward, UK). The system was evacuated by an oil diffusion pump backed by an oil rotary pump. The chamber could be evacuated to a pressure less than 10^{-5} Torr. The glass substrate were masked with 0.08mX0.08mX 0.001 m engraved brass sheet for the electrode deposition. The electrode assembly used in the study is shown in Fig.3.8. The glass substrates with mask were supported by a metal rod 0.1 m above the tungsten filament. For the electrode deposition Al was kept on the tungsten filament. The filament was heated by low-tension power supply of the coating unit. The low-tension power supply was able to produce 100 A current at a potential drop of 10 V. During evacuation of the chamber by diffusion pump, the diffusion unit was cooled by the flow of chilled water and its outlet temperature was not allowed to rise above 305K. When the penning gauge reads about 10^{-5} Torr, the Al on tungsten filament was heated by low-tension power supply until it was melted.
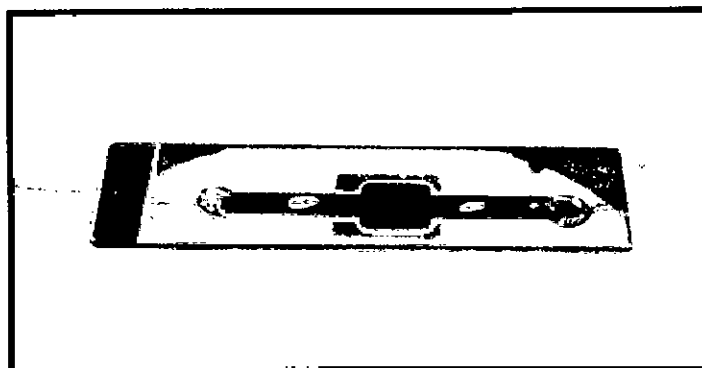
Fig.3.7 Photograph of PPTMA thin film.
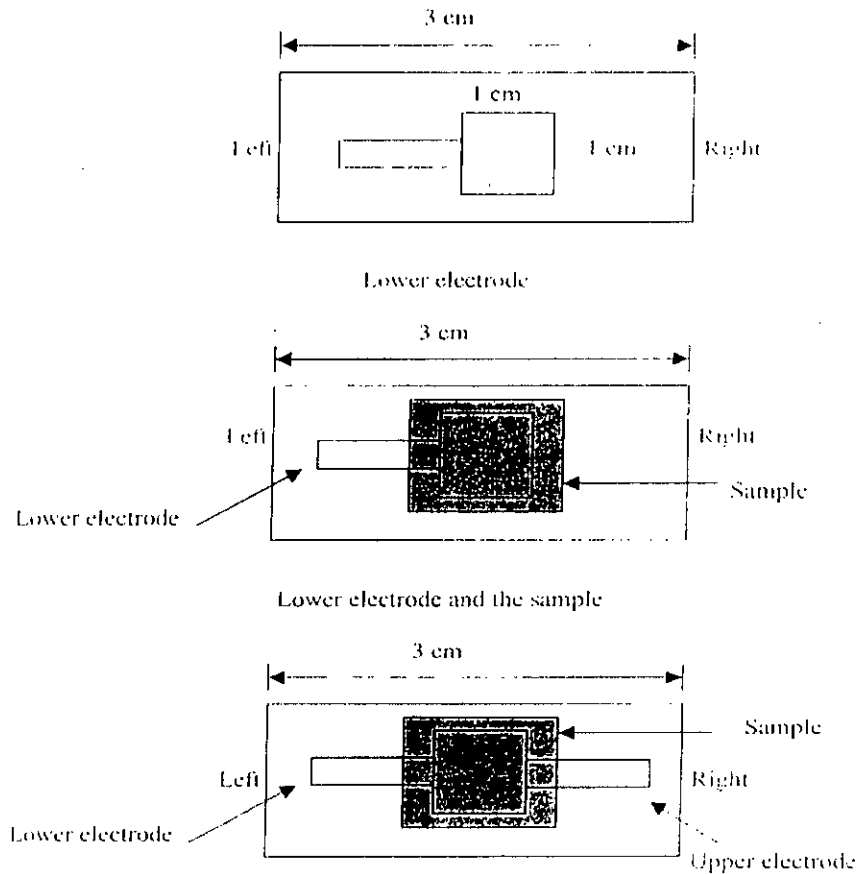
Fig.3.8 The electrode assembly.

The Al was evaporated, thus lower electrode onto the glass slide was deposited. Al coated glass substrates were taken out from the vacuum coating unit and were placed on the middle of the lower electrode of the plasma deposition chamber for TMA thin film deposition under optimum condition. The top Al electrode was also prepared on the PPTMA film as described above [10-12].

3.10 Samples for Different Measurements

PPTMA thin films were deposited on to chemically cleaned microscope glass substrates for UV-Visible spectroscopy analyses. For EA, DTA, TGA study and IR spectroscopy the films were scraped off from the substrate. Metal/ PPTMA/Metal sandwich structures, shown in Fig. 3.8, were prepared for all shorts of electrical investigations.

References

1. H. Yasuda, "Plasma Polymerization" Academic Press, Inc, Tokyo (1985).

2. F.-U.-Z. Chowdhury, A.B.M.O. Islam, A.H. Bhuiyan, " Chemical analysis of plasma- polymerized diphenyl thin films", Vacuum, **57** (2000) 43-50.

3. S.D. Anghel, T. Frentiu, E.A. Cordos, A. Simon, A. Popescu,"Atmospheric pressure capacitively coupled plasma source for the direct analysis of non-conducting solid samples", J.Anal. At. Spectrom, **14** (1999) 541-545.

4. N. Inagaki, "Plasma surface modification and plasma polymerization", Technomic Publishing Co. Inc., New York (1996).

5. F.F. Chen, "Introduction to plasma physics", Plenum Press, New York (1974).

6. M.A. Lieberman, A.J. Lichtenberg, "Principles of plasma discharges and materials processing", Wiley, New York (1994).

7. A. Bogaerts, E. Neyts "Gas discharge plasma and their applications", Spectrochimica Acta Part B, **57** (2002) 609-658.

8. M.A. Lieberman, A.J. Lichtenberg, "Principles of plasma discharges and materials processing", Wiley, New York (1994).

9. S. Tolansky, "Multiple Beam Interferometry of surfaces and films", Clarendon Press, Oxford (1948).

10. A.B.M. Shah Jalal, S. Ahmed, A.H. Bhuiyan and M. Ibrahim, "On the conduction mechanism in plasma polymerized m-xylene thin films", Thin Solid Films, **295** (1997) 125-130.

11. S. D. Phadke, K. Sathianandan and R. N. Karekar, "Electrical conduction in polyferrocene thin films", Thin Solid Films, **51** (1778) 9-11.

12. R.D. Gould and T.S. Shafai, "Condction in lead phthalocyanine films with aluminim electrodes", Thin Solid Films, **373** (1-2) (2000) 89-93.

CHAPTER 4

CHEMICAL, THERMAL AND OPTICAL PROPERTIES OF PPTMA

4.1 Introduction

This chapter deals with the investigation of structural, thermal and optical behaviors of PPTMA thin films. The investigation of the composition and structure of PPTMA by EA and IR spectroscopy respectively are discussed. The DTA and TGA of PPTMA are also discussed.

Plasma polymers have received much attention for their potential applications as light guide material, optical fibers, as photovoltaic energy converters, photodiodes, optical coatings to inhibit corrosion, etc.[1-3]. For these kinds of applications, plasma polymerized thin films need optical investigations. The optical energy gaps, the allowed direct transition and allowed indirect transitions, Tauc parameter, B and extinction coefficient have been determined from the Uv-vis spectroscopic studies and are discussed in this chapter.

4.2 Elemental Analysis(EA)

The elemental analysis is a useful technique for chemical investigation of organic or inorganic materials. The chemical compositions of plasma-polymerized materials can be characterized by elemental analyses technique. The elemental composition of plasma-polymerized materials generally differs substantially from that of monomer, which does not usually happen in case of conventional polymers.

The technique used for the determination of CHN is based on the quantitative "dynamic Flash Combustion" method as shown in Fig.4.1. The samples are held in a tin container, placed inside the auto samples drum where they are purged with a continuous flow of helium and then dropped at constant intervals into a vertical quartz tube maintained at 1293K (Combustion reactor). When the sample dropped inside the furnace, the helium stream is temporarily enriched with pure oxygen and the sample and its container melt and the tin promotes a violent reaction (Flash Combustion) in a temporary enriched atmosphere of oxygen.

Sample in a tin capsule

Quantitative
Dynamic   Flash
Combustion
1800° C

$S_n \rightarrow S_nO_2$
$N_2 + N_X O_Y$
CO_2
H_2O
$SO_2 + SO_3$
1000" C

Catalyst
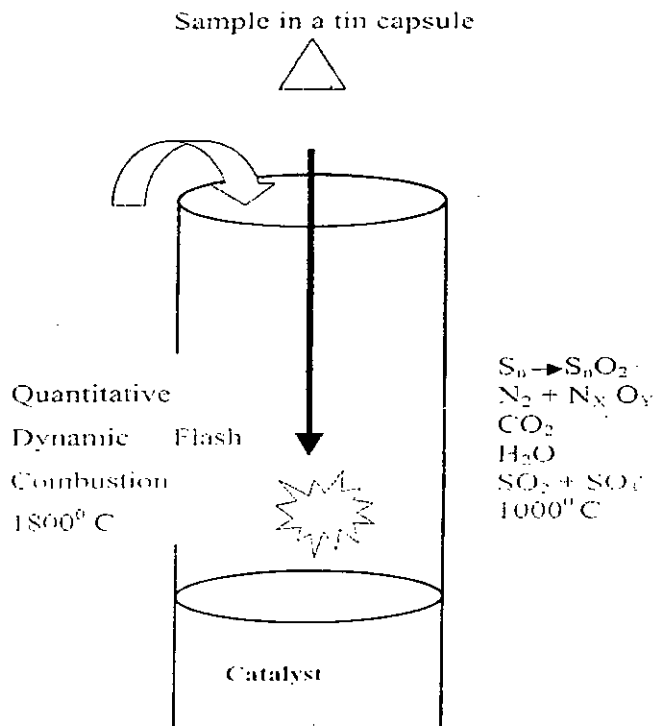
Fig. 4.1 The principle of operation of elemental analyzer.

Under these favorable conditions even thermally resistant substances are completely oxidized. The resulting combustion gases are separated and detected by a thermal conductivity detector, which gives an output signal proportional to the concentration of the individual components of the mixture.

4.2.1   Experimental procedure

The PPTMA powder was collected from the monomer deposited substrates by scrapping process. The scrapped PPTMA was then made fine powder using agate mortar and pastle. The C, H and N contents of PPTMA films were determined by an elemental analyzer EA 1180 of Carlo Erba Instruments, TYCHN, Milan, Italy. The analyzed has the following specification:

Measuring range 100 ppm; accuracy<0.3% absolute; repeatability<0.20%; sample required 0.1 to 100 mg.; analysis time CHNS<12 min.; CHN<7 min.

4.2.2   Results and discussion

The percentages (wt) of carbon, hydrogen and nitrogen in PPTMA detected by elemental analysis are presented in Table 4.1.

Table 4.1 The percentages (wt) of C, H, N and O in PPTMA thin films .

Sample	Elements detected(weight %)				Formula	Empirical formula
	C	H	N	O		
TMA(monomer)					$C_{10}H_{15}N$	
PPTMA	62.10	6.88	7.47	23.55		$C_{7.70}H_{10.30}N_{1.50}O_{0.80}$

It is seen that the amount of C and H in PPTMA are decreased and N is increased relative to the amount of constituent elements in the monomer TMA. The percentage of oxygen content was calculated on subtraction from the results of other element [4].

The incorporation of oxygen and nitrogen in PPTMA may be due to the:

i)   post-deposition reaction of the PPTMA after exposure to air owing to reactions with radical species and dangling bonds in the structure and /or,

ii)   from the glow discharge chamber during polymerization.

The deficiency of carbon and hydrogen contents in PPTMA may be due to the breakdown of bonds owing to the complex reaction during plasma polymerization.

4.3 Infrared Spectroscopy

Infrared spectroscopic analysis is an important and familiar technique for obtaining structural information and identification of functional groups in organic compounds. Infrared spectroscopy deals with the interaction of infrared light with matter. When a beam of electromagnetic radiation of intensity is passed through a substance, it can either be absorbed or transmitted, depending upon its frequency, and the structure of the molecules. If a transition exists which is related to the frequency of the incident radiation by Planck's law, then the radiation can be absorbed. The type of absorption spectroscopy depends upon the type of transition involved and accordingly the frequency range of the electromagnetic radiation absorbed. If the transition is from one

vibrational energy level to another, then the radiation is from the infrared portion of the electromagnetic spectrum and the technique is known as infrared spectroscopy [5,6].

The portion of the infrared region most useful for analysis of organic compounds is not immediately adjacent to the visible spectrum, but is that having a wavelength range from 2,500 to 16,000 nm, with a corresponding frequency range from 1.9×10^{13} to 1.2×10^{14} Hz.
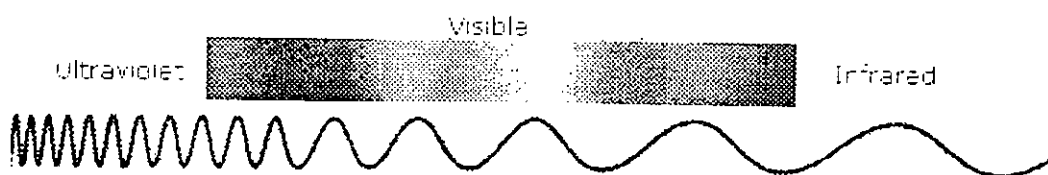
Fig. 4.2 Optical wave in Uv-vis and IR spectroscopy.

Photon energies associated with this part of the infrared radiation are not large enough to excite electrons, but may induce vibrational excitation of covalently bonded atoms and groups. Any structural change like addition substitution, of groups or atoms in a molecule affects the relative mode of vibration of the group.

Organic functional groups differ from one another both in the strength of the bonds, and in the masses of the atoms involved. Molecules are flexible, moving collections of atoms. The atoms in a molecule are constantly oscillating around average positions. Bond lengths and bond angles are continuously changing due to this vibration. A molecule absorbs infrared radiation when the vibration of the atoms in the molecule produces an oscillating electric field with the same frequency as the frequency of incident IR "light". All of the motions can be described in terms of two types of molecular vibrations. One type of the vibration, a stretch, produces a change of bond length. A stretch is a rhythmic movement along the line between the atoms so that the interatomic distance is either increasing or decreasing. The second type of vibration, a bend, results in a change in bond angle. These are also sometimes called scissoring, rocking, etc. motions. Each of these two main types of vibration can have variations. A stretch can be symmetric or asymmetric. Bending can occur in the plane of the molecule

or out of the plane; it can be scissoring, like blades of a pair of scissors, or rocking, where two atoms move in the same direction.

A molecule absorbs only those frequencies of IR light that match vibrations that cause a change in the dipole moment of the molecule. In a complicated molecule many fundamental vibrations are possible, but not all are observed. Some motions do not change the dipole moment for the molecule; some are so much alike that they coalesce into one band. Even though an IR spectrum is characteristic for an entire molecule, there are certain groups of atoms in a molecule that gives rise to absorption bands at or near the same wavenumber, v,(frequency) regardless of the rest of the structure of the molecule. These persistent characteristic bands enable to identify major structural features of the molecule.

Assignment for stretching frequencies can be approximated by the application of Hook's law. In the application of the law, two atoms and their connecting bond are treated as a simple harmonic oscillator composed of two masses joined by a spring. The following equation derived from Hook's law states the relationship between frequency of oscillation, atomic masses, and the force constant of the bond.

$$\nu = \frac{1}{2\pi c} \left(\frac{f}{\dfrac{M_x M_y}{M_x + M_y}} \right)^{1/2} \qquad 4.1$$

where ν is vibrational frequency (cm^{-1}), c is velocity of light (cm /sec), f is force constant of bond (dynes/cm) and M_x and M_y are mass(gm) of atoms x and y respectively. The values of f are approximately 5×10^5 dynes per cm for single bonds and approximately 2 and 3 times this value for double bonds and triple bonds, respectively.

An infrared spectrum shows the frequencies of IR radiation absorbed and the % of the incident light that passes through the molecule without being absorbed. For organic molecules, the IR spectrum can be divided into three regions. Absorptions between 4000 and 1300 cm^{-1} are primarily due to specific functional groups and bond types. Those between 1300 and 909cm^{-1}, the fingerprint region, are primarily due to more

complex interactions in the molecules; and those between 909 and 650 cm^{-1} are usually associated with the presence of benzene rings in the molecule.

There are no rigid rules for interpreting an IR spectrum. Certain requirements, however, must be meet before an attempt is made to interpret a spectrum.

i.)   The spectrum must be adequately resolved and of adequate intensity.

iii)   The spectrum should be that of a reasonable pure compound.

iv)   The spectrophotometer should be calibrated so that the bands are observed at their proper frequencies or wavelengths. Proper calibration can be made with reliable standards, such as polystyrene film.

v)   The methods of sample handling must be specified. If a solvent is employed, the solvent, concentration, and the cell thickness should be indicated.

4.3.1   Experimental procedure

IR spectra of the monomer liquid and plasma polymerized thin films were recorded at room temperature using a double-beam IR spectrometer Shimadzu-IR 470 (Shimadzu Corporation, Tokyo, Japan). A drop of each of the respective liquid monomer was placed between two thin KBr pellets to record the IR spectrum of the monomers. Plasma polymerized films of different precursors prepared on glass substrates were used for the IR analysis. Specimens were scraped off from the substrates and a little amount of sample was taken to prepare pellets after mixing with potassium bromide(KBr). The strength of an IR absorption spectrum is dependant on the number of molecules in the beam. With a KBr disk the strength will be dependant on the amount and homogeneity of the sample dispersed in the KBr powder. The spectrometer has its repeatability of the transmittance, 0.5%, except the wavenumber range, where the absorption bands of the water vapor exist. Its wavenumber range is 4000-400 cm^{-1}.

4.3.2   Results and Discussion

Fig.4.3 shows the IR spectra of the monomer N,N,3,5 Tetramethylaniline(TMA) and PPTMA which are represented by M and N respectively.

The asymmetric N-H stretching band at 3475 cm^{-1}(A) and the symmetric N-H stretching band at 3340 cm^{-1} (B) are observed in the spectrum M of the monomer N,N,3,5 tetramethylaniline. Relatively strong bands at 2935 (C) and 2793 cm^{-1} (D) correspond to the C-H stretching vibrations. The wide band at 1680-1645 cm^{-1} (E) and the absorption peaks at 1484 and 1595 cm^{-1}(F) may be attributable to C=C in aromatic ring stretching vibration of the benzenoid and quinoid rings respectively. Bands at 1351(G) and 1307 cm^{-1} (H) are observed due to conjugation of the electron pair of the nitrogen atom with the ring imparting double-bond character to the CN bond and a lower frequency band at 1223-1030 cm^{-1} (I) may be due to aliphatic CN stretching. The band character of tetra substituted benzene is present between 814-776 cm^{-1} (J) in the spectrum[7-9].

Table 4.2. Assignments of IR absorption peaks for TMA and PPTMA

Vibrations	Wave number (cm^{-1})	
	Monomer	PPTMA
Assy N-H stretching vibration (A)	3475	3435
Sym N-H stretching vibration. (B)	3340	
C-H. stretching vibration (C, D)	2935, 2793	2935
C=C stretching vibration (E)	1680-1645	1650-1603
C=C stretching vib. in benzenoid and quinoid (F)	1595, 1484	1570, 1472
C-N stretching vibration.(G, H)	1351, 1307	1340
C-N stretching vibration (I)	1223-1030	
Tetra substituted Benzene (J)	814-776	

In the IR spectrum of PPTMA represented by N in Fig 4.3, the absorption bands at around 3435, 2935, 1850-1603, 1570, 1472 and 1340 cm^{-1} in the wide absorption envelope corresponds to the regions A, C, E, F and G of the monomer spectrum, resulting from the presence of N-H stretching vibration, C-H stretching vibration, an aromatic ring C=C stretching vibration in benzenoid and quinoid rings and CN stretching vibration respectively. The wide band around 1850-1603 cm^{-1} may also include the contribution due to C=O stretching vibration which is typical for plasma polymers. The formation of carbonyl group is usually attributed to the oxidation of the

hydrocarbon part of the PPTMA after exposure to air owing to oxygen reactions with a radical species (dangling bonds) trapped in the structure of the plasma polymer. Cross-linking may also occur between different carbons of the chains due to the loss of hydrogen, particularly in the plasma-polymerized films because of the impact of energetic particles within the plasma during deposition. Here the PPTMA shows a widening of the band corresponding to the C=C stretching vibration of benzenoid and quinoid and slight down-shifting of CN stretching vibrations, probably caused by cross-linking interactions intrinsically associated with plasma polymers.

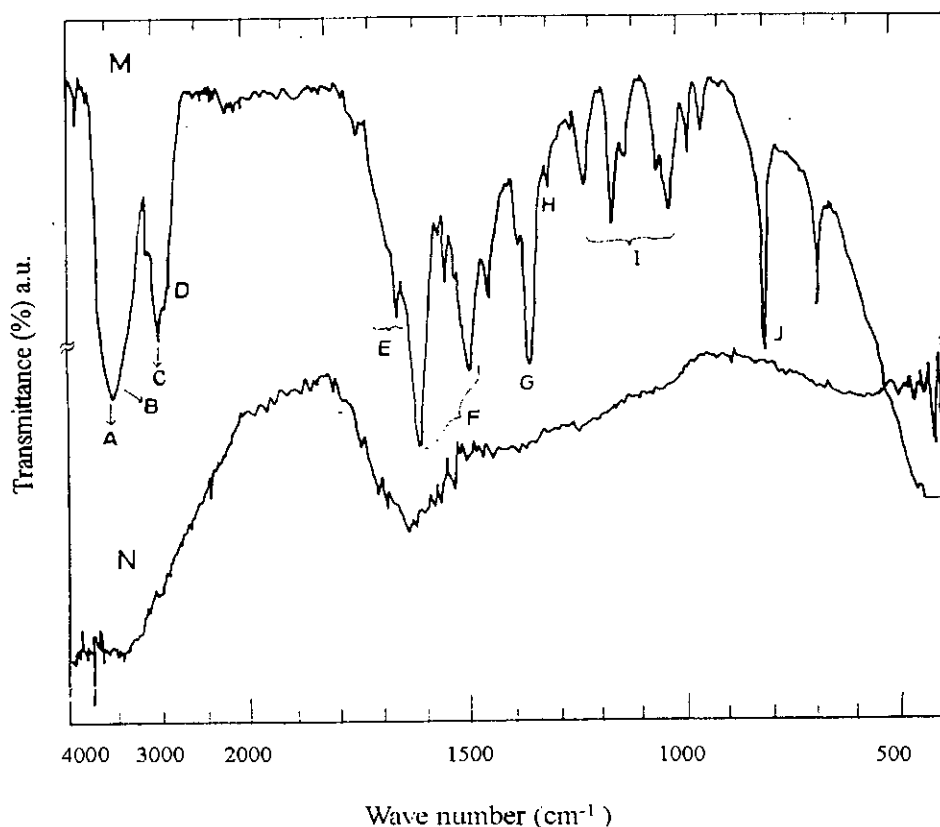Fig.4.3   The IR spectra of monomer N,N,3,5 tetramethylaniline(TMA), spectrum M; and PPTMA, spectrum N.

The IR observations reveal that the PPTMA contain an aromatic ring structure with NC and CH side groups. From the above discussion it is understood that the PPTMA film deposited by the plasma polymerization technique does not exactly resemble to that of the monomer N,N,3,5 tetramethylaniline structure.

4.4 Differential Thermal Analysis (DTA)and
Thermogravimetric Analysis (TGA)

The thermal properties of plasma polymerized thin films are important from the technological point of view. The term thermal analysis is frequently used to describe analytical experimental techniques, which was used to investigate the behavior of a sample as a function of temperature [10-13].

Differential Thermal Analysis (DTA)

Differential thermal analysis (DTA) is a process of accurately measuring the amount heat that are taken up from or emitted to the surroundings per unit time during heating or cooling or during isothermal measurements. DTA is an important tool to study the structural and phase changes occurring both in solid and in liquid materials during heat treatment. These changes may be due to dehydration, transition from one crystalline form to another, destruction of crystalline structure, oxidation, decomposition etc.
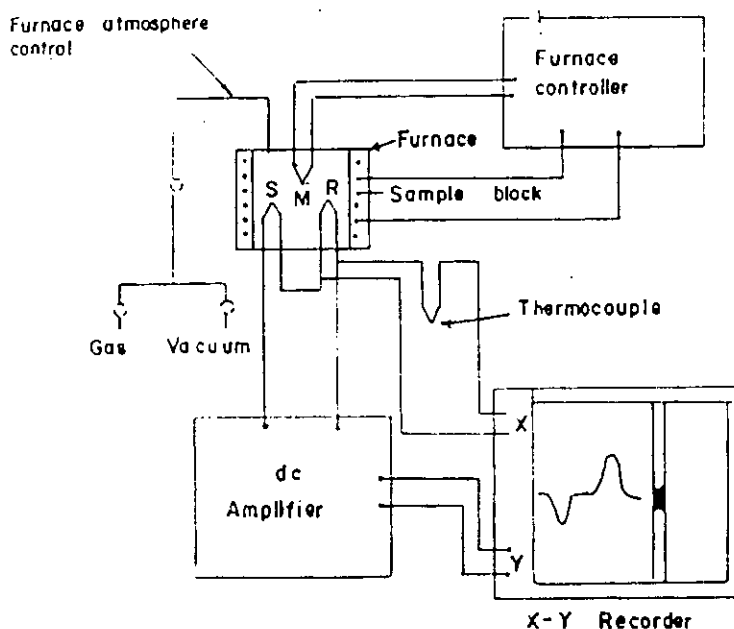

Fig.4.4 A schematic diagram showing different parts of a DTA apparatus.

The principle of DTA consists of measuring heat changes associated with the physical or chemical changes occurring when any substance is gradually heated. The

The principle of DTA consists of measuring heat changes associated with the physical or chemical changes occurring when any substance is gradually heated. The thermocouple(platinum-platinum rhodium 13%) for DTA measurement is incorporated at the end of each of the balance beam ceramic tubes, and the temperature difference between the holder on the sample side and the holder on the reference side is detected. This signal is amplified and becomes the temperature difference signal used to measure the thermal change of the sample.

Thermogravimetric Analysis (TGA)

The TGA is a branch of thermal analysis, which examines the mass change of a sample as a function of temperature in the scanning mode or as a function of time in the isothermal mode. under a variety of conditions, and to examine the kinetics of the physico-chemical processes occurring in the sample. Sample weight changes are measured as described below in Fig.4.5.

Figure shows the sample balance beam and reference balance beam are independently supported by a driving coil/pivot. When a weight change occurs at the beam end, the movement is conveyed to the opposite end of the beam via the driving coil/pivot, when optical position sensors detect changes in the position of a slit. The signal from the optical position sensor is sent to the balance circuit.
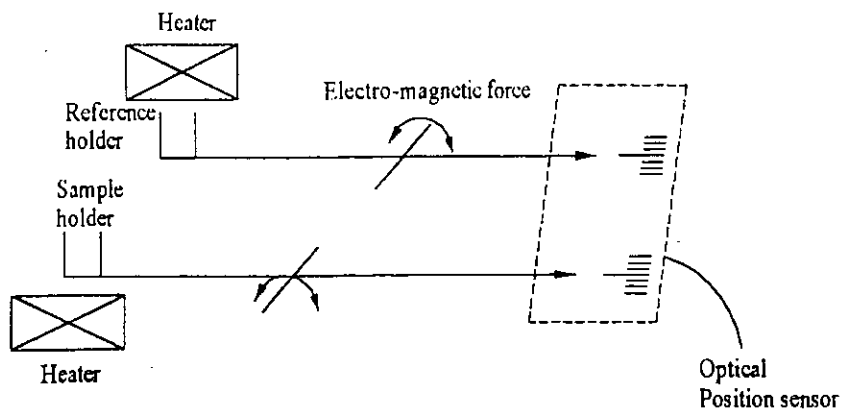

Fig.4.5 TGA measurement Principle.

The TGA is used to characterize the decomposition and thermal stability of materials. The balance circuit supplies sufficient feedback current to the driving coil so that the slit returns to the balance position. The current running to the driving coils on the sample side and the current running to the driving coil on the reference side is detected and converted into weight signals.

4.4.1 Experimental procedure

The PPTMA films were scrapped off from the substrate to use as the sample for the DTA/TGA investigations. The DTA/TGA scans of PPTMA thin films were taken using a computer controlled TG/DTA 6300 system connected to an EXSTAR 6000 station, Seiko Instruments Inc., Japan. The TG/DTA module uses a horizontal system balance mechanism.

The specifications of the instrument are: sample weight ≤ 200mg, Temperature range; room temperature to 1573 K, Heating rate; 0.01°K/min. to 100.00 °K/min., TGA Measuring Range; ± 200 mg(0.2 μg), DTA Measuring Range; ± 1000 μV(0.06 μV), Gas flow; ≤ 1000m/min.

4.4.2 Results and discussion

The DTA and TGA traces taken at 10 K/min for PPTMA are shown in Fig. 4.6. The DTA thermogram shows an exotherm, which reaches a maximum at around 571K. The corresponding TGA trace of PPTMA has been taken from 303 to 1023K and showed different stages of thermal decomposition, which divided in three regions (A, B, and C). Every region may be associated with a different rate of weight loss. The weight losses in A, B, and C regions are about 3 %, 3%, and 28% respectively. In the first region A, the weight loss may be due to the removal of water content, which is not necessarily associated with any change in the structure. The 3% of weight loss in the region B may be attributed to the loss of non-constitutional or adsorbed water and unreacted monomer settled on PPTMA films surface and/ or due to evolution of hydrogen and low molecular mass hydrocarbons gases. The maximum change in the PPTMA structure has been occurred in the region C. The weight loss of 28% in this region is important because the DTA curve exhibits a wide peak. In region C the weight

loss may be caused by the thermal breakdown of the PPTMA structure and expulsion of higher molecular mass hydrocarbons, oxygen containing compounds, etc. Thus, it may be attributed that PPTMA films are thermally stable up to about 505 K.
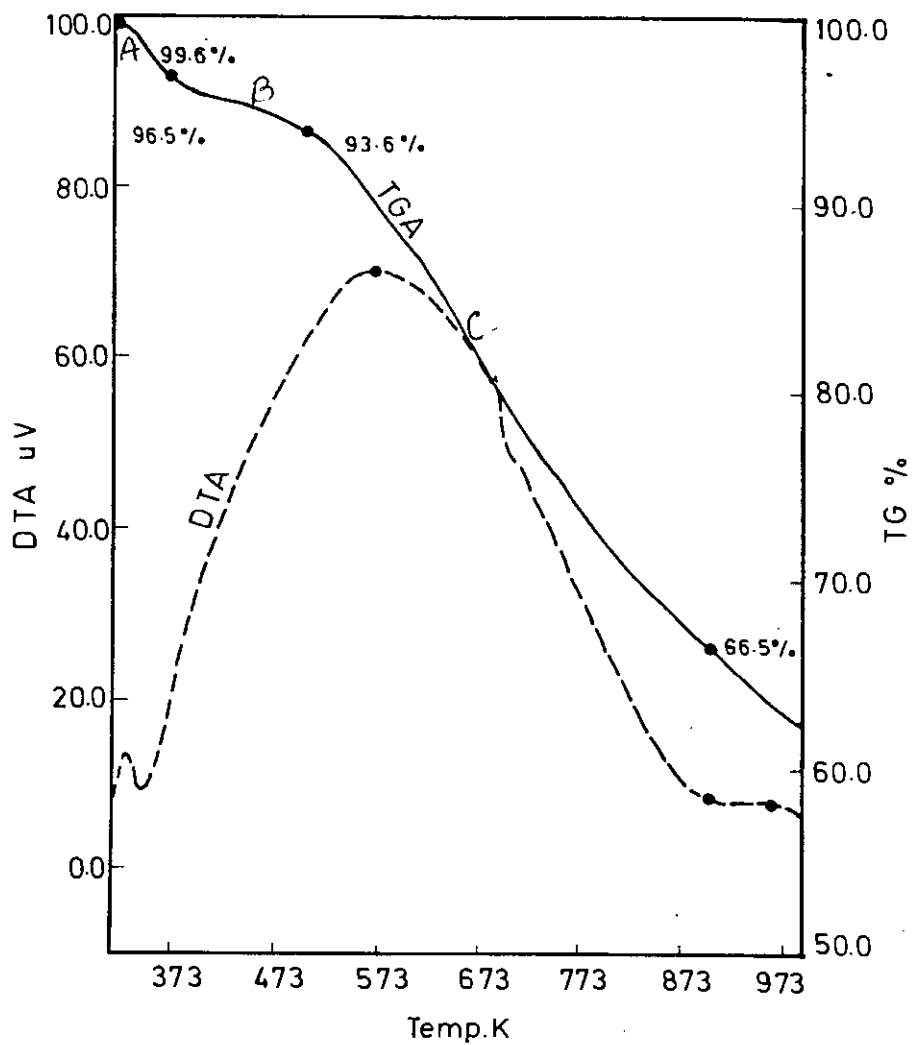

Fig.4.6 The DTA/TGA traces of PPTMA thin films.

4.5 UV-Visible Optical Absorption Spectroscopic Analysis

Ultraviolet/visible spectroscopy is useful as an analytical technique for two reasons. First it can be used to identify some functional groups in molecules and secondly, it can be used for assaying. This second role - determining the content and strength of a substance is extremely useful. The optical energy gaps and the allowed direct transitions and allowed indirect transitions and forbidden transitions of optically active substances can be determined from the Uv-visible spectroscopic studies for the potential applications such as light guide material, optical fibers, optical coating to inhibit corrosion, etc. [14-16]. The most important application of Uv-vis spectroscopy is to determine the presence, nature and extent of conjugation present in the material. Increasing conjugation length generally moves the absorption spectrum to longer wavelengths and finally into the visible region.

When light either visible or ultraviolet is absorbed by valence electrons these electrons are promoted from their ground states to higher energy states. The energies of the orbital involved in electronic transitions have fixed values. Because energy is quantised, it seems safe to assume that absorption peaks in an Uv-vis spectrum will be sharp peaks. This is because there are also vibrational and rotational energy levels available to absorbing materials, shown in Fig.4.7. These vibrations and rotations also have discrete energy levels, which can be considered as being packed on top of each electronic level. The absorption of Uv or visible radiation corresponds to the excitation of outer electrons. There are three types of electronic transition, which can be considered;

    i)   Transitions involving π, σ, and n electrons

    ii)   Transitions involving charge-transfer electrons

    iii)   Transitions involving d and f electrons

Absorption of Uv-visible radiation in organic molecules is restricted to certain functional groups(chromophores) that contain valence electrons of low excitation energy. The spectrum of a molecule containing these chromophores is complex. This is because the superposition of rotational and vibrational transitions on the electronic transitions gives a combination of overlapping lines. This appears as a continuous absorption band.
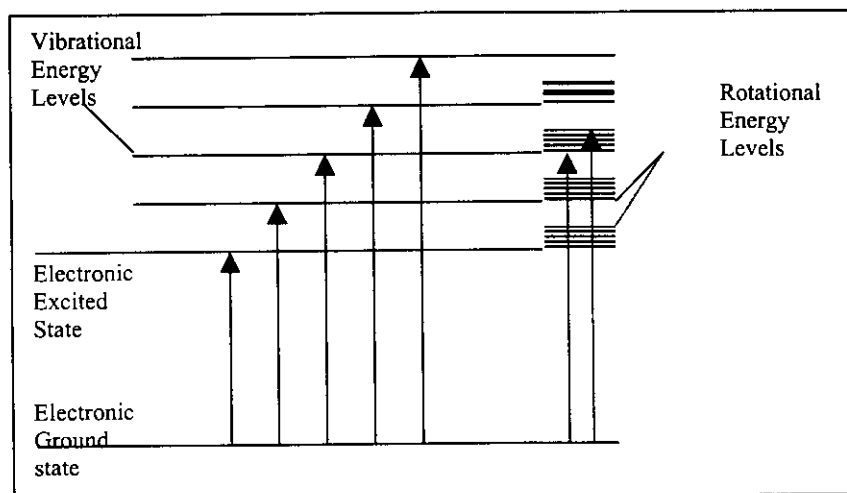
Fig.4.7 Vibrational and rotational Energy levels of absorbing materials.
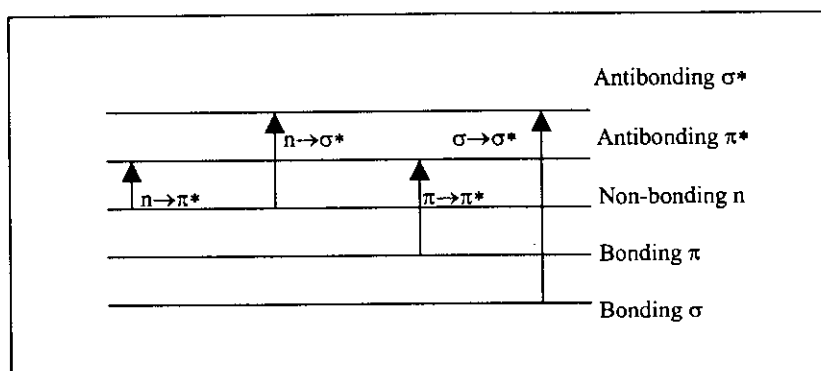
Fig.4.8 Summery of electronic energy levels.

Possible electronic transitions of π, σ, and n electrons are

$\sigma \rightarrow \sigma^*$ Transitions

An electron in a bonding σ orbital is excited to the corresponding antibonding orbital. The energy required is large. Absorption maxima due to $\sigma \rightarrow \sigma^*$ transitions are not seen in typical Uv-vis spectra (200-800 nm).

$n \rightarrow \sigma^*$ Transitions

This transition needs less energy than $\sigma \rightarrow \sigma^*$ transitions. They can be initiated by light whose wavelength is in the range 150-250 nm. The number of organic functional groups with $n \rightarrow \sigma^*$ peaks in the UV region is small.

$n \rightarrow \pi^*$ and $\pi \rightarrow \pi^*$ Transitions

Most absorption spectroscopy of organic compounds is based on transitions of n or π electrons to the π^* excited state. This is because the absorption peaks for these transitions fall in an experimentally convenient region of the spectrum (200-800 nm). These transitions need an unsaturated group in the molecule to provide the π electrons. Molar absorbtivities from $n \rightarrow \pi^*$ are relatively low, and range from 10 to 100 L mol^{-1} cm^{-1}. $\pi \rightarrow \pi^*$ transitions normally give molar absorbtivities between 1000 and 10,000 L mol^{-1} cm^{-1}.

The solvent in which the absorbing species is dissolved also has an effect on the spectrum of the species. Peaks resulting from $n \rightarrow \pi^*$ transitions are shifted to shorter wavelength (**blue shift**) with increasing solvent polarity. The reverse (**red shift**) is seen for $\pi \rightarrow \pi^*$ transitions. This effect is greater for the excited state, and so the energy difference between the excited and unexcited states is slightly reduced resulting in a small red shift. This effect also influences transitions but is overshadowed by the blue shift resulting from salvation of lone pairs.

Many inorganic species show charge-transfer absorption and are called charge-transfer complexes. For a complex to demonstrate charge-transfer behavior one of its components must have electron-donating properties and another component must be able to accept electrons. Molar absorbtivities from charge transfer absorption are large(greater that 10,000 L mol^{-1} cm^{-1}).

4.5.1 Beer-Lambert Law

For most spectra the solution obeys Beer's Law. This states that the light absorbed is proportional to the number of absorbing molecules. This is only true for dilute solutions.

A second law- Lambert's law tells us that the fraction of radiation absorbed is independent of the intensity of the radiation. Combing these two laws gives the Beer-Lambert law:

$$I = I_o e^{-\alpha d} \qquad\qquad 4.2$$

$$\log_e\left(\frac{I_o}{I}\right) = \alpha d \qquad\qquad 4.3$$

where is I_o the intensity of the incident radiation, I is the intensity of the transmitted radiation, d is the path length of the absorbing species and α is the absorption co-efficient. The absorption spectrum can be analyzed by Beer-Lambert law which governs the absorption of light by the molecules and states that, "When a beam of monochromatic radiation passes through a homogeneous absorbing medium the rate of decrease in intensity of electromagnetic radiation in Uv-vis region with thickness of the absorbing medium is proportional to the intensity of incident radiation".

The intensity of transmittance is expressed as the inverse of intensity of absorbance. The absorption co-efficient α, can be calculated from the absorption data using the relation(4.3)

$$\alpha = \frac{2.303A}{d} \qquad\qquad 4.4$$

where $A = \log_{10}\left(\frac{I_o}{I}\right)$ is the Absorbance.

To estimate the form of absorption a random phase model is used where the momentum selection rule is completely relaxed. The integrated density of states $N(E)$ has been used and defined by

$$N(E) = \int_{-\infty}^{+\infty} g(E)dE \qquad\qquad 4.5$$

The density of states per unit energy interval may be represented by $g(E) = \frac{1}{V}\sum \delta(E - E_n)$, where V is the volume, E is energy at which $g(E)$ is to be evaluated and E_n is the energy of the nth state.

If $g_v \propto E^p$ and $g_c(E) \propto (E - E_{opt})^q$, where energies are measured from the valance band mobility edge in the conduction band (mobility gap), and substituting these vales into an expression for the random phase approximation, the relationship obtained $v^2 I_2(v) \propto (hv-E_o)^{p+q+1}$, where $I_2(v)$ is the imaginary part of the complex permittivity. If the density of states of both band edges is parabolic, then the photon energy dependence of the

absorption becomes $\alpha \nu \infty \nu^2 I_2(\nu) \infty (h\nu - E_{opt})^2$. So for higher photon energies the simplified general equation is

$$\alpha h\nu = B(h\nu - E_{opt})^n \qquad \qquad 4.6$$

where $h\nu$ is the energy of absorbed light, n is the parameter connected with distribution of the density of states and B is the proportionality factor. The index n equals ½ and 2 for allowed direct transition and indirect transition energy gaps respectively [17]. Thus, from the straight-line plots of $(\alpha h\nu)^2$ versus $h\nu$ and $(\alpha h\nu)^{1/2}$ versus $h\nu$ the direct and indirect energy gaps respecting of insulators and /or dielectrics can be determined.

4.5.2   Experimental procedure

UV-Vis spectrum of the TMA monomer liquids was obtained in absorption mode with a spectrophotometer Shimadzu UV-160A (Shimadzu Corporation, Tokyo, Japan) and those of the PPTMA thin films on glass substrates were recorded with a Shimadzu UV-1201V spectrophotometer (Shimadzu Corporation, Tokyo, Japan) in the wavelength range 200 to 800 nm and 325 to 800 nm respectively at room temperature. The reflectance at an incident angle of 5° was also recorded using the later one.

4.5.3   Results and discussion

Different molecules absorb radiation of different wavelengths. The absorption spectrum shows a number of absorption bands corresponding to structural groups within the molecule. The Uv-vs absorption spectra for TMA and PPTMA have been recorded at room temperature. These Uv-vis spectra for different thickness are presented in Fig.4.9. In the spectra, it is observed that the absorption increases with increasing thickness. The reflectance versus wavelength curve in Fig.4.10 shows that the reflectance is weakly dependent on wavelength and the reflectance is about 10%. Fig. 4.11 represents the absorption spectrum of PPTMA thin film of 500 nm thickness for further analysis. It is seen that there is a sharp rise of the absorption in the low wavelength side and then rapidly decreases up to about 500 nm with a peak at around 380 nm; above 500 nm absorption decreases slowly.
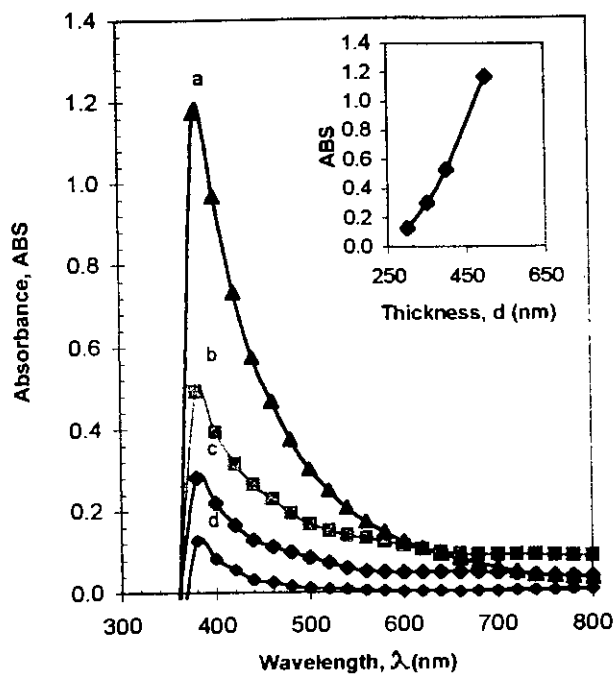
Fig. 4.9 Variation of absorbance (ABS) with wavelength, λ, for various PPTMA thin films; 500 nm, spectrum a; 400 nm, spectrum b; 350 nm, spectrum c; 300 nm, spectrum d (Inset: ABS vs d plot).
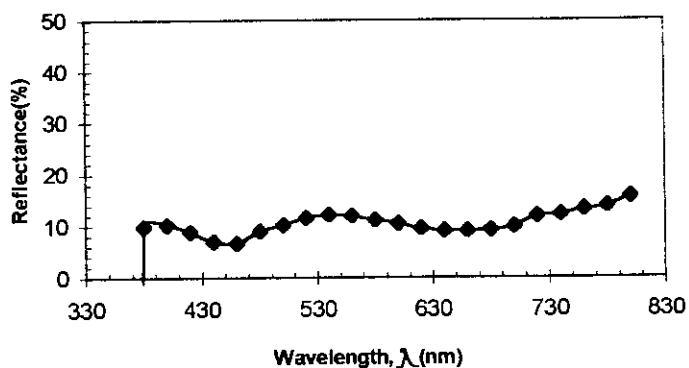

Fig. 4.10 Variation of reflectance with wavelength, λ, for PPTMA thin films.
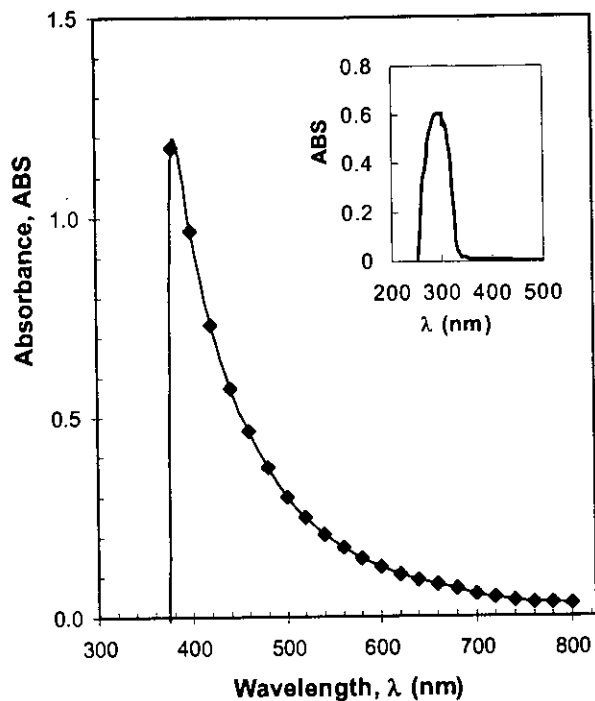
Fig.4.11 Variation of absorbance (ABS) with wavelength, λ, for PPTMA thin films(inset : monomer).
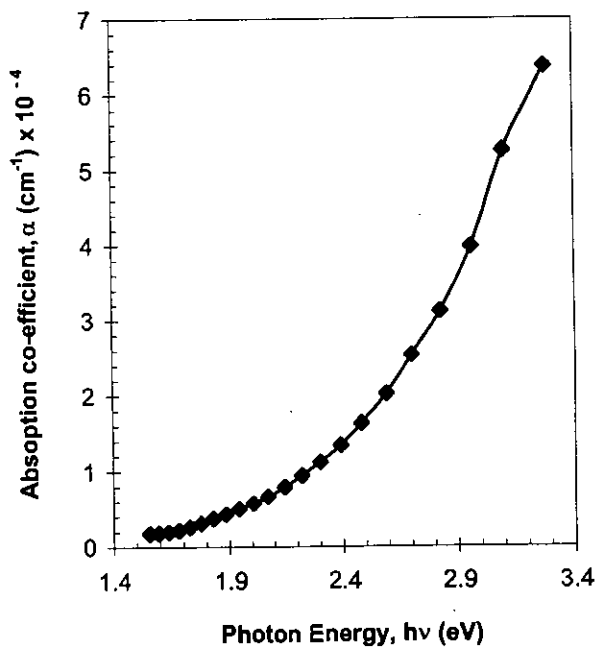

Fig.4.12 Plot of absorption co-efficient, α, as a function of photon energy, hν, for PPTMA thin films.

It is observed in the Uv-vis spectrum of PPTMA that the peak value shifts to higher wavelength compared to the peak wavelength (λ_{max}) value, 300 nm (inset of Fig.4.11) of the liquid monomer. Thus, there is a red shift of about 79 nm in λ_{max} as compared to the absorption wavelength peak of the liquid monomer. It is well known that increasing conjugation generally moves the absorption to longer wavelength [18]. This red shift in PPTMA may demonstrate presence of an increased degree of conjugation in the resulting films.

The absorption co-efficient α was calculated from the absorbance data of Fig.4.11 using the eqn. 4.4. The spectral dependence of α as a function of photon energy, hν, for the sample is shown in Fig.4.12. It is observed that in the low energy region the edges follow linear fall for values of α below about 10,000 cm^{-1}. This linear falling edge may either be due to lack of long-range order or due to the presence of defects in the thin films.

One of the most significant optical parameters, which are related to the electronic structure, is the optical band gap. Two different slopes could characterize the curve in Fig.4.12. This may indicate the presence of direct and indirect transitions in the materials. The allowed direct transition energy gap can be evaluated from the plot of $(\alpha h\nu)^2$ as a function of hν shown in Fig.4.13. The allowed direct transition energy gap was determined from the intercept of the extrapolation of the curve to zero α in the photon energy axis. In Fig.4.14, $(\alpha h\nu)^{1/2}$ as a function of hν is plotted to obtain the allowed indirect transition energy gap. The intercept of the extrapolated curve to zero α in the photon energy axis was taken as the indirect transition energy gap. The values of allowed direct transition energy gap, E_{qd}, is 2.80 eV and that of allowed indirect transition energy gap, E_{qi}, is 1.44 eV.

Physical processes that control the behavior of gap states in non-crystalline materials are structural disorder responsible for the tail states and structural defects in deep states [19]. The Tauc parameter, B, is a measure of the steepness of band tail (Urbach region)
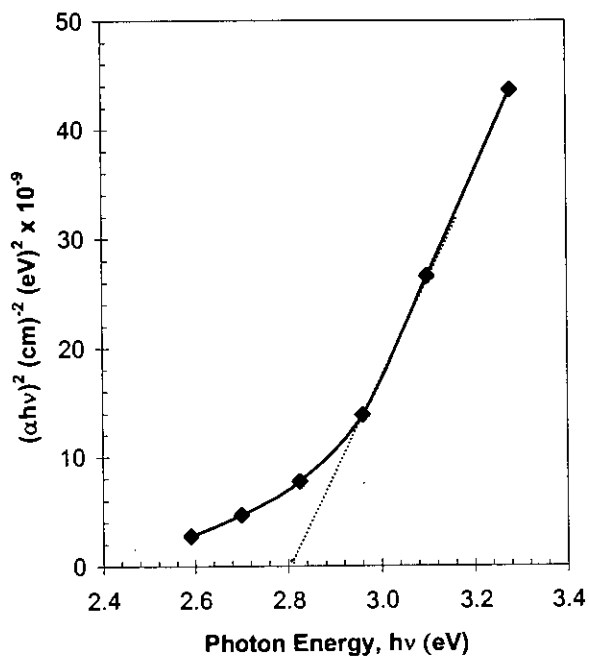
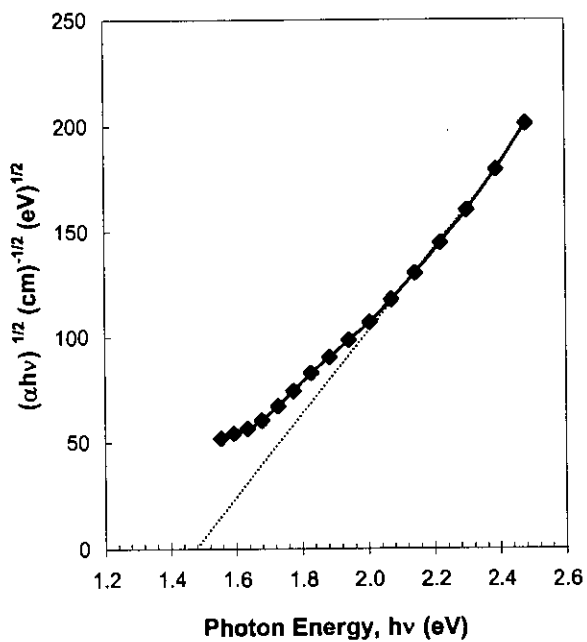Fig 4.13 $(\alpha h\nu)^2$ versus hν curve for PPTMA thin film.

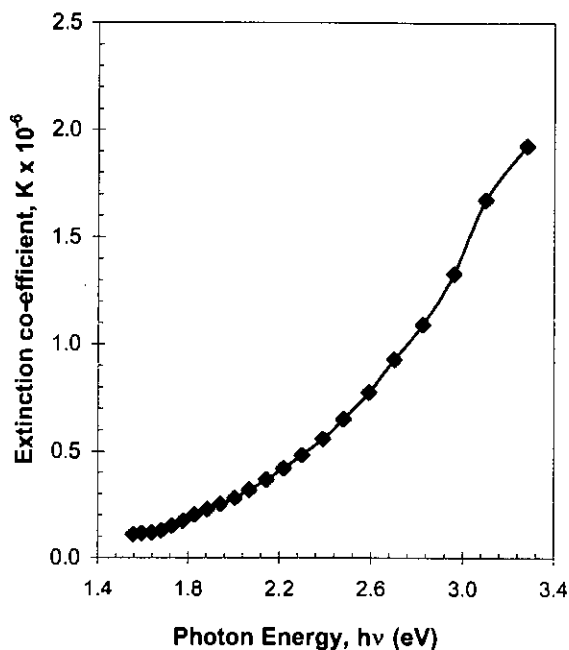Fig.4.14 $(\alpha h\nu)^{1/2}$ versus hν curve for PPTMA thin film.

Fig.4.15 Plot of extinction co-efficient, K, as a function of hv for PPTMA thin
films.

density of states. Higher value of B in thin film is due to less structural disorder. The B
values for camphoric carbon and graphitic carbon films have been reported to be 320
and 250 cm$^{-1/2}$ (eV)$^{-1/2}$ respectively[20]. The value of B obtained from Fig. 4.14 for
PPTMA is almost 188 cm$^{-1/2}$ (eV)$^{-1/2}$.

The extinction co-efficient, K, was computed from α using the relation $\alpha = \dfrac{4\pi K}{\lambda}$ where

λ is the wavelength. The variation of the K for PPTMA thin films with hv is shown in
Fig.4.15. It is seen from the plot that the increase of K with the increase in photon
energy indicating that the probability of electron transfer across the mobility gap rises
with the photon energy.

Thus, it can be attributed from the EA, IR, DTA/TGA and Uv-vis spectroscopic
observations that the chemical structure of PPTMA is little different than that of TMA.
It contains a little amount of non monomeric oxygen. It is stable upto 505K. PPTMA
may have short-range order structure with an aromatic ring structure.

References

1. N. Morosoff, "An introduction to plasma polymerization", in "Plasma deposition, treatment, and etching of polymers", R. d'Agostino Ed, Academic Press, San Diego, CA (1990).

2. N. Morosoff, "Surface modification by plasma polymerization", in "Innovations in materials processing", Plenum, New York (1985).

3. J. Tauc, in "Optical Properties of Solids", F. Abeles Ed., North-Holland, Amsterdam (1972) chap.5.

4. H. Yasuda, "Glow discharge polymerization in thin film processes", Academic, New York (1978).

5. R.M. Silverstein, G.C. Bassler, T.C. Morrill, "Spectrometric identification of organic compounds", John Willey & Sons, New York (1981).

6. K. Nakamura, M. Watanabe, M. Zhou, M. Fujishima, M. Tsuchiya, T. Handa, S. Ishii, H. Noguchi, K. Kashiwagi and Y. Yoshida, "Plasma polymerization of cobalt tetraphenylporphyrin and the functionalities of the thin films produced", Thin Solid Films, 345 (1999) 99-103.

7. R.K. John, D.S. Kumar, "Structural, electrical, and optical studies of plasma polymerized and Iodine-doped poly pyrrole" J. Appl. Polym Sci, 83 (2002) 1858-1859.

8. F.-U.-Z Chowdhury and A.H. Bhuiyan,"An investigation of the optical properties of plasma-polymerized diphenyl thin films", Thin Solid Films, 306(1-2) (2000) 69-74.

9. X. Gong, L. Dai, A.W.H. Mau, and H. J. Griesser, " Plasma-polymerized polyaniline films: synthesis and characterization", J. Polym. Sci.: PartA: Polym. Chem., 36 (1998) 633-643.

10. C.J. Keattch, D. Dollimore, " An Introduction to Thermogravimetry", Heyden & Son Ltd, New York (1969).

11. T. Hatakeyama and F.X. Quinn, "Fundamentals and applications to polymer science", John Wiley & Sons Ltd, London (1997).

12. L. Katsikas, K. Jeremic, S. Jovanovic, J. S. Velickovic and I.G. Popovic, "The thermal degradation kinetics of dextran and pullulan", J. Therm. Anal., 40 (1993) 511-517.

13. M. S. Erogla, M.M. Akilli and O. Guven, "Spectroscpic, Thermal and mechanical characterization of carboxyl terminated polybutadieno- based carbon black filled networks", J. Appl. Polym. Sci., 66(2) (1997) 355-366.

14. Y. C. Quan, S. Yeo, C. Shim, J. Yang, and D. Jung, "Significant improvement of electrical and thermal properties of low dielectric constant plasma polymerized paraxylene thin films by postdeposition H_2+He plasma treatment", J. Appl. Phys, **89(2)** (2001) 1402-1404.

15. M.C. Kim, S.H. Cho, J.G. Han, B.Y. Hong, Y.J. Kim, S.H. Yang and J.H. Boo,"High-rate deposition of plasma polymerized thin films using PECVD method and characterization of their optical properties", Surface and Coatings Technology, **169-170** (2003) 595-599.

16. A.H. Bhuiyan and S.V. Bhoraskar, " Electrical, optical and ESR study of thin films of plasma-polymerized acrylonitrile", J. Mater. Sci., **24** (1989) 3091-3094.

17. A.B.M. Shah Jalal, S. Ahmed, A.H. Bhuiyan and M. Ibrahim, "UV-Vis absorption spectroscopic studies of plasma-polymerized m-xylene thin films", Thin Solid Films, **288** (1996) 108-111.

18. Xiaoyi Gong, Liming Dai, Albert W.H. Mau, and Hans J. Griesser, " Plasma-polymerized polyaniline films: Synthesis and Characterization", J. Polym. Sci.: PartA: Polym. Chem., **36** (1998) 633-643.

19. J. H. Lambert, David A. Lightner, Herbert F. Shurvell, and R. Graham Cooks, Introduction to organic spectroscopy, Macmillan Publishing Co., New York (1987).

20. S.M. Mominuzzaman, T. Soga, T. Jimbo, M. Umeno, "Camphoric soot: a new target for deposition of diamond-like carbon films by pulsed laser ablation", Thin Solid Films, **376** (2000) 1-4.

CHAPTER 5

DC ELECTRICAL PROPERTIES
OF PPTMA

5.1 Introduction

This chapter begins with a brief account of the existing theories on dc electrical conduction mechanism which are followed by descriptions of the experimental techniques used in the measurements of current density-voltage (J-V) and thermally activated current in the successive sections.

Electrical measurements on many organic materials have been reported [1-3] and different type of mechanisms, such as space charge limited (SCL), Poole-Frenkel (PF) and Schottky mechanisms, have been found. An analysis of the observations indicates that the electrical conduction in PPTMA is mostly due to SCLC process.

5.2   DC electrical conduction mechanism

In the dc electrical conduction in plasma-polymerized materials, the carriers may either be electronic or ionic in nature and conduction is considered through the film, rather than along the plane of the film. The low field properties, which are usually ohmic in nature, but the high field electrical properties cannot describe by a single conduction process; usually the various field strength ranges manifest different electrical conduction phenomena. The materials, which have energy gaps more than 2 eV or above, the electrical properties may bear no resemblance to what is intrinsically expected of such an insulating material. So this is clear that the electrical properties of thin film insulators are determined not only by the intrinsic properties of the insulator but also by other properties, such as the nature of the electrical-insulator contact. The dc conduction mechanisms in different plasma-polymerized thin films reported are the following [4-11]:

    i)   Schottky mechanism: In this mechanism, the injection of carriers from electrode is performed by means of thermal or field-assisted emission.

    ii)   PF mechanism: If the carriers are produced by the dissociation of donor-acceptor centers in the bulk of the material, the process of conduction is then called PF mechanism.

    iii)   SCL conduction mechanism: In case of SCL conduction the transport by the carriers is slower than the generation and it constitutes a rate-determining step.

In general, if the carrier generation process is slower than transport of the carriers through a dielectric, the conduction is controlled either by Schottky or PF mechanism. At reasonable applied fields there will normally be a sufficient supply of carriers available to enter the insulator from the cathode(negatively biased electrode) to replenish the carriers drawn out of the bulk of the insulator. Under these conditions the J-V characteristics of the sample will be determined by the bulk properties of the insulator; this conduction process is thus referred to as bulk-limited. At high fields, or if the contact is blocking, the current capable of being supplied by the cathode to the insulator will be less than that capable of being carried in the bulk of the insulator. Under these conditions the J-V characteristics of the sample will be controlled primarily by conditions existing at the cathode-insulator interface; this conduction process is referred to as being emission-limited or contact-limited.

A power law can express the variation of current density with voltage in a material generally:

$$J \propto V^n \qquad\qquad 5.1$$

where, n is a power factor. When n is unity, the conduction is ohmic. If the value of n is more than unity, then the conduction process is other than ohmic. These are described in the following sections.

5.2.1 Schottky mechanism

The Schottky effect is the image force induced lowering potential energy for charge carrier emission when an electric field is applied. The image force effect plays an important role in the conduction process. The potential step at a neutral barrier in the presence of image force as a function of distance (x) from the metal-insulator interface is given by

$$\varphi(x) = \varphi_o + \varphi_{im}(x) = \varphi_o - \frac{e^2}{16\pi\varepsilon_o\varepsilon x} \qquad\qquad 5.2$$

where, $\varphi_{im}(x) = -\dfrac{e^2}{16\pi\varepsilon_o\varepsilon x}$ is the potential energy of electron due to image force. The

barrier $\varphi(x)$ in the presence of image forces is illustrated by the line AB in Fig. 5.1. Eqn.5.2 is not valid at the electrode surface, since $\varphi = -\infty$ there.
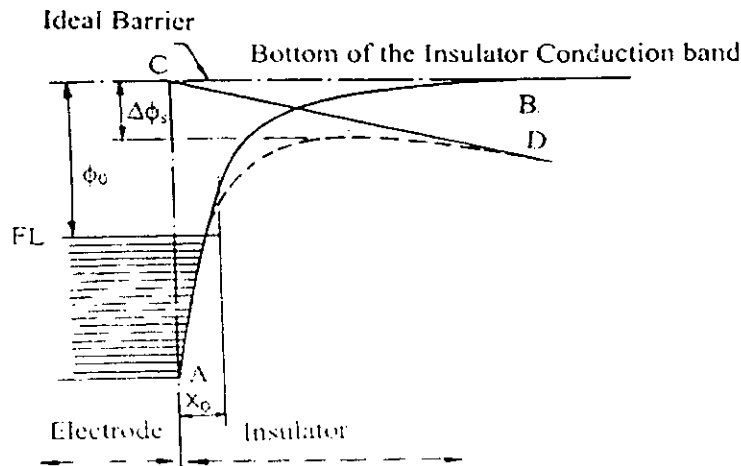
Fig. 5.1 Schottky effect at a neutral contact.

The potential energy with respect to the Fermi level of the electrode is now given by

$$\varphi(x) = \varphi_o - \frac{e^2}{16\pi\varepsilon_o\varepsilon x} - eFx \qquad 5.3$$

The change $\Delta\varphi_s = \varphi_o - \varphi(x)$ in the barrier height due to the interaction of the applied field with the image potential is given by

$$\Delta\varphi_s = -\left(\frac{e^3}{4\pi\varepsilon_o\varepsilon}\right)^{1/2} F^{1/2} = \beta_s F^{1/2} \qquad 5.4$$

where $\beta_s = \left(\dfrac{e^3}{4\pi\varepsilon_o\varepsilon}\right)^{1/2}$ 5.5

is Schottky coefficient. Because of the image force lowering of the barrier, the electrode-limited current obeys the Richardson-Schottky law

$$J = AT^2 \exp[-(\varphi_o - \Delta\varphi_s)/kT] \qquad 5.6$$

This equation was first applied successfully to metal-vacuum interfaces.

5.2.2 Poole-Frenkel (PF) mechanism

The PF effect is the bulk analog of the Schottky effect at an interfacial barrier. This effect is also known as field-assisted thermal ionization process. As the potential energy

of an electron in a Coulombic field $-e^2/4\pi\varepsilon x$ is four times that due to the image force effects, the Poole-Frenkel attenuation of a Coulombic barrier $\Delta\varphi_{PF}$, uniform electric field is twice that due to the Schottky effect at a neutral barrier:

$$\Delta\varphi_{PF} = 2\Delta\varphi_s = 2\left(\frac{e^3}{4\pi\varepsilon_o\varepsilon}\right)^{1/2} F^{1/2} = \beta_{PF}F^{1/2} \qquad 5.7$$

With the applied field, the Coulombic barrier height between electrode and the film is lowered, and the carrier can escape more easily giving rise to field assisted conductivity:

$$\sigma = \sigma_o \exp\left[\frac{\beta_{PF}F^{1/2}}{2kT}\right] \qquad 5.8$$

where $F = V/d$, is the dc applied field, k is Boltzmann constant, T is the absolute temperature, σ_0 is the low field conductivity, β_{PF} is the Poole-Frenkel co-efficient and is given by

$$\beta_{PF} = 2\left[\frac{e^3}{4\pi\varepsilon_o\varepsilon}\right]^{1/2} = 2\beta_s \qquad 5.9$$
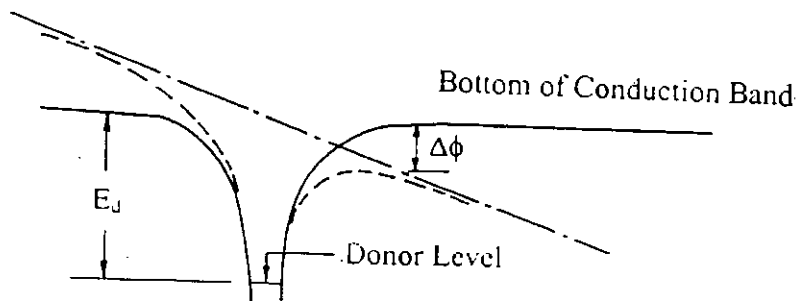

Fig.5.2 Poole-Frenkel effect at a donor center.

The general expression for J that is equally valid for both the PF and Schottky mechanisms is of the form

$$J = J_o \exp\left[\frac{\beta F^{1/2} - \varphi}{kT}\right] \qquad\qquad 5.10$$

where J_o is the low field current density; β is the coefficient: F is the static electric field and φ is the ionization energy of the localized centers in Poole-Frenkel conduction (it involves the emission of trapped electrons (holes) from localized centers or potential wells within the dielectric) and Coulomic barrier height of the electrode-polymer interface in Schottky conduction (it results from injection of electrons or holes from the electrodes into the conduction band of the dielectric. .

5.2.3 Space charge limited (SCL) conduction mechanism

The mechanism of electrical conduction in thin insulating films has been discussed by Lamb and several important theoretical modes have been put forwarded. Dielectric materials, which are basically insulators, are capable of carrying electric currents by virtue of carriers injected at one or both the electrodes. According to the basic assumptions, if an ohmic contact is made at the surface of an insulator, electrons flow from the metal to the conduction band of the insulator.
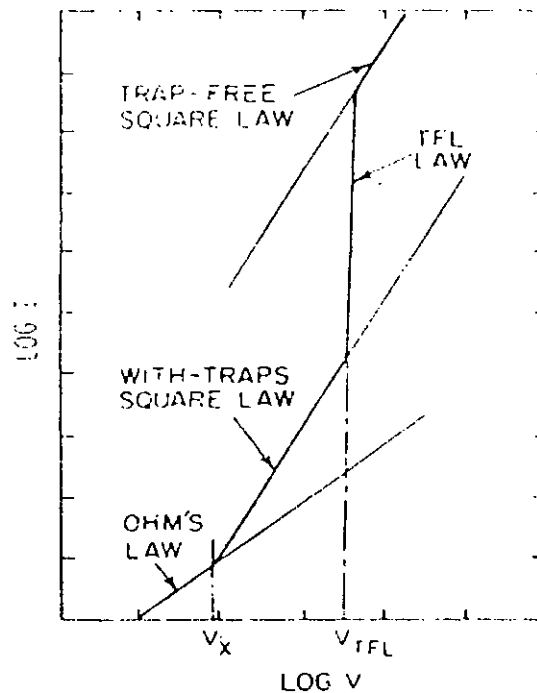

Fig. 5.3 Space charge limited conduction mechanism.

Due to the injected charges near the electrodes, there is a generation of space charge near the electrodes, which affect the conduction mechanism. As an effect, ohmic conduction changes into SCL conduction as the applied electric field is increased.

When a bias is applied to the system shown in Fig.5.3 that is, an insulator having two ohmic contacts on its surface. The result of the applied bias is to add positive charge to the anode and negative charge to the cathode. As the voltage bias increases, the net positive charge on the anode increases and that on the cathode decreases then the current density would be

$$J = \frac{9}{8}\varepsilon\varepsilon_o\mu\frac{V^2}{d^3}$$
<div align="right">5.11</div>

Where μ is the mobility of charge carriers, ε is dielectric constant, ε_o is the permittivity of free space, V is the applied voltage, d is the thickness eqn 5.11 predicts that SCL current is directly proportional to V^2 and inversely proportional to d^3.
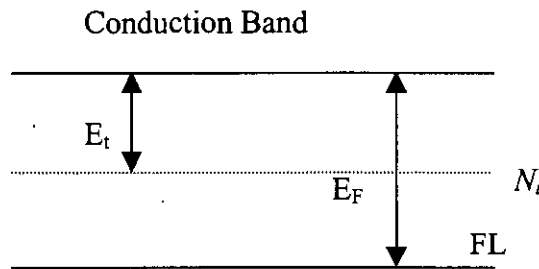

Fig 5.4. Energy diagram showing shallow traps in an insulator.

Practically, the character and the magnitude of SCL conduction are modified due to the presence of localized trapping centers which try to immobilize the injected charge carriers. If the insulator contains N_t shallow traps positioned an energy E_t below the conduction band and N_o is the number of charge carriers, shown in Fig. 5.4 then the free component of the space charge

$$p_f = eN_c \exp\left(\frac{-E_F}{kT}\right)$$
<div align="right">5.12</div>

and trapped component of the space charge

$$p_t = eN_t \exp\left[-\frac{(E_F - E_t)}{kT}\right]$$ 　　　　　5.13

thus the trapping factor, θ is defined as

$$\theta \equiv \frac{p_f}{p_t} = \frac{N_c}{N_t} \exp\left(\frac{-E_t}{kT}\right)$$ 　　　　　5.14

The SCL current density with traps is defined by:

$$J = \frac{9}{8}\varepsilon\varepsilon_o\mu\frac{V^2}{d^3}\theta$$ 　　　　　5.15

For a shallow trap SCLC and trap-free SCLC, $\theta = 1$. According to eqn 5.15 J varies as d^{-1} in the ohmic region and as d^{-3} in the SCLC region except for the trap-filled SCLC part. In eqn 4.15 it can be seen that for a fixed V, the dependence of ln J on ln d should be linear with slope $1 \geq -3$.

The voltage at which transition from the ohmic region to the shallow trap SCLC region (V_{tr}) occurs is given by

$$V_{tr} = \frac{8}{9}n_0\frac{ed^2}{\varepsilon}$$ 　　　　　5.16

where n_o is independent of both μ and J. This value will be defined from the extrapolated parts of the respective current region in the lnJ - lnV curves.

5.3　Thermally activated conduction processes

5.3.1　Electronic conduction

The band theory of solids has been applied to understand the electrical behavior of polymers. An important featured of the band system is that electrons are delocalized or spread over the lattice. Some delocalization is expected when an atomic orbital or any atom overlaps appreciably with those of more than one of its neighbors, but delocalization reaches an extreme form in the case of a regular 3-D lattice. The band theory assumes that the electrons are delocalized and can extend over the lattice. When electronic conduction is considered in polymers, band theory is not totally suitable

because the atoms are covalently bonded to one another, forming polymeric chains that experience weak intermolecular interactions. But macroscopic conduction will require electron movement, not only along the chains but also from one chain to another.

The carrier mobility in organic molecules is usually very low. This is due to the fact that electrons, while jumping from one molecule to another, lose some energy. But the mobilities of electrons are found to increase with molecular size in such type of compounds. In polymer system, the conductivity is influenced by the factors such as dopant level, morphology of polymer, concentration of conducting species, temperature, etc. The temperature dependence of conductivity can be described by an Arrhenius type of eqn.

$$J = J_o \exp[-\Delta E/kT]$$ 5.17

where ΔE is the activation energy for carrier generation. The plot of $\log\sigma$ vs $1/T$ must be linear for thermally activated conduction.

5.3.2   Hopping conduction

Disorder in a lattice affects both the energetic and spatial distribution of electronic states. For a random distribution of atoms the density of electronic energy states tails into what is the electrons in these tails are localized. When the electrons are excited to higher energy, conduction via localized electron implies discrete jumps across an energy barrier from one site to the next as shown in Fig.5.5.

An electron may either "hop" over or "tunnel" through the top of the barrier; the relative importance of these two mechanism depending on the shape of the barrier and the availability of the thermal energy.
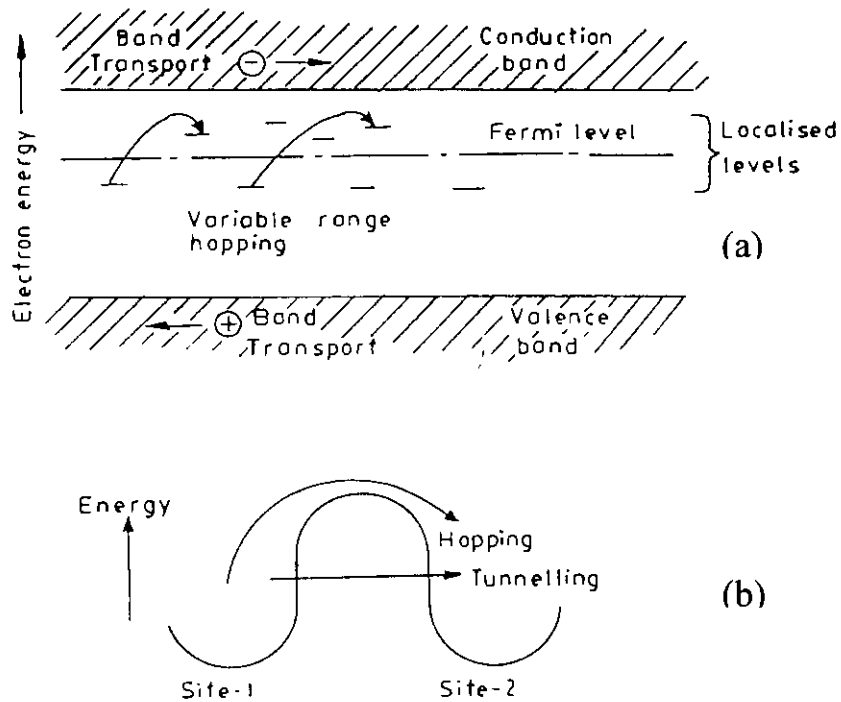
Fig. 5.5 Diagram of electron-transfer mechanisms between adjacent sites separated by a potential-energy barrier.

For variable range hopping the electrical conductivity is given by

$$\sigma = \sigma_o \exp - \left(\frac{T_o}{T} \right)^{\frac{1}{d+1}}$$

5.18

Where "d" is the dimensionality of transport, σ is the conductivity, σ_o is the initial value of conductivity, T is the absolute temperature and T_o is the activation energy in terms of temperature.

5.3.3 Ionic conduction

In bulk material ionic conduction occurs due to the drift of defect under the influence of an applied electric field. The degrees of ionic impurities that may be totally ignored in the context of other properties may have a significant effect on conductivity. A theoretical expression may be derived for the current density,

$$J = \sin h \, (eaE/2kT)$$

5.19

Where E is the electric field and a is the distance between neighboring potential wells, e = electronic charge.

5.4 Experimental Procedure

The specimens investigated were in the form of metal/PPTMA/metal sandwich structures and the top and bottom aluminium contact electrodes were deposited at a pressure of about 10^{-5} torr onto chemically cleaned microscope glass substrate as described in Chap.3. The PPTMA films were deposited on the bottom contact electrode and then the top contact electrode was deposited.
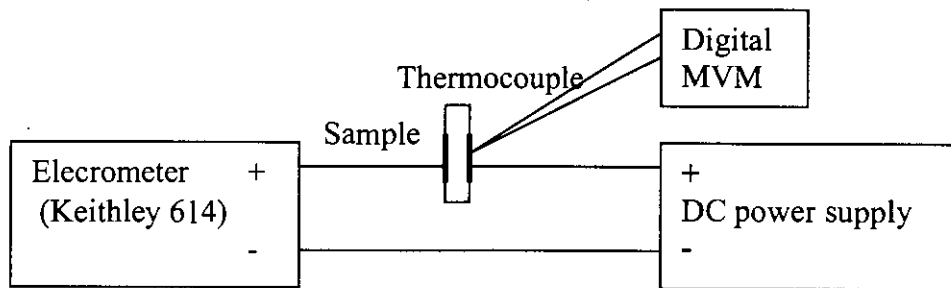

Fig. 5.6 A schematic circuit diagram of DC measurements.

The circuit diagram for current-voltage measurements is shown in Fig. 5.6. The current across the different thickness PPTMA thin films was measured at different temperatures by a digital Keithley 614 electrometer, USA, and the voltage was supplied using a stabilized dc E 3610A power supply (Hewlett Packard, England).
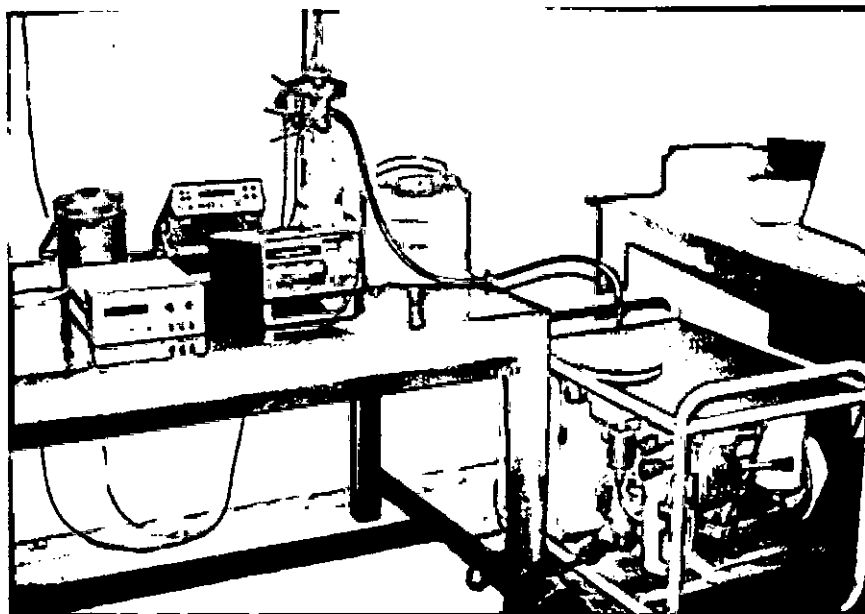
Fig. 5.7 DC measurement setup.

The thermally activated current or the temperature dependence of current across the PPTMA thin films was measured at applied voltages 2.0 and 10 V using the above-mentioned electrometer. The measurements were performed from 300 to 450 K.

In both measurements the samples were heated by heating the specimen chamber externally by a heating coil. The temperature was recorded by a Chromel-Alumel (Cr-Al) thermocouple placed very close to the sample which was connected to a Keithley 197 A digital microvolt(DMV) meter. To avoid oxidation, all the measurements were performed in a vacuum of about 10^{-2} torr.

5.5 Results and Discussion

5.5.1 J-V characteristics

Current density-Voltage(J-V) characteristics of PPTMA thin films of different thicknesses at temperatures 300, 375 and 423K were recorded in the voltage region from 0.2 to 13.0 V. The observed J-V characteristics of the films are presented in Figs.5.8 to 5.11. The J-V curves follow a power law, eqn 5.1 with different slopes in the lower and higher voltage regions. The values of the slope n, is around 1 in the lower

voltage region which corresponds to the ohmic region and in the higher voltage region the slope is around 2 for all samples corresponding to the non ohmic region. The values of the slopes are depicted in Table 5.1.

Table 5.1 The slopes in the two voltage regions at different thicknesses and different temperatures.

Thickness of PPTMA thin films d (nm)	Measurement temperature	Value of slopes	
		Low voltage region (ohmic)	High voltage region (non ohmic)
300	300	1.03	1.70
	373	1.00	2.06
	423	1.26	2.30
350	300	1.02	1.95
	373	1.04	2.05
	423	1.03	2.18
400	300	0.80	1.70
	373	0.95	1.90
	423	1.00	2.02
500	300	0.93	2.40
	373	1.03	2.10
	423	1.08	2.30

The thickness and voltage dependence of current at higher voltage region predict that the current may be due to SCL conduction, Schottky or PF mechanism in PPTMA thin films[12, 13]. To ascertain the type of conduction mechanism, the dependence of J on film thickness d for a series of different samples at constant voltage(10V) is presented in Fig. 5.12. The linear slope derived from these data has a value of about-3.5.
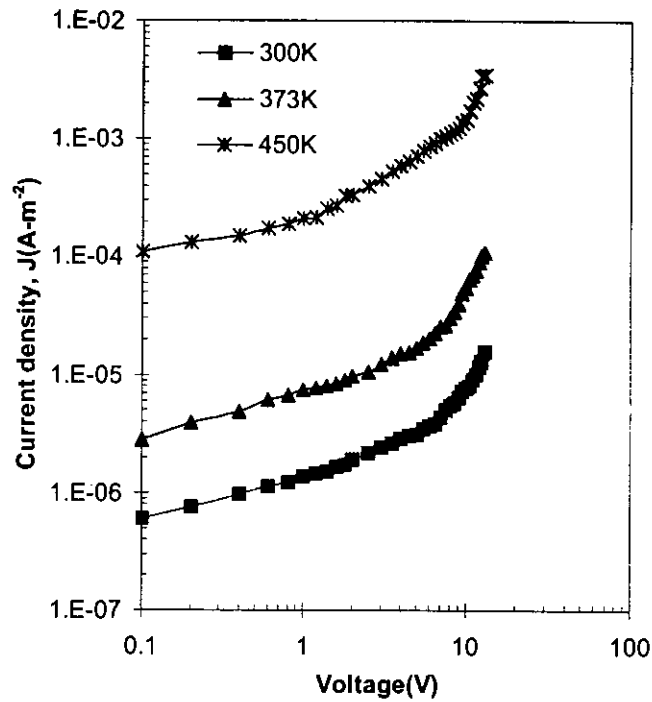
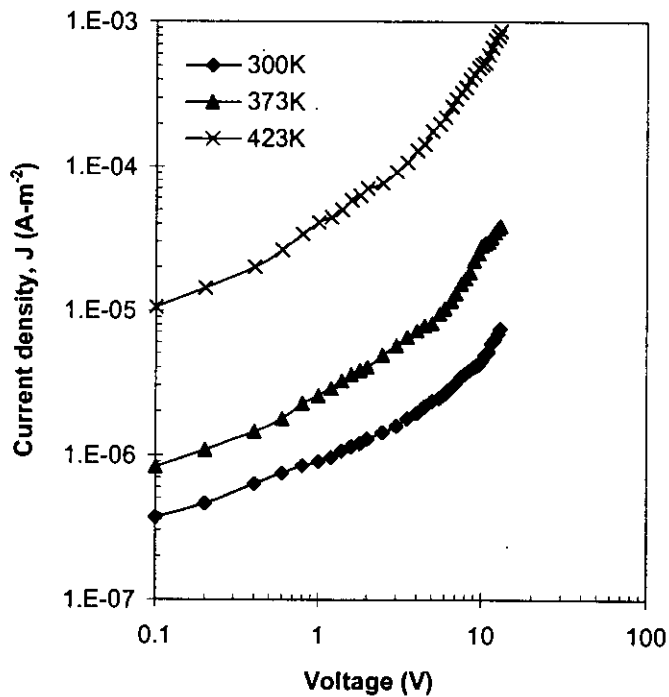Fig. 5.8. Plots of current density against applied voltage at different temperatures for PPTMA film (d = 300 nm).

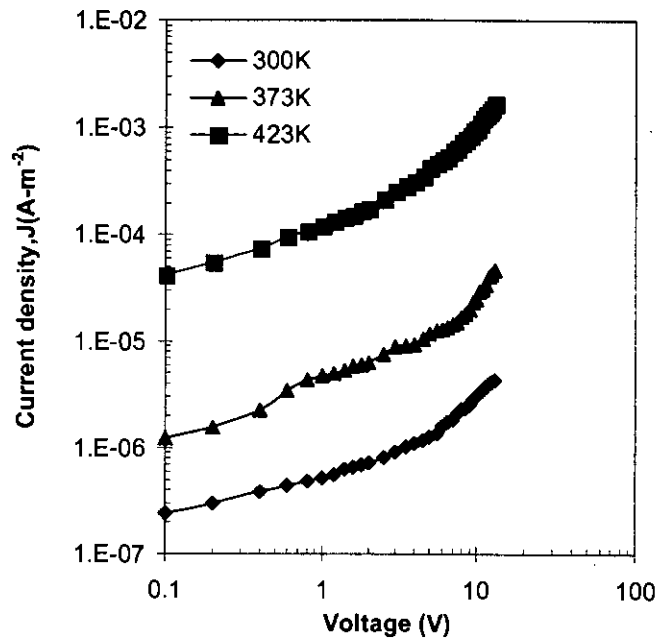Fig. 5.9 Plots of current density against applied voltage at different temperatures for PPTMA film (d = 350 nm).

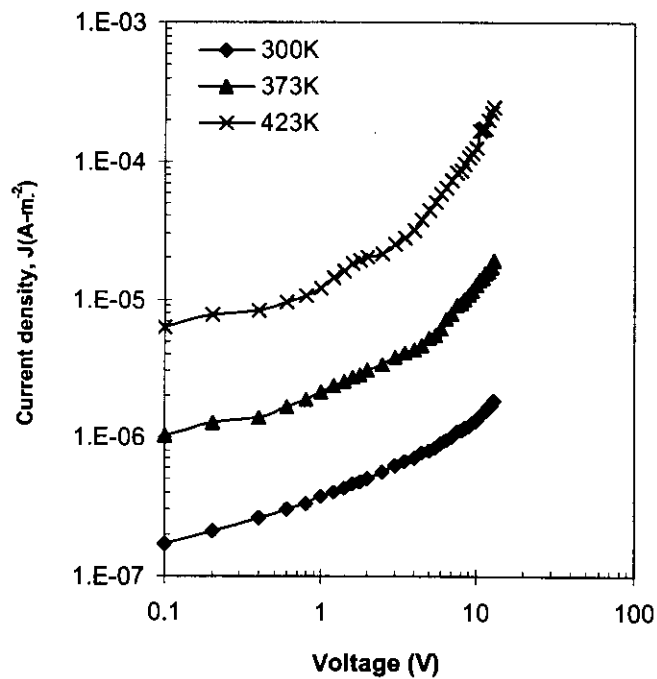Fig. 5.10 Plots of current density against applied voltage at different temperatures for PPTMA film (d = 400 nm).

Fig. 5.11　Plots of current density against applied voltage at different temperatures for PPTMA film (d = 500 nm).

It is seen that in the non-ohmic region the slope is much higher than that corresponding to Schottky and PF conduction mechanisms. This value satisfied the condition for SCLC mechanism as discussed in section 5.2.3. Thus, it can be inferred that the type of conduction mechanism in PPTMA most probably be SCLC.
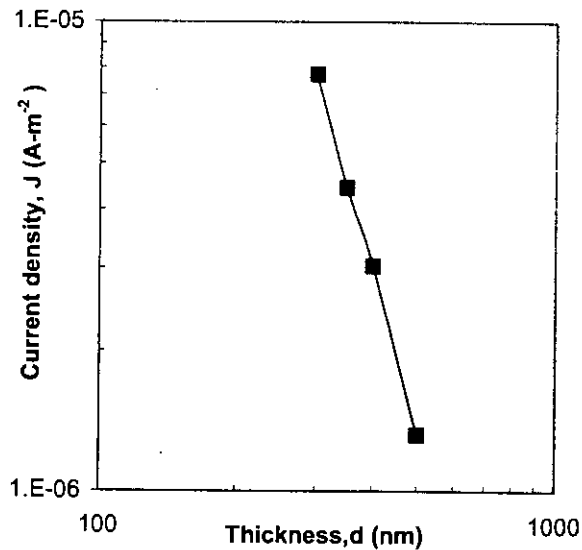

Fig. 5.12　Plot of current density against different thicknesses for PPTMA film in non ohmic region.

5.4.1 Temperature dependence of current

Figs.5.13 to 5.16 show the dependence of J on inverse absolute temperature, 1/T, for PPTMA thin films of different thicknesses. There are two curves, one in the ohmic region with an applied voltage, 2V, and other in the SCLC region with an applied voltage, 10V. Each of the curves has two different slopes in the low temperature and the high temperature regions. The activation energies calculated from the slopes of plots of Figs.5.13 to 5.16 for all samples are reported in Table 5.2.

From the Table 5.2, for applied voltage 2V(ohmic), the activation energy is observed to be about 0.19 ± 0.01 eV at the low temperature region and that at the higher temperature region is about 0.81 ± 0.02 eV. Whereas for 10V(SCLC) applied voltage, the activation energies are observed to be about 0.19 ± 0.02 eV at the low temperature region and about 0.85 ± 0.05 eV at the higher temperature region.

Table5.2 Values of activation energy ΔE (eV) for PPTMA thin films of different thicknesses.

Thickness d (nm)	Activation energies ΔE (eV)			
	2.0 V		10.0 V	
	Temperature		Temperature	
	low	high	low	high
300	0.20	0.89	0.18	0.90
350	0.18	0.76	0.22	0.79
400	0.17	0.72	0.18	0.82
500	0.19	0.88	0.18	0.88

The low activation energy, about 0.19 ± 0.01 and 0.19 ± 0.02 eV, at the lower temperature region and the high activation energy, about 0.81 ± 0.02 and 0.85 ± 0.05 eV, at the higher temperature region may be attributed to a transition from a hopping regime to a regime dominated by distinct energy levels. In this kind of transition process, the localized carrier may be bound with the agglomerates itself. As a result the carriers cannot take part in the conduction throughout the bulk of the material. The low temperature activation energy is too high to draw a correlation with conventional hopping behavior having activation energy of a few meV, although a decrease in ΔE with decreasing temperature may indicate a gradual transition to the hopping regime[14-16].

The band gap between the valence and conduction band can be explained in terms of SCLC and optical measurements. PPTMA thin films deposited using identical conditions have an indirect optical band gap of 1.44 eV and activation energy for conduction of 0.8 eV. It is seen that the activation energy is about half of the indirect band gap. It may be imagined that the energy gap is filled upto the middle where the Fermi level may be situated. Similar results have been reported for dimond like carbon[17] and for disorder solids [18].
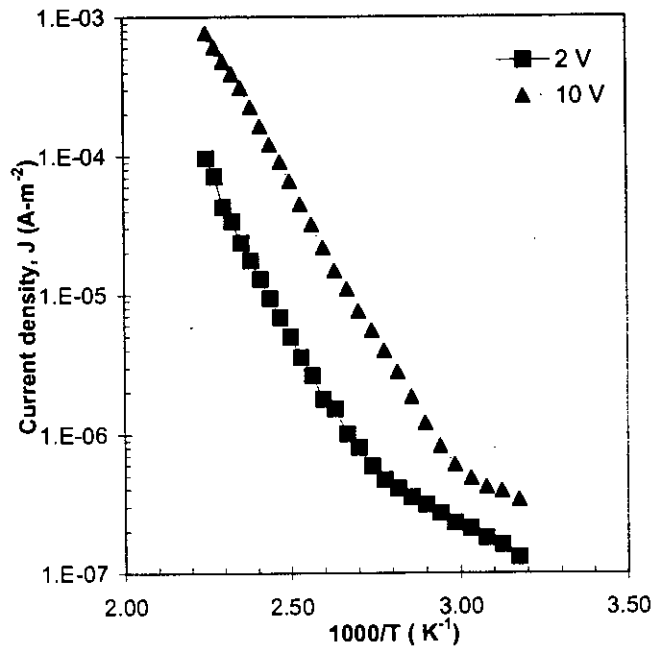
Fig.5.13 Plots of current density against inverse absolute temperature for PPTMA thin film in ohmic and non ohmic regions (d = 300 nm).
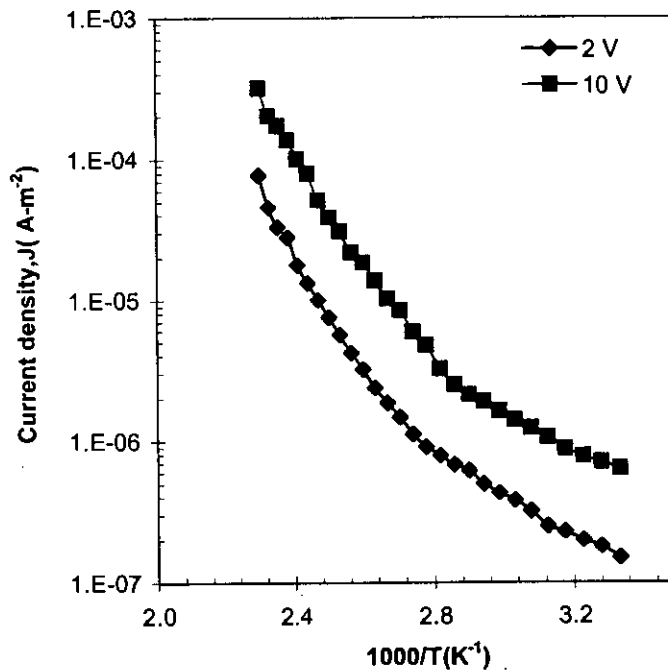

Fig.5.14 Plots of current density against inverse absolute temperature for PPTMA thin film in ohmic and non ohmic regions (d = 350 nm).
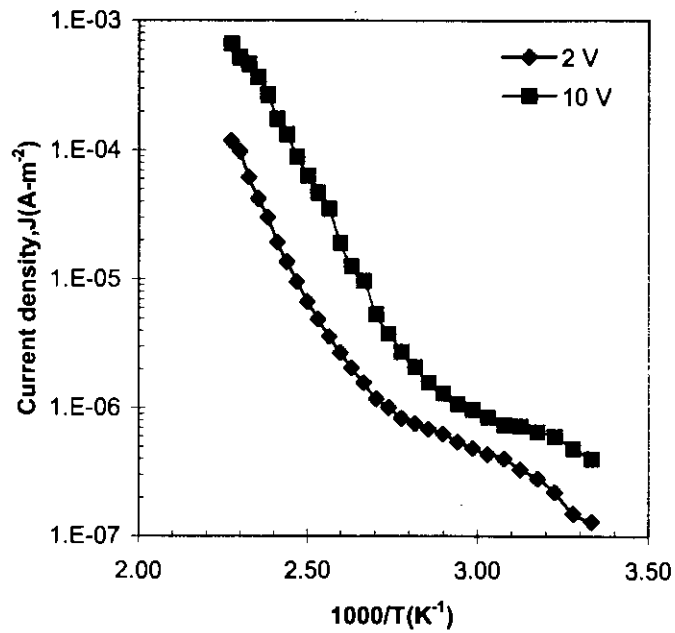
Fig.5.15　Plots of current density against inverse absolute temperature for PPTMA thin film in ohmic and non ohmic regions (d = 400 nm).
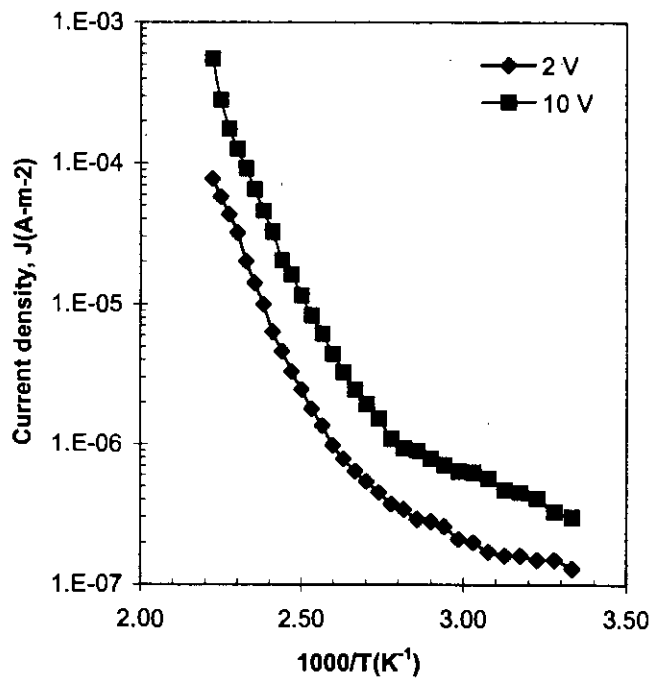

Fig.5.16　Plots of current density against inverse absolute temperature for PPTMA thin film in ohmic and non ohmic regions (d = 500 nm).

References

1. A.S. Saleh, K. Hassan, R. D. Gould, "DC conduction processes and electrical parameters of the organic semiconducting zinc phthalocyanine, ZnPc, thin films", Current Appl. Phys., **3(4)** (2003) 345-350.

2. H. Yasuda, "Plasma Polymerization" Academic Press, Inc, Tokyo (1985).

3. J. H. Lambert, D. A. Lightner, H. F. Shurvell, and R. G. Cooks, Introduction to Organic Spectroscopy, Macmillan Publishing Co., New York (1987).

4. W. Gao and A. Kahn, "Electronic structure and current injection in zinc phthalocyanine doped with tetrafluorotetracyanoquinodimethane: interface versus bulk effects", Organic Electronics **3** (2002) 53-63.

5. R. Valaski, S. Ayoub, L. Micaroni, I.A. Hummelgen, " Influence of film thickness on charge transport of electrodeposited polypyrrole thin films", Thin Solid Films, **415** (2002) 206-210.

6. R.D. Gould and T.S. Shafai, "Condction in lead phthalocyanine films with aluminim electrodes", Thin Solid Films, **373**(1-2) (2000) 89-93.

7. R.D. Gould and M.G. Lopez, "Poole-Frenkel condctivity prior to electroforming in evaporated Au-SiO$_x$-Au-sandwich structures", Thin Solid Films, **342-344** (1999) 94-97.

8. N. Amar, R.D. Gould and A.M. Saleh, "Space-charge-limited conductivity in evaporated α-form metal-free phthalocyanine thin films", Vacuum, **50(1-2)** (1998) 53-56.

9. W.M. Sayed, T.A. Salem,"Preparation of polyaniline and studying its electrical conductivity", J. Appl. Polym. Science, **77** (2000) 1658-1665.

10. M.G. Han and S.S. Im, "Dielectric spectroscopy of conductive polyaniline salt films", J. Appl. Plyom. Sci., **82** (2001) 2760-2769.

11. A.S. Riad, M. El-Shabasy and R.M. Abdel-Latif, "D.C. electrical measurements and temperature dependence of the Schottky-barrier capacitance on thin films of β–MgPc dispersed in polycarbonate", Thin Solid Films, **235** (1993) 222-227.

12. G. W. Bak and A. Lipinski, "Space charge limited currents in thin film solid dielectrics with non-uniform deep-trap distributions: numerical solutions", Thin Solid Films, **238** (1994) 290-294.

13. F.-U.-Z. Chowdhury and A.H. Bhuiyan, " Dielectric properties of plasma-polymerized diphenyl thin films", Thin Solid Films, **370** (2000) 78-84.

14. A.B.M. Shah Jalal, S. Ahmed, A.H. Bhuiyan and M. Ibrahim, " On the conduction mechanism of plasma-polymerized m-Xylene thin films", Thin Solid Films, **288** (1996) 108-111.

15. S. D. Phadke, K. Sathianandan and R. N. Karekar, "Electrical conduction in polyferrocene thin films", Thin Solid Films, **51** (1778) 9-11.

16. S. D. Phadke, "Space-charge-limited currents and carrier trapping in plasma-polymerized malononitrile films", Thin Solid Films, **55** (1978) 391-397.

17. S.R.P. Silva and G.A.J. Amaratunga, "Use of space-charge-limited current to evaluate the electronic density of states in diamond-like carbon thin films", Thin Solid Films, **253** (1994) 146-150.

18. N.F. Mott and E. A. Davis, "Electronic Processes in non-crystalline materials", Clarendon, Oxford (1971).

CHAPTER 6

CONCLUSIONS

6.1   **Conclusions**
6.2   **Suggestions for Future Work**

6.1 Conclusions

Plasma polymerization technique was successfully used to prepare good and reproducible thin films of desired thickness from TMA. TMA is an aniline derivative with $-N(CH_3)_2$ group. Although studies on polyaniline have been reported, there are no reports on experimental studies on TMA based materials. So TMA was chosen as a potential organic monomer for thin film preparation and study of its different properties. Here structural, thermal, optical and dc electrical properties of PPTMA produced from TMA were studied.

The chemical composition of PPTMA was analyzed by elemental analysis technique. The empirical formula of the PPTMA film was determined to be $C_{7.70}H_{10.30}N_{1.50}O_{0.80}$. Non-monomeric oxygen was incorporated into the PPTMA films due to the post-deposition reaction with radical species (danging bonds) trapped in the structure and from the glow discharge chamber during polymerization. The deficiency of carbon and hydrogen contents in PPTMA may be due to the breakdown of bonds owing to the complex reaction during plasma polymerization. The IR investigation shows that the PPTMA is structurally different from monomer. This observation reveals that the PPTMA may contain an aromatic ring structure with NC and CH side groups.

In DTA/TGA investigations, DTA shows a broad exothermic peak around 571K and TGA shows different regions with different percents of weight loss. The maximum change in the PPTMA structure has been occurred in the temperature region 373-873K, where the DTA curve exhibits the exothermic peak. In TGA, the weight loss might occur by thermal breakdown of the PPTMA structure and expulsion of higher molecular mass hydrocarbons, oxygen containing compounds, etc above 505K. It may be attributed from TGA that PPTMA films are thermally stable upto about 505K.

Both allowed direct transition(E_{qd}) and allowed indirect transition(E_{qi}) were identified in PPTMA thin films. The E_{qd} and E_{qi} are found to be 2.80 and 1.44 eV respectively. The calculated value of Tauc parameter, B, is 188 $cm^{-1/2}$ $(eV)^{-1/2}$. The dependence of K,

on photon energy indicates that the probability of electron transfer across the mobility gap rises with the photon energy.

J-V measurements at different temperatures on PPTMA films with aluminiuum(Al) electrodes showed a power law dependence with a linear ohmic dependence at low voltages followed by a non ohmic dependence with an exponent about 2 at higher voltage levels. The thickness dependence of current density in the higher voltage region predicts that space-charge-limited conduction (SCLC) mechanism is operative in PPTMA.. J vs 1/T measurements allowed to derive values of the activation energy. The activation energies are founded to be 0.19 ± 0.01 and 0.19 ± 0.02 eV in the lower temperature region for 2(ohmic) and 10 V(non ohmic) respectively and that are 0.81 ± 0.02 and 0.85 ± 0.05 eV for ohmic and non ohmic region in the higher temperature region respectively. It reveals that in the low temperature region the conduction may be due to hopping of the electrons/ions from traps and/or sub levels and conduction may be due to movement of carriers between distinct energy level in the high temperature region.

6.2 Suggestions for Future work

In this work an attempt was made to investigate the structural, optical and the dc electrical behavior of PPTMA. But, more investigations on PPTMA thin films are required to know different characteristics, which will help finding suitable applications of these materials. The following investigations on PPTMA thin films may be carried out for elucidation of different properties.

The thermal analysis by DSC, DTA and TGA at different heating rates will be helpful to ascertain the reaction kinetics in the PPTMA films. The XPS investigation should be carried out in order to see the bonding of different functionalities found present chemical states in the PPTMA thin films. It also can provide quantitative information of the element present. The electron spin resonance (ESR) study may be carried out to see the nature and source of radicals in this material.

The dielectric constant, dielectric loss factor and dielectric relaxation parameters may be measured to find the dielectric application of the materials. For studying the charge storage and charge relaxation the thermally stimulated depolarization current(TSDC) can be measured.

PPTMA can be modified to change electrical properties by heat treatment and doping. Doping of these films can be carried out while preparing those films in the plasma chamber or by exposing them in dopant gases. All measurements mentioned above can be performed on the modified material to evaluate different properties.